FACULTY OF ELECTRICAL ENGINEERING
UNIVERSITY OF BANJA LUKA

ELECTRONICS

VOLUME 21, NUMBER 2, DECEMBER 2017

FACULTY OF ELECTRICAL ENGINEERING
UNIVERSITY OF BANJA LUKA

Address: Patre 5, 78000 Banja Luka, Bosnia and Herzegovina
Phone: +387 51 211824
Fax: +387 51 211408
Web: www.etf.unibl.org

E L E C T R O N I C S

Web: www.electronics.etfbl.net
E-mail: els-journal@etf.unibl.org

Publisher:

Faculty of Electrical Engineering, University of Banja Luka, Bosnia and Herzegovina

Number of printed copies: 100

Dear reader,

This year, 2017, we celebrate 20 years since the first issue of Electronics Journal was published. In the first years, papers were published in Serbian. Science does not know borders and scientists wish that their research is available all over the world. Therefore, we decided to start publishing papers in English, as of vol. 3 issue 1, published in 2000, thus increasing the visibility of our authors' works in the world of science. Today, Electronics Journal is currently indexed and abstracted in several globally recognized scientific databases. The most prominent ones are certainly Scopus and Ei Compendex from Elsevier. The journal is covered by these databases starting from 2012 and its CiteScore is currently 0.62, according to Scopus (last update on 8 February, 2018). Other metrics, retrieved from Scimago Journal and Country Rank platform, in 2016, were: 0.114 (SJR), 0.178 (SNIP) and 5 (h-index). CiteScore indicator and citation analysis show that Electronics Journal steadily receives more and more citations, which clearly demonstrates that its international visibility follows increasing trend. This conclusion is also supported by the website visits analysis.

In the past few years, editorial board of Electronics Journal also made a significant effort to attract papers from authors worldwide. In that regard, the papers published in the journal are authored by researches from universities and research institutes in countries from almost all continents (India, China, USA, Serbia, Egypt, Algeria, Czech Republic, Latvia, Russian Federation, UK, just to mention few of them). We will continue our work in making the journal internationally recognized.

The next logical step is to extend the coverage of Electronics Journal to other important scientific databases. The ultimate goal is to enter the most respectful one – SCIE (Science Citation Index Expanded) from Clarivate Analytics. To this end, we already defined a roadmap for 2018, and we expect the journal will be included in ESCI (Emerging Sources Citation Index) by the end of the year. This would highly contribute to further international visibility of the journal, which would be beneficial both to the journal and the authors.

I would like to use this opportunity to express gratitude to all authors who trusted Electronics Journal to publish results achieved by their scientific research. Furthermore, I would like to thank all the reviewers, without whose effort invested in careful selection and suggestions the journal would not hold the rating it does today. A special thanks goes to all of the members of the Editorial Board – both current and previous – including the guest editors: prof. dr M. Stojic, prof. dr V. Litovski, prof. dr V. Katic, prof. dr Milovanovic, prof. dr Milojkovic, prof. dr Vukovsavic, prof. dr Pejovic, prof. dr Z. Jaksic.

Editorial Board has selected two guest editors, professors M. Stojic and V. Litovski to print special issues dedicated to their 70th birthdays. Electronics Journal vol. 15 issue 1 (2011) is dedicated to prof. M. Stojic and this issue is dedicated to prof. Litovski. I would like to use this opportunity to express sincerest thanks to prof. Litovski for long-lasting support he has given to this journal, as well as for taking the time and effort to select his associates all over the world to provide contribution for this special issue.

Next issue of Electronics Journal publication will be coordinated by the new Editorial Board, lead by prof. dr Mladen Knezic. The Board will include five section editors: prof. dr Branko Blanusa, prof. dr Tatjana Pesic-Brdjanin, prof. dr Milorad Bozic, prof. dr Vladimir Risojevic and prof. dr Zoran Djuric. I will remain in the Board as the honorary editor-in-chief.

Congratulations to prof. dr M. Knezic for being elected to the position of Electronics Journal editor-in-chief position. I wish him to succeed in our common goal as soon as possible – that Electronics Journal makes it to the Thompson-Reuters list.

Banja Luka, December 2017

Branko Dokic

Professional Biography
Vančo B. Litovski

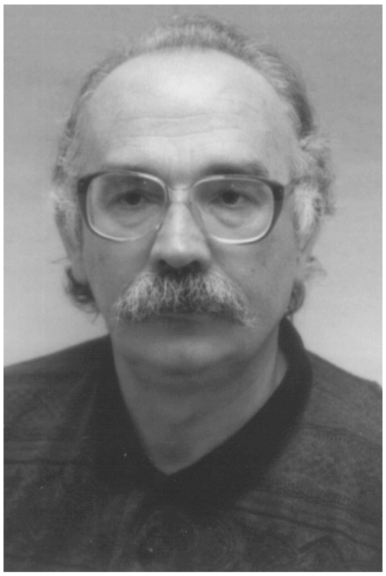

http://leda.elfak.ni.ac.rs/?page=people/Vanco%20Litovski/

1. Introduction

Prof. Litovski was born in 1947in Rakita, South Macedonia, Greece. He graduated the primary school and „gymnasium“ in Bitola, Republic of Macedonia. He enrolled the Faculty of Electronic Engineering in Niš in 1965 where he graduated in March 1970. He was appointed teaching assistant at the Chair of Electronics at the Faculty of Electronic Engineering in Niš on March 20, 1970. He got his Magisterium in June 1974. He served his one year obligatory military service in 1974/75. He got his Ph.D. in June 1977. He was elected a full professor at the Faculty of Electronic Engineering in Niš in 1987. He was appointed visiting professor at the University of Southampton, UK, on November 1999. He retired at the University of Niš on October 2012. He joined the University of Bath, UK, in 2015. He was performing the duty of head of the Chair of Electronics at The Faculty of Electronic Engineering in a period of 12 years. He was teaching the following subjects “Electronics I“ , “Design of electronic circuits“, “Fundamentals of electronics”, “Amplifiers”, “Testing of Electronic circuits”, “Neural networks” and “System on chip design”. He was teaching also at the Universities of Priština, Sarajevo, Novi Sad, and Banja Luka.

As an expert he was serving for several years as a consultant for research and development of the CEO of “Elektronska Industrija Niš“.

Prof. Litovski was member “The Institute of Electrical and Electronic Engineers“ for 20 years, and member of “The Association for Computing”. He was member of the presidency of ETRAN and now is Lifelong Member of the presidency Honoris Causa. He was the founder and the first president of the Yugoslav Simulation Society.

Prof. Litovski is regular member of the Academy of Engineering Sciences of Serbia.

He is winner of several awards delivered by the Town of Niš, The University of Niš, and The Faculty of Electronic Engineering (in 1966, 1967, 1980, 1985, and 1995). He got similar recognitions from the Faculties of Electrical Engineering of Banja Luka and Eastern Sarajevo for special contribution to the development of these faculties. He got a special recognition of the journal “TEHNIKA” in 1985 and the ETRAN award in 1986. He got the “High recognition” from ETRAN for special contribution to the cause of ETRAN. He was awarded the “Tesla” award given by the independent Tesla foundation, for “exceptional achievements in engineering and technology” in 1994. On July 1998 he was awarded the “Savastano” award for best paper published in the previous three years period, by The European Federation of Simulation Societies. The Regional Chamber of Commerce of the Niš region granted him with the “Award for life achievements” on February 2015.

His efforts in improving the quality of teaching wherever he was engaged were mostly expressed by implementation of investments via European projects. He was in charge for the University of Niš’s part of the projects TEMPUS_JEP-17028-2002 and TEMPUS_JEP_41107-2006. He was also i charge for the project CDP+ N° 20/IS/06, financed by WUS Austria for the Faculty of Electrical Engineering in Eastern Sarajevo.

Prof. Litovski founded and developed the first international journal in the field of electronics at the University of Niš: “Facta Universitatis, series: “Electronics and Energetics”. In addition he was a member of the first editorial board of the journal “Elektronika“ which was published in a period of five years by Elektronska Industrija from Niš. He is also a member of the editorial board of the journal „Electronics“ published by the Faculty of Electrical Engineering in Banja Luka.

Prof. Litovski proudly claims that he was the one who brought to the Faculty of Electronic Engineering: computer graphics, Unix operating system, TCP-IP protocol, supercomputing in Beowulf technology, simulation of electronic circuits and systems, design of electronic integrated circuits, electronic testing, electronic diagnosis, sustainable electronic design, artificial neural networks, and he was the first to introduce NIDAQ-LabView technology in laboratory teaching at the Faculty.

He was the first to establish a research laboratory, LEDA, at the Faculty. In: Stephan Pascal (Advisor, Directorate C, »Lisbon strategy and policies for information society«), »Serbia – ICT RTD technological audit«, published by the European Commission Information Society and Media, on March 2010, LEDA was identified as one among 17 centres of excellence of Research and development in Serbia.

http://ebookbrowse.com/serbia-ict-rtd-technological-audit-final-report-pdf-d115707490

2. Scientific activities

The scientific opus of Prof. Litovski is mainly related to design of electronic circuits and systems (discrete and integrated). Being a pioneer in the field he practically paved the research road for research in the subject in Serbia. In his earliest research phase he was investigating computer-aided synthesis of electronic communication filters. He made his doctoral thesis in that field while his results were published in the most distinguished journals in the USA and Yugoslavia. Together with his mentor Prof. Branko Raković he introduced a new class of filtering functions named Lest-Squares Monotonic (LSM). Toward the end of the seventies of the twentieth century, he started his research in integrated circuits design. The research work was performed within the Laboratory for electronic design automation (LEDA). In the field of CAD of electronic circuit, thanks to his personal efforts and to efforts coordinated by him, the first Yugoslav electronic-circuit simulators were developed (named LIFT and MOST) in the early eighties. After that this research task was further fostered so that LEDA became a leading research centre in the field. Software packages for simulation mixed-signal and mixed-level described circuit and systems developed in LEDA were implemented at several universities in Western Europe.

Automation of IC layout design was the next activity undertaken within LEDA. The first Yugoslav integrated software package for gate-array design named ISPGM was developed and implemented. It was presented as an invited lecture at the »3rd MidEuropean Custom Circuit Conference, in Sopron, 1991". This package was directly used in the Niš Elektronska Industrija for design CMOS gate arrays. Based on these results decisions were made at the federal level for investments into CAD equipment for electronic design.

Prof. Litovski started research in electronic testing and design for testability in Serbia. The later is especially related to the introduction of the IEEE 1149.1 standard. His main research results in this area are related to establishment of methodology for fault modelling, fault simulation, and its implementation within the system for automatic test pattern generation for analog and digital circuits. Recently he introduced electronic circuit diagnostic as a research subject in Serbia. He published the first textbook on the subject of testing and diagnosis of electronic circuits in Serbian.

Implementation of artificial neural network in computer-aided design of electronic circuits and systems was a research subject where LEDA and Prof. Litovski gave a significant scientific contribution to the overall research efforts. The first international meeting on ANNs in Serbia took place at the Faculty of Electronic Engineering in the year 1990. Prof. Litovski was the first to implement ANNs for electronic device modelling (which is globally recognized). In that way he opened a completely new way of black-box modelling of electronic components and circuits. That may be confirmed by the fact that the British EPSRC granted a research project on this subject to Prof. Litovski in the war year of 1999/2000.

Prof. Litovski was the first in Serbia to introduce research in the field of sustainable electronic design. His social engagement in the subject helped seriously to the recognition of the problem of the electronic waste and the need for sustainable and eco-electronic design in the Serbian community.

To his name is connected the implementation of ANNs for prediction based on short time series. These concepts were implemented for prediction in various fields such as electricity loads prediction, production of electrical energy, production of microelectronic components, prediction of technological developments in electronics, prediction in eco-developments etc.

In the last decades his research interest was partly oriented to electrical power systems. That includes power electronics for smart-grid, prediction of loads, measurement and characterisation of small loads, power grid modelling, and arc simulation and detection.

3. Publications and citations

Prof. Litovski published 25 textbooks (one in English). The latest versions of them add up to 4,500 pages.

Prof. Litovski published several hundreds of publications. He had 92 co-authors while the average number of authors per publication on his publications was around 2.7.

According to https://scholar.google.co.uk/citations?user=Z5I-hjdYAAAAJ&hl=en his works were cited 1069 times (April, 2017). According to his own statistics, when self-citations and citations by his co-authors are excluded, his publications were cited 452 times. 98 publications of his were cited in this way.

His works were cited by researchers coming from the most advanced research centres in the world such as IBM, Intel, Motorola, Nokia, Synopsis, Cadence Design Systems, Mentor Graphics, AT&T Bell Laboratories, Fraunhoffer Institute, University of California at Berkeley, Ecole Nationale Supérieure des Télécommunications, Technische Universitaet Muenchen and many others.

Prof. Litovski was a coordinator of a large number of national and international scientific and research projects.

Modular Environment for Development and Characterization of Tunable Energy Harvesting Systems

Javier Casatorres-Agüero and Octavio Nieto-Taladriz

***Abstract*—This paper presents the design and development process for an electromagnetic self-tuned vibrational energy harvester prototype. Most state-of-the-art publications present non-tunable or manually tunable vibrational energy harvesters, even the market provides some commercial models of these categories for specific applications. On the other hand, self-tuned energy harvesters are yet rarely seen on the research community. The presented work follows the complete process of designing a prototype to work as a second-order oscillatory system in the form of a cantilever. Three different approaches to tune the resonant frequency of the harvester were considered, each based in changing a property of the cantilever that modifies its resonant frequency. Firstly, it was changed the effective vibrating length of the cantilever. Secondly it was introduced an axial load to the system. Then, the use of a dual cantilever wishbone structure was studied as it allows changing the equivalent stiffness of the system. Finally a prototype based on the first strategy was built and tested, including control algorithms for the maximum electrical energy harvesting point tracking which are presented.**

***Index Terms*—Energy harvesting, self-tuned vibrational energy harvester, Internet of Things, sensor autonomous nodes.**

Original Research Paper
DOI: 10.7251/ELS1721053C

I. Introduction

Even though currently there is no "killer application" that demands the very low energy produced by common vibrational energy harvesters (with the notable exception of the automotive industry mainly in the United States, where incorporating tire pressure monitoring systems within the tires of any new vehicle is mandatory [1]), in the context of low-energy nodes that the Internet of Things trend will soon bring, this kind of energy-harvesting devices and technologies are most likely to play a major role as enablers. By providing enough energy for a low power node to operate, autonomy of such nodes would be greatly improved, with the corresponding reduction in the operational costs of a wireless sensor network. However, as there is not a significant demand for such systems nowadays, there exist few commercial solutions yet [2] [3], though many state-of-the-art investigations and prototypes have shown their effectiveness.

Energy harvesting can be achieved in a wide variety of ways, each suiting a different application. While solar modules have the largest energy density (energy per unit volume or mass), they rely on an intrinsically unpredictable source of energy, and are obviously not adequate for indoor applications. Aero-generators lack predictability, too, and are not "down-scalable": there is a minimum size for such systems to operate efficiently. Vibrational energy-harvesters, conversely, are able to become a predictable low-power source even in small scales, as long as the external vibration continues. Besides its wide projected use in automotive applications, this feature makes "*wearables*" a perfect target/perfect targets for mechanical energy harvesters, along with any other general application where motion is available.

There exist three different families of vibrational energy harvesters. Electrostatic vibrational energy harvesters rely on variations in capacitance due to changes in their geometry that appear when a vibration occurs. Their major drawback is their low energy density, and the fact that their capacitance must be pre-charged with an external power supply to operate correctly. Conversely, piezoelectric energy harvesters use the voltage that appears between their plates when submitted to a mechanical effort as a means to produce energy. They are the ones with the highest energy density at a macro and even microscopic level, but don't seem to operate well in the Nano scale, where are outperformed by their electrostatic and electromagnetic counterparts. Furthermore, the piezoelectric materials required are expensive and the resulting harvester is quite complex.

Finally, electromagnetic devices are based on Faraday's Law of Induction: they work by moving a coil within a magnetic field. As coils and permanent magnets have a non-despicable size, electromagnetic harvesters are difficult to miniaturize to micron scales, but have proven to be a simple and promising solution at a macroscopic level.

A typical electromagnetic mechanical energy harvester consists on a cantilever fixed on one end, and with a mass on the other. External vibrations produce a forced oscillation on the cantilever, so that its non-fixed end behaves like a 2nd order spring-mass system. By fixing a permanent magnet in the non-fixed end of the cantilever and a coil in the vibrating base (or vice versa: a coil on the non-fixed end and a permanent magnet on the vibrating base), the relative displacement between the two elements induce an electromotive force in the coil's terminals as predicted by Faraday's Law of Induction. As far as the

Manuscript received: May 18th, 2017
Received in revised form: May 18th, 2017

Casatorres-Agüero J. is with the Research Group "B105 Electronic Systems Lab", Departamento de Ingeniería Electrónica, E.T.S.I. de Telecomunicación, Universidad Politécnica de Madrid, SPAIN

Nieto-Taladriz, O. is the Head of the Research Group "B105 Electronic Systems Lab", Departamento de Ingeniería Electrónica, E.T.S.I. de Telecomunicación, Universidad Politécnica de Madrid, SPAIN

external vibration does not stop, the device keeps generating energy, which makes it very adequate to power sensors situated in indoor areas that are difficult to reach, as those in common industrial environments or ship engines.

However, systems as the one described above have a very high quality factor (Q). What this means is if the external vibration frequency doesn't perfectly match the one the energy-harvester has been designed for, the energy production falls dramatically to near-zero values, which makes the device useless, as depicted in Fig.1. Consequently, if the frequency of the external vibration changes over time, the energy production drops to zero. Various strategies are then to overcome the problem, ranging from devices that are manually tunable so they can be manually adjusted to any application, to non-linear harvesters designed to have a much lower Q, so they can produce energy in a wider frequency range. While the former strategy is obviously not suited to those "difficult to reach areas", the latter has the problem of having a much lower power density: devices following that strategy produce much less energy than a linear harvester correctly tuned, as long as the external vibration has one dominant frequency, and is not a broadband signal or white noise.

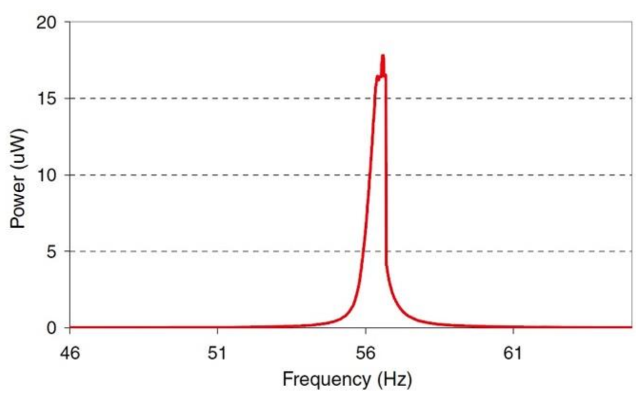

Fig.1. Example of power generation vs. frequency in our test platform

The most promising solution seems to be that harvesters are automatically tuned, without any kind of human intervention. However, this implies both a mechanical tuning mechanism and a closed-loop control system that ensures that the device is operating in its maximum power point, with its subsequent increase in complexity. Furthermore, it leads to the need for some power auto-consumption: some of the energy produced is used to power the tuning mechanism, reducing the amount of energy produced.

In this paper, some strategies for mechanical tuning are presented, along with some algorithms for the control system. A prototype is made and measured, and its problems are shown as guidelines for future research work.

II. Theoretical basis: 2nd order systems and energy harvesting

As has been said, the simplest way to create a vibrational energy harvester is by using a cantilever: a thin plate of material which is clamped to a rigid base on one of its ends, and free at the other, where an inertial mass is fixed. The equations that govern the behavior of such systems are well known, and a full development can be found in [4]. However, some facts should be highlighted:

When the system is under an external vibration, it is forced to oscillate at the same frequency that the external vibration, which is called forced oscillation. The only difference is the phase of the oscillation that appears in the free-end.

- A 2nd order system such as the one described above, when submitted to a punctual excitation, has a response that highly depends on the damping coefficient. For a typical cantilever system, the first mode response is under damped, which means that it tends to oscillate at a given frequency called *damped natural frequency*, with amplitude that decays exponentially over time. If the damping coefficient became zero, the system would oscillate indefinitely at a frequency called *un-damped natural frequency*. Higher order modes are also excited, but their relative power to the first mode is very low. Analysis is usually carried out only for the first mode, as it will often be the only one excited in the frequencies of interest.
- When an under-damped 2nd order system is forced to oscillate at a frequency that matches its un-damped natural frequency, it occurs what is usually called *resonance*, which means that the energy transmitted from the environment to the system has a maximum. It is this state of resonance that frequency tuning seeks in an energy harvester, as produced power is maximum when the un-damped natural frequency matches the external vibration frequency, and nearly zero when it doesn't. The un-damped natural frequency is often called *resonant frequency*, and it does not depend on the damping of the system.
- When the 2nd order system is purely mechanical, the only damping that appears is the mechanical damping (which is function of the characteristics and shape of the cantilever and its free-end mass, as a result of its friction with air). However, when the system produces energy by means of moving a coil in a magnetic field, with a load connected to the terminals of the coil, an electrical damping coefficient appears, to be added to the mechanical damping. It shall, however, not be seen as an undesirable effect, as it is precisely because of that damping that the system generates energy.
- Of the total generated power, characterized by that electrical damping, part is dissipated as electrical losses, and part is dissipated on the load, being the actual generated power, which is what it is intended to maximize. Furthermore, there exists an optimal load that produces the exact electrical damping to extract maximum power from the energy harvester. This is an additional degree of freedom for this kind of systems, where not only the resonant frequency but also the load should be tuned to ensure maximum power is extracted. In the simplest approach, both parameters are addressed independently, as

changes in the value of the load should not affect the resonant frequency of the system.

There is confusion in which the value of the optimal load should be. It is many times stated that the optimal load is the one that matches the value of the conjugated output impedance of the harvester (equal to the impedance of the coil). This maximizes the power dissipated on the load out of the overall electrical power generated, but does not maximize the electrical power.

On the other hand, it is sometimes said that the optimal load makes the electrical and mechanical damping equal. Again, this maximizes the electrical power generated, but most of it is dissipated in non-desirable ways, becoming electrical losses. In [4] it is shown that the optimal load matches the coil impedance plus the electrical equivalent impedance of the mechanical damping. This means that the mechanical damping is modeled as an additional electrical element, with a resistive impedance capable of dissipating power in series with that of the coil. Therefore, the optimal load should be the conjugate of the sum of both impedances, as in any other impedance matching problem.

III. Mechanical solutions for frequency tuning

It has previously been mentioned the extreme importance that matching the resonant frequency of the system with that of the external vibration has in terms of the generated power. The un-damped natural frequency of an under-damped second order system can be computed as in Eq.1.

$$f_n = \frac{1}{2\pi}\sqrt{\frac{K}{m}} \qquad with \quad K = \frac{Ywh^3m}{4L^3(m+0{,}24m_c)}$$

Eq.1

Where m is the equivalent mass, which can be approximated by that of the free end of the cantilever; m_c is the mass of the cantilever, *Y* is its Young's modulus, *L* is its length, *W* is its width and *h* is its thickness.

By simple observation of the above formulas, some techniques for changing the resonant frequency can be suggested. While changes in the mass on the free end of the cantilever, or in its position are extremely difficult to implement effectively, and dynamically modifying the cantilever's width or thickness is nearly impossible, there are not many strategies left. It is possible to change the resonant frequency by changing the *effective length* of the cantilever, meaning the length that vibrates freely. This can be simply achieved by moving the point where the cantilever is attached to the vibrating base, as described in [5].

Another way of changing the resonant frequency can be by changing the *equivalent stiffness* of the system. A method for doing so is presented in [6], where adjusting the distance between the clamped ends of two parallel cantilevers attached in their free-end allows tuning the frequency at which the system resonates.

In addition, if an axial load is applied to the cantilever, its resonant frequency can be shifted [7] according to the expression:

$$f'_r = f_r \cdot \sqrt{1 - \frac{F}{F_b}} \qquad with \ F_b = \frac{\pi^2 \cdot Y \cdot w \cdot h^3}{48 \cdot l^2}$$

Eq.2

Where F_b is the compressive force necessary to buckle the cantilever, or the tensile force that makes it behave like a string.

The easiest way to apply and adjust that axial force is by changing the distance between two permanent magnets, one on the free end of the cantilever and another one at exactly the same height, attached to the vibrating base. By moving the position of the latter, the axial force changes, modifying consequently the resonant frequency of the cantilever.

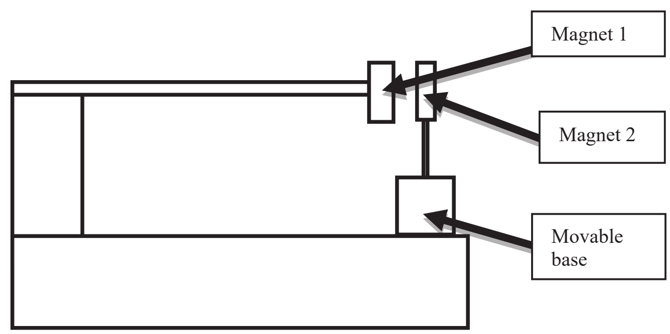

Fig.2. Magnet configuration for axial force tuning

Though the three strategies should be able to dynamically change the resonant frequency while being reasonably easy implementable, there is a major difference among them, namely the tuning range. The system is intended to work in the range of 30 to 80 Hz, as most engine vibrations fall within that interval. To do so, the following values are used to carry out the simulations:

Table 1. Parameters for simulations

Material	Stainless steel 301	
Young's modulus	$1.98 \cdot 10^{11}$	N/m^2
Density	$7.9 \cdot 10^3$	kg/m^3
Length	45	mm
Width	5	mm
Thickness	0.5	mm
Mass on free end	10	g

In the first approach, changing the vibrating length has a dramatic impact on the value of the resonant frequency. A simple plot of the formula shows that if the nominal resonant frequency –i.e. the one that the system has when the whole cantilever vibrates- is adjusted to ~30 Hz, changing the vibrating length to 50% is enough to reach the 80 Hz intended limit:

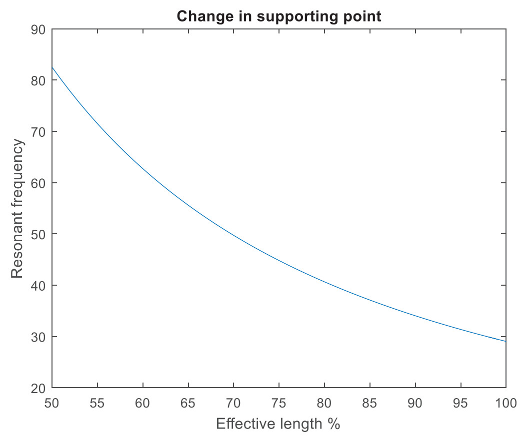

Fig.3. Resonant frequency dependence on vibrating length

One main problem the graph shows is that reducing the equivalent length makes the sensitivity quite large. Consequently, even small deviations in the correct position would yield non-despicable deviations in the desired resonant frequency. In very a high Q system as the one described, the output power would drop. If the total length of the cantilever is about 45 mm, changes of about 1 mm mean a frequency shift of more than 10 Hz.

The second strategy lacks a theoretical model, so simulations are not performed. Despite the curves given in [6], it is intended to build a prototype to evaluate the tuning range that the technique is capable of, setting a frequency of 30 Hz as the mandatory lower end of the interval. This, however falls of the scope of the present article and is under current development.

Finally, the third strategy has a major drawback: if the harvester has to be minimized, the permanent magnets size is not enough to give a reasonable tuning range. To illustrate so, another simulation was performed, using the work presented in [8] with the "*Matlab"* code in [9] to compute the forces between magnets, both in the tensile and the compressive cases. The nominal frequency was set to ~30 Hz in the tensile force case, and to ~40 Hz in the compressive force simulation.

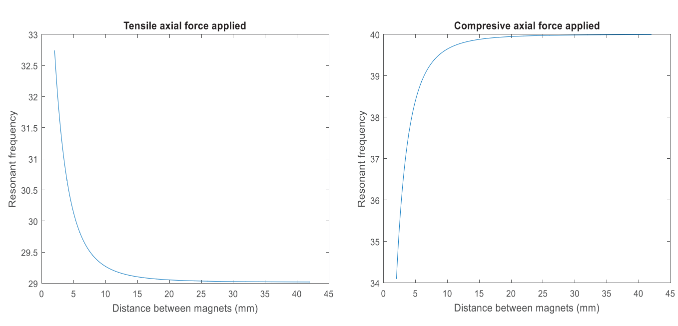

Fig.4. Resonant frequency vs. distance between tuning magnets

The simulated magnets sizes were 5 x 5 x 5 mm for the one on the cantilevers free end, and 5 x 5 x 10 mm for the moving magnet (being the third dimension the one along the movement axis), and they were type N52 magnets, the category that produces the highest magnetic flux per unit volume. As stated before, the tuning range is way too small to be useful. Furthermore, the permanent magnets presence does (though slightly) affect the magnetic flux through the harvester's coil, in a difficult to predict manner

IV. The design environment

In the process of designing a vibrational energy harvester, a design and testing environment has been developed. Its modular nature allows separating the physical design of the harvester from the algorithms to be implemented, and the test-bench used to measure the prototypes.

The physical design has been made through two separate stages. The first stage consists of the mechanical simulation of the tuning strategies where the behavioral model – i.e. the equations that describe its behavior - was available. The simulations have been carried away in "*Matlab"*, and are indispensable to define the parameters of the model (dimensions, mass, material…) to a first degree, which is intended to be refined after measuring the corresponding prototypes. Furthermore, they are useful to discard the strategies that seem less promising, as happened with the axial-load approach. Some of the resulting graphs have been shown above.

Once determined the correct dimensions and topologies to be tested, the second stage starts, where the models are 3D modeled using the software "*SolidWorks®*" so they can be 3D-printed afterwards. Examples of the prototypes that are currently under development can be seen in Fig.5. 3D printing offers a relatively cheap way of optimizing the design, as some parameters that were coarsely determined in the simulations can be finely tuned through measures.

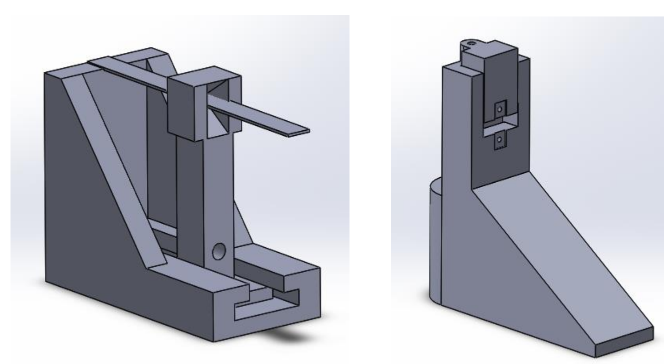

Fig.5. 3D Modeled prototypes. (a) based in changing vibrating length, (b) based in changing equivalent stiffness

As the prototype was designed, a test-bench for measuring was also built. A vibration-generator was acquired and characterized, and some electronics for power conditioning had to be done to allow proper functioning. The design of such test-bench, however, falls of the scope of the present paper, though is of extreme usefulness for the designing process and testing of different algorithms.

V. The prototype

The first prototype, which is presented in this article, uses the first described frequency tuning technique. In order to mitigate the high sensitivity problem described, it is designed so that its length is slightly larger than the one simulated simulate. In particular, its length is 55 mm. The prototype base is built using a 3D printer, with a special piece –tuner from now on-designed to be movable along the prototype's axis, effectively changing the vibrating length. A motor connected to a worm screw maxes this longitudinal movement possible, while some other pieces are printed for support.

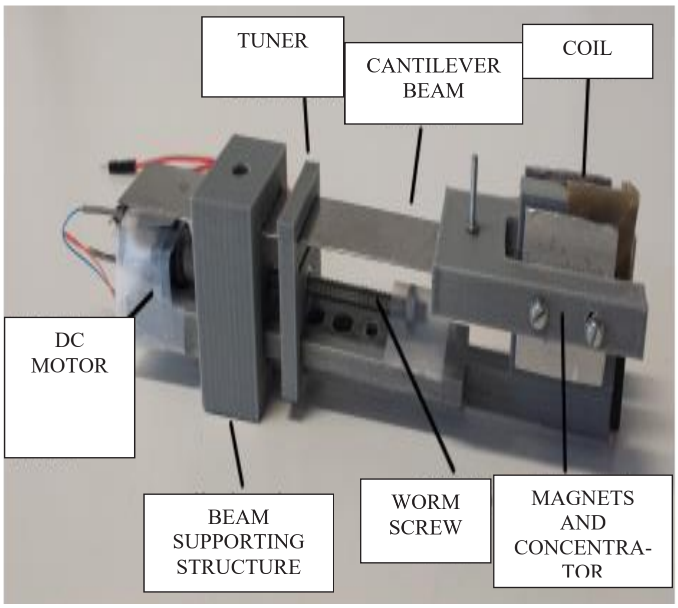

Fig.6. The prototype

The chosen topology for electrical power generation consists of 4 small N52 magnets attached to a u-shaped piece clamped in the free end of the cantilever. A coil is then fixed to the vibrating base so that is between the two arms of the u-shaped piece. The magnets are glued to a pair of metal pieces that act both as support and as a concentrator of the magnetic flux, maximizing the flux that goes through the coil. Fig.7 shows a front view.

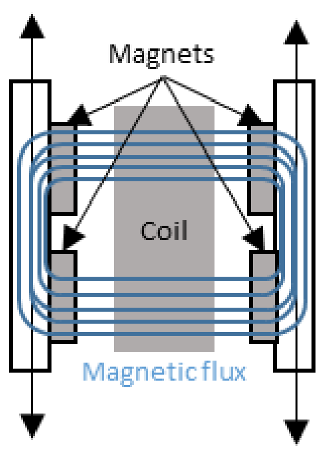

Fig.7. Coil-magnets configuration

The reason why this topology is used, instead of others such as moving the coil while a magnet is inside, or using only one magnet while the coil is directly underneath it, is because it has been proven to maximize the generated power. This experimental result while comparing various coupling topologies can be found in [10].

The obtained output voltage value is very small (~0.5 V peak in the best case), and not constant, which makes it useless for most electronic applications. A voltage multiplier in used to get a rectified voltage high enough to work with. It is used an 8-or-4-stage Villard multiplier, with a switch to change the multiplying factor. "*Schottky*" diodes are used instead of regular PN diodes because the output voltage value without multiplication is lower than a regular diode forward voltage, so the multiplier would not work if using regular diodes. As can be seen from Fig.8., the chosen configuration gives the predicted results, both rectifying and multiplying the output voltage.

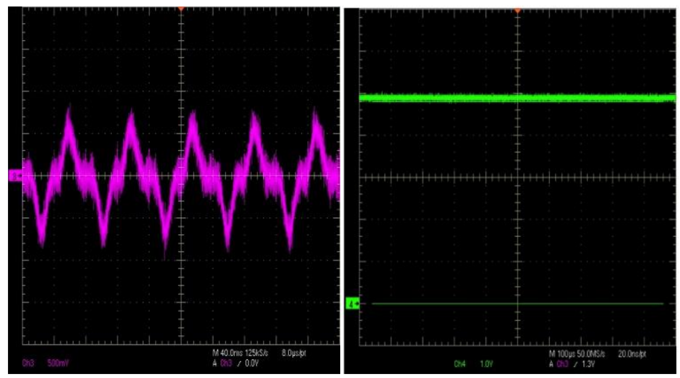

Fig.8. Output voltage (a) before the Villard multiplier (b) after the Villard multiplier

The microcontroller used to implement the tuning algorithm is a Microchip's PIC 16LF1503 [11], whose 30 uA consumption at 1.8 V (54 uW) make it perfectly suitable for controlling the system. Finally, the DC motor that has been chosen to tune the harvester is the model 212-008 of Precision Microdrives, which can take up to 2.5 V [12]. An H bridge is used to change its rotation direction, so that it can both increase and decrease the vibrating length.

Whilst the microcontroller is perfect for the application, the DC motor consumes an amount of power various orders of magnitude above that the harvester can produce, making the total produced energy balance negative unless tuning is very rarely done. Any contemporary macroscopic general-purpose DC motor is likely to have that high consumption problem, so their use for mechanical tuning in this kind of devices won't be a competitive solution until application-specific low power actuators are developed, as those used in common wristwatches.

VI. Tuning algorithms

As has been stated many times before, a second order mechanical energy harvester has a very large Q, so precise self-tuning of its resonant frequency is mandatory. Two stages integrate the tuning algorithm: monitoring to detect if the system is out of tune, and adjusting its resonant frequency if it is. There are two main strategies to follow: those that imply a constant monitoring and adjustment of the operating point while always consuming, and those that rely on periodic sampling and adjusting, thus only consuming power within a fraction of the operating time of the harvester. It is the second strategy which is followed as very tight power consumption constraints must be considered in mechanical energy harvesters.

When monitoring the operating point and detecting whether or not it is the most desirable, both operating frequency and output power can be used. Monitoring the output power – or equivalently the output voltage - has the advantage of being very simple while not needing additional sensors. The voltage level could be measured both before and after the voltage multiplier. If measured before, the algorithm ought to be aware of the operating frequency, or it would detect that the system is out of tune on every cycle. If measured after, it should be taken into account that the response would be slow, as the multiplier capacitors prevent the signal from changing abruptly. Despite the point where the voltage is measured, detecting a voltage drop might trigger an unnecessary tuning process if that drop was caused by a reduction in the amplitude of the external vibration. Using the frequency as an indicator, on the other hand, avoids that problem but requires additional hardware and computing power. A particularly interesting method for detecting the optimal working point lies on the resonance phenomena: when the harvester is perfectly tuned there appears a phase difference between its free end and the vibrating base (or the external vibration) of exactly π/2. This difference appears in all position, velocity and acceleration signals, which makes possible to use a pair of accelerometers to detect the phase shift. If it is different from π/2 an adjustment process could be triggered. As it seems to be a promising solution, it is a present line of work.

Once detected a deviation in the operating point, the adjusting algorithm starts. This process is highly dependent on the architecture used for mechanical tuning. For the motor driven tuning used in the prototype, it means powering the motor until the correct vibrating length is reached. Some different approaches can be programmed on the microcontroller. If the environment is well known, so that its different vibration frequencies are characterized, these can be saved in the system's memory so it can power the motor the exact amount of time to get to the correspondent vibrating length. The output voltage is then measured and compared to a threshold to determine whether the frequency is correct, restarting the process if it is not. This would mean that all the frequencies are progressively "checked" according to their probability of occurrence. For the architecture used in the prototype, the time needed for a given displacement pf the tuner can be found as $t = L \cdot \frac{60}{P \cdot RPM}$ being L the displacement, P the pitch of the worm screw (0.7 mm in the prototype) and RPM the angular speed the motor has in *revolutions per minute* (42 in the prototype). This way the time that the motor has to be powered to switch to the next frequency can be computed, as long as both the equivalence between length and resonant frequency, and the current position of the tuner are known. A calibration period is therefore needed to give the microcontroller information about the tuner's initial position, which also needs additional (possibly passive) hardware.

However, in the most generic case there is no knowing at all about the environment. This means that the whole range of vibrating lengths must be gone over when tuning, by implementing a *sweeping* algorithm. The easiest way do this is with a *linear* sweep, by starting at the last resonant frequency known and then increasing the vibrating length until a new resonant frequency, characterized by an increase in the output voltage, is found. If it is not, the sweep should restart from the last resonant frequency, but reducing the vibrating length. No resonant frequency should be found, the system would go to sleep mode to perform a new analysis later.

An *alternating sweep* is far more suited to situations where the external vibration frequency has changed to a slightly lower value. It would first increase the vibrating length slightly, and if no voltage peak were detected, it would start reducing it twice as much as it was previously increased. Again, if no resonant frequency were found, the vibrating length would be increased by 4 times the initial increase. In this two-times increase fashion, the algorithm would solve very quickly the situations where the new resonant frequency is very close (either larger or smaller) than the previous one. However, if the change is big, this algorithm would take an unreasonably large amount of time.

Approaches based on gradient descend would be nearly optimal if the Q of the system were lower, as it is a convex problem. However, trying to use such strategies would mean an enormous sensitivity to minimal voltage changes, as when far from the resonant frequency, the output voltage is extremely low, and the voltage difference between successive steps would be extremely low.

It should be noted, however, that this problems only occur when using the output power – or voltage - to detect if the system is correctly tuned. By using its frequency or the previously described phenomena of phase shift in resonance, it could be easily determined if the vibrating length of the harvester ought to be increased or decreased. Furthermore, if the phase shift is subtracted to π/2, the error value can be converted into an electrical signal to feed the tuning motor, possibly through a Pulse Width Modulation. A PID controller that optimizes the convergence speed would then be the best solution to solve the problem.

VII. Results

An operational prototype has been built and tested under a controlled environment. The system has been designed to be modular so that different modules and approaches can be built, characterized and tested, Fig.9.

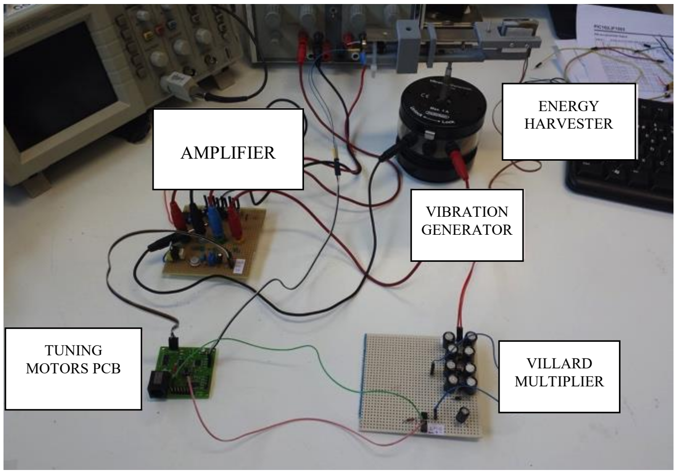

Fig.9. Complete testing environment

First result is that the available energy is quite low in most environments to get it as a usable power supply for the state of the art electronic technology, mainly regarding mechanical actuators. Specific cases as automotive applications where vibrating energy is high will be the first to use these technologies. However, as very low energy nodes are becoming available, this is a quite promising technology in many other fields

Several tuning algorithms have been programmed and tested, and a wide field for new developments is presented in terms of predicting the mechanical spectrum and deciding whether is better to continue in the same frequency or moving to another closer to the optimum operating point.

VIII. Conclusion

A platform for designing, testing and characterization of self-tunable mechanical energy harvesting systems has been designed and a first prototype has been used as validation of the principles presented. Some other mechanical, electronic and algorithmic approaches are under current development.

IX. Future work

Some lines of future work have been presented along the paper. The following are currently under development:

- Miniaturization of the vibrating-length approach prototype and correction of some mechanical issues related.
- Design, construction, testing and characterization of an energy harvester using the wishbone structure presented in [5]
- Optimization of the voltage-level-detection tuning algorithms presented before in terms of their convergence speed and robustness,
- Implementation of a phase-detection tuning algorithm to overcome the problems presented before.
- -Study and optimization of suitable energy storage options.

References

[1] DEPARTMENT OF TRANSPORTATION (USA), *Federal Motor Vehicle Safety Standards; Tire Pressure Monitoring Systems;*, 2005.

[2] MicroStrain, “MagnetoInductive Vibration Energy Harvester,” [Online]. Available: http://files.microstrain.com/MVEH_Datasheet_Rev_1.02d.pdf. [Accessed 5 1 2017].

[3] Perpetuum, “Perpetuum PMG Energy Harvester,” [Online]. Available: https://perpetuum2016.files.wordpress.com/2016/09/perpetuum-ltd-vibration-energy-harvester-data-sheet-21october2013.pdf. [Accessed 5 1 2017].

[4] N. G. Stephen, “On energy harvesting from ambient vibration,” *Journal of sound and vibration,* vol. 293, pp. 400-425, 2006.

[5] K.-A. L. Shyh-Chin Huang, “A novel design of a map-tuning piezoelectric vibration energy harvester,” *Smart materials and structures,* vol. 21, no. 8, 2012.

[6] J. D. Heit, Thesis: A framework to estimate power output as a function of input vibration parameters for vibration energy harvesting, Utah, 2014.

[7] D. Zhu, M. J. Tudor and S. P. Beeby, “Frequency Tuning of Vibration Energy Harvesters using Compressive and Tensile Axial Loads,” in *PowerMEMS*, Seoul, Korea, 2011.

[8] W. S. P. Robertson, Thesis: Modelling and design of magnetic levitation systems for vibration isolation, Adelaide: University of Adelaide, 2013.

[9] W. S. P. Robertson, “Magcode,” [Online]. Available: https://github.com/wspr/magcode.

[10] D. Spreemann, B. Folkmer and Y. Manoli, “Comparative study of electromagnetic coupling architectures for vibration energy harvesting devices,” in *PowerMEMS*, Sendai, Japan, 2008.

[11] MicroChip, *PIC 16LF1503 Datasheet.*

[12] MicroDrives, *212-008 DC Motor.*

High Efficiency Photovoltaic System with Fuzzy Logic Controller

Branko Blanuša, Željko Ivanović and Branko Dokić

Abstract — **In this paper is presented high efficiency photovoltaic system (PV) with fuzzy logic controller. This system consists of PV panel, boost DC/DC converter and 24V DC load. Control module is realized with fuzzy controller. This controller has double function and it gives references for duty factor and switching frequency of the converter control signal. In this way the PV system works with applied maximum power point tracking (MPPT) method and switching frequency is changed on the way so the converter works with maximum efficiency in continuous current mode. Functionality of proposed model is tested through computer simulations in Matlab and on laboratory prototype.**

Key words: PV system, DC/DC converter, fuzzy controller, MPPT, efficiency optimization.

Original Research Paper
DOI: 10.7251/ELS1721060B

I. Introduction

Electrical energy production from renewable energy sources, increasingly grows and significant, one can say the leading, place have PV panels. This method of power generation from PV systems is one of the cleanest and safest, and there is no acoustic pollution that is characteristic for wind plants.

Although new materials and production techniques of photovoltaic cells were developed, silicon is still in over of 80% the produced photovoltaic cells. The reason is wide accessibility of silicon and the fact that it is not toxic. Monocrystalline and polycrystalline PV cells are two basic types of silicon photovoltaic cells. There is a third type, amorphous silicon, but the efficiency of these cells is lower than in the previous two types and is less used.

One of the basic requirement that is set in front of PV systems is their efficiency. Therefore, there is an intensive research that is carried out into several directions:

- Development of materials for PV panels with a better ratio efficiency/price,
- Optimization of solar system topology from the standpoint of electrical energy production and consumption,
- Maximum utilization of available power of solar panels,
- Maximum efficiency of power converters used in solar systems.

There are significant researches and many methods which are used for a better utilization of available power from PV panels. They are well known as MPPT technique like gradient methods[1], perturbation and observation (P&O) [2], the incremental conductance (IncCond) [3], ripple correlation [4], short circuit current (SCC) and open circuit voltage (OCV) technique [5] etc. Also, there are many techniques based on fuzzy logic [6-7] and the use of artificial intelligence [8-9]. In some papers, a comparison between different MPPT techniques were performed [10-11]. Generally, these techniques vary in complexity, cost, speed of convergence, hardware implementation, and effectiveness.

Application of DC/DC converters in PV systems are wide and significant. These converters are used to connect PV panel to DC consumers. Also, converters can be used as battery chargers, or interfaces between solar panels and DC/AC converters, or electrical grid. One of the significant characteristics of the converters used in solar systems is their efficiency.

Central place in this paper has control module based on fuzzy logic controller. Efficiency optimization algorithm for DC/DC converter and MPPT algorithm are implemented in this module. So, two functions are realized with the one fuzzy controller. Fuzzy based MPPT controller is fast and the output voltage of the PV panel adjusts to meteorological changes, so the maximum power at the panel output is obtained. Also, using the same controller, an adaptive search algorithm for efficiency improvement of the DC/DC converter is implemented. This algorithm is applicable regardless of converter topology.

Simple PV system is discussed in this paper. It consists from PV panel, boost DC/DC converter and 24V DC load. (Fig. 1.). Similar controller with some modifications can be used in more complex PV systems.

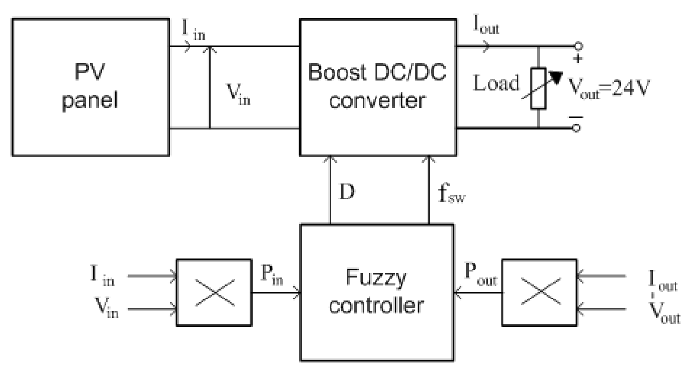

Fig. 1. Block diagram of the PV system.

Manuscript received: May 18th, 2017
Received in revised form: February 2nd, 2018

Branko Blanuša is with the Faculty of Electrical engineering, University of Banja Luka, phone: +387 51 221 824; email: branko.blanusa@etf.unibl.org

Željko Ivanović is with the Faculty of Electrical Engineering, University of Banja Luka, phone: +387 51 221 846; email: zeljko.ivanovic@ etf.unibl.org

Branko Dokić is with the Faculty of Electrical engineering, University of Banja Luka, phone: +387 51 221 820; email: branko.dokic@etf.unibl.org

Organization of paper is as follows:

Loss model of boost DC/DC converter is presented in second section. The realization of control module with the fuzzy controller is given in the third section Proposed controller is tested through computer simulation and laboratory tests. This is presented in the fifth section. Obtained results are summarized in conclusions.

II. Boost Converter Losses

In this PV system boost DC/DC converter is realized in standard topology of this converter [12] (Fig. 2.).

Energy losses in elements of the boost DC/DC converter can be divided into: conduction, dynamic and fixed losses [13]. Total energy loss P_{loss} is expressed as [14]:

$$P_{loss} = P_{cond} + P_{fixed} + W_{TOT} \cdot f_{sw} \quad (1)$$

where: P_{cond} – conduction losses, P_{fixed} – fixed losses, W_{TOT} – total energy of dynamic loss during one switching period. Product $P_{sw} = W_{TOT} \cdot f_{sw}$ is average value of dynamic power loss, which is directly proportional to switching frequency f_{sw}.

Equivalent scheme of boost converter is presented in Fig. 2. In this case MOSFET is used as basic switch component [15,16] .

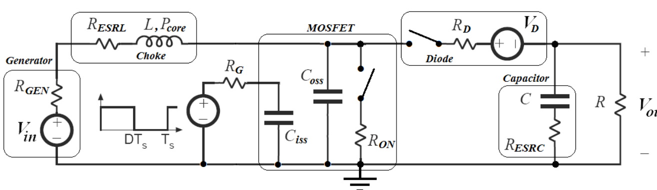

Fig. 2. Equivalent scheme of boost converter with parasitic elements [14].

Conduction losses are directly dependant on loads, and very little dependant on switching frequency. Fixed losses are dependent on neither switching frequency nor load. Semiconductor elements are major source of dynamic losses in the converter. Dynamic losses are very little dependent on power load, but directly depend on switching frequency.

So, It is possible to reduce switching losses by adjusting switching frequency to working conditions. From that reason, the focus in the analysis of power losses is on the dynamic losses.

A Dynamic losses

Dynamic losses in the converter consist of losses in inductor core, transistor and diode. Dynamic MOSFET losses are losses in gate, output capacitance and losses which occur during switch mode change [17,18]. Detailed analysis of dynamic losses in boost DC/DC converter is given in [14].

Total switching losses are equal to the sum of individual switching losses of converter elements and they can be expressed as follows:

$$P_{din} = P_{iss} + P_{Tsw} + P_{oss} + P_{Tdiode} + P_{core} \quad (2)$$

where P_{iss} is power loss in the MOSFET gate, P_{Tsw} are dynamic losses occur in transition process of switches, P_{oss} is power loss during the process of discharging the output capacitance C_{oss} of MOSFET, when MOSFET is turning on, P_{Tdiode} is transistor dynamic losses, coming from diode recovery time and P_{core} are inductor core losses due to hysteresis and eddy currents

Relations (2) shows that the switching losses in semiconductor elements are function of switching frequency.

Depending on the duty factor, load and switching frequency, the converter can operate in continuous current mode (*CCM*) or discontinuous current mode (*DCM*). In this application it works in CCM. This mode enables independent control of duty factor (D) and frequency (f_{sw}) of converter control signals.

III. Control module with fuzzy controller

The control module regulates operation of boost DC/DC converters. It is based on fuzzy controller. This controller controls duty factor and frequency of the converter control signal. In this way two important functions are realized. One is control of PV output voltage, so the MPPT algorithm is realized. Output voltage of the PV panel is changed in the dependency of the temperature and solar radiation intensity, so the maximum output power is achieved This is realized by the duty factor control. The second function of controller is efficiency improvement of the converter, what is achieved by control of switching frequency (Eq.(1) and (2)).

A. Implementation of MPPT algorithm

PV panel is current source, whose output current and voltage, and on that way the power depend from many factors, among which the most important are temperature and intensity of solar radiation.

The dependence of the PV panel output power from its voltage is nonlinear (Fig. 3).

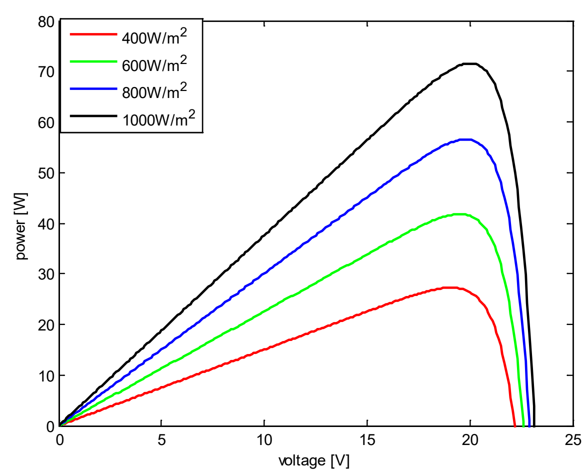

Fig. 3. Output power of PV panel in a funcion of panel voltage for different values of solar radiation

For the realization of MPPT algorithm simple fuzzy controller is used (Fig. 5.). Input in the fuzzy controller is difference of two successive samples of PV panel output power:

$$\Delta P_{in}(n) = P_{in}(n) - P_{in}(n-1), \tag{3}$$

where $P_{in}(n)$ is PV panel output power in moment nT_1, and T_1 is time interval between two successive samples of the panel output power. In this application T_1=0.1s. Output from the fuzzy controller is duty factor (ΔD). By changing of duty factor, output voltage of PV panel is changed, so it works with maximum output power.

Sign of ΔD is determined based on panel output power. If ΔP_{in} increases, sign of ΔD is retained. Otherwise, the sign is opposite.

$$sgn\left(\Delta(\mathrm{D}(n))\right) = \begin{cases} sgn\left(\Delta(\mathrm{D}(n-1))\right) & if\ P_{in}(n) \geq P_{in}(n-1) \\ -sgn\left(\Delta(\mathrm{D}(n-1))\right) & if\ P_{in}(n) < P_{in}(n-1) \end{cases} \tag{4}$$

where $\Delta D(n)$ is change of duty factor in the moment nT_1.

B. Efficiency optimization of boost converter

Algorithm for efficiency optimization of boost DC/DC converter is realized as search algorithm with fuzzy controller (Fig. 4). Boost converter efficiency for given operating conditions (input power and output voltage) can be optimized by adjusting switching frequency what is discussed in Section 2. Changing the switching frequency must not disturbed defined operating conditions of the converter, relating to maximum change of inductor current, maximum ripple of the output voltage and maximum induction in the inductor core.

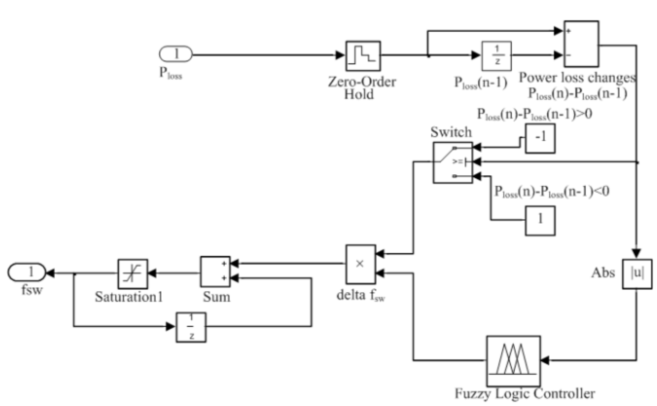

Fig. 4. Search algorithm for efficiency optimization of boost DC/DC converter

This algorithm works as follows. Power loss is calculated as difference between the input and output power of the converter

$$P_{loss}(n) = P_{in}(n) - P_{out}(n) \tag{5}$$

where $P_{loss}(n)$ is converter power loss and $P_{in}(n)$ and $P_{out}(n)$ converter input and output power respectively in the moment nT_2. In this aplication T_2=10ms. The difference of two power loss successive samples is:

$$\Delta P_{loss}(n) = P_{loss}(n) - P_{loss}(n-1). \tag{6}$$

If $\Delta P_{loss}(n)$ is negative, switching frequency f_{sw} keeps its direction. Otherwise, sign of Δf_{sw} is opposite

$$sgn\left(\Delta(f_{sw}(n))\right) = \begin{cases} sgn\left(\Delta(f_{sw}(n-1))\right) & if\ P_{loss}(n) \leq P_{loss}(n-1) \\ -sgn\left(\Delta(f_{sw}(n-1))\right) & if\ P_{loss}(n) > P_{loss}(n-1) \end{cases} \tag{7}$$

Based on $|\Delta P_{loss}(n)|$, value of $|\Delta f_{sw}(n)|$ is determined in the fuzzy controller so the new value of switching frequency in the moment nT_2 is equal to

$$f_{sw}(n) = f_{sw}(n-1) + sgn\left(\Delta f_{sw}(n)\right)|\Delta f_{sw}(n)|. \tag{8}$$

C. Implementation of fuzzy controller

Fuzzy controller has two inputs and two outputs. One input is output power of PV panels (P_{in}) and second are power losses of DC/DC converter (P_{in}-P_{out}) (Fig. 5). Outputs are duty factor (D) and switching frequency (f_{sw}). Block diagram of the realized control module is shown in Fig. 5.

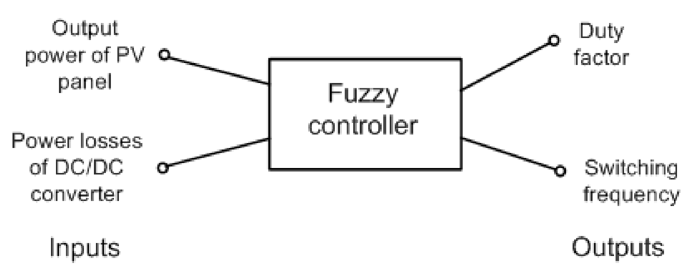

Fig. 5. Block diagram of the realized control module

Fuzzy system has total 12 rules. Set of fuzzy rules is given in Table I.

Table I.
Set of Fuzzy Rules implemented in Application

Number of fuzzy rule	Fuzzy rule
1.	If $\Delta P_{in}(n)$ is big and sgn($\Delta P_{in}(n)$) is positive then $\Delta D(n)$ is positive big
2.	If $\Delta P_{in}(n)$ is medim and sgn($\Delta P_{in}(n)$) is positive then $\Delta D(n)$ is positive medium
3.	If $\Delta P_{in}(n)$ is small and sgn($\Delta P_{in}(n)$) is positive then $\Delta D(n)$ is positive small
4.	If $\Delta P_{in}(n)$ is big and sgn($\Delta P_{in}(n)$) is negative then $\Delta D(n)$ is negative big
5.	If $\Delta P_{in}(n)$ is medium and sgn($\Delta P_{in}(n)$) is negative then $\Delta D(n)$ is negative medium
6.	If $\Delta P_{in}(n)$ is small and sgn($\Delta P_{in}(n)$) is negative then $\Delta D(n)$ is negative small
7.	If $\Delta P_{loss}(n)$ is big and sgn($\Delta P_{loss}(n)$) is positive then Δf_{SW} (n) is negative big
8.	If $\Delta P_{loss}(n)$ is medium and sgn($\Delta P_{loss}(n)$) is positive then Δf_{SW} (n) is negative medium
9.	If $\Delta P_{loss}(n)$ is small and sgn($\Delta P_{loss}(n)$) is positive then Δf_{SW} (n) is negative small
10.	If $\Delta P_{loss}(n)$ is big and sgn($\Delta P_{loss}(n)$) is negative then Δf_{SW} (n) is positive big
11.	If $\Delta P_{loss}(n)$ is medium and sgn($\Delta P_{loss}(n)$) is negative then Δf_{SW} (n) is positive medium
12.	If $\Delta P_{loss}(n)$ is small and sgn($\Delta P_{loss}(n)$) is negative then Δf_{SW} (n) is positive small

Fuzzy type is mamdani. Centroid method of defuzzification is used.

IV. Simulation Results

Simulations of discussed PV system are implemented in MATLAB-Simulink. Experimental verification of the proposed algorithm is tested on the laboratory setup.

There is a linear and step change of the parameters that have the most important impact to the characteristics of the PV panels, temperature (T) and solar radiation intensity (λ) (Fig. 6). Total duration of simulations is 10s. Simulation results which show the performance of the described MPPT algorithm are shown in the figure 7. and 8. Output voltage, output current and the output power of PV panel for the excitation from Fig. 6. are shown in Fig. 7.

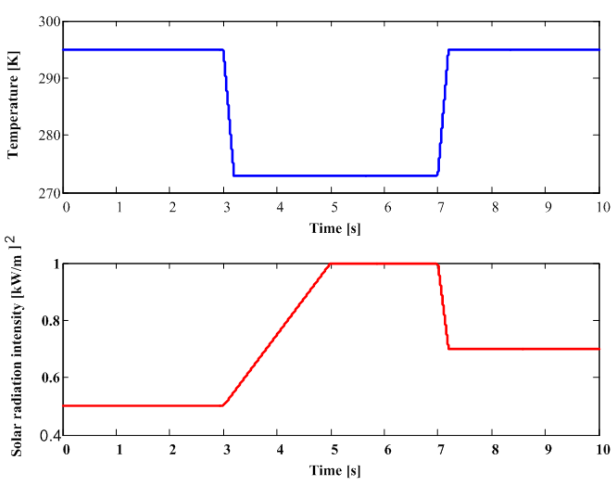

Fig. 6. Graphic of outside temperature and solar radiation intensity used in simulation.

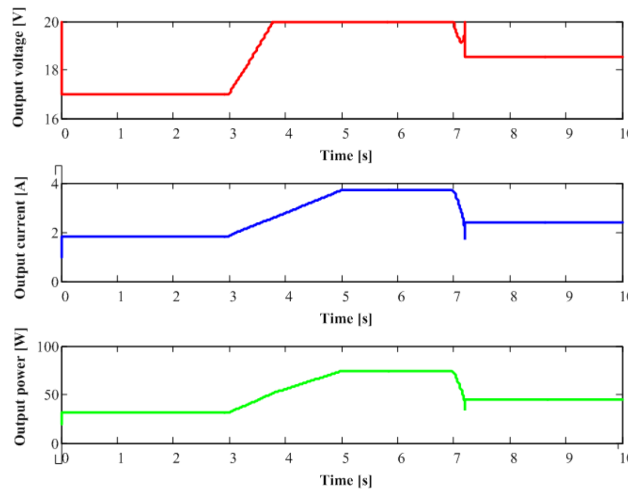

Fig. 7. Graphics of panel output voltage, output current and output power for applied MPPT algorithm based on fuzzy logic and the working conditions shown in Fig. 6.

Graphics of PV panel output power when MPPT algorithm is applied and for constant output voltage V_{po}=0.7V_{oc} (V_{oc} is open circuit voltage for the used PV panel) and specified working conditions (Fig. 6.) are shown in Fig. 8.

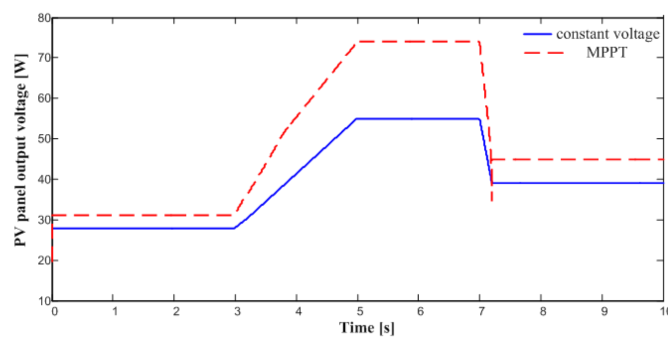

Fig. 8. Graphics of panel output power for constant voltage V_{po}=0.7V_{oc} and applied MPPT algorithm and the working conditions shown in Fig. 6.

Based on Figs. 7 and 8 It can be concluded that the proposed MPPT algorithm is fast and comparable with the fastest MPPT algorithms. Also, for a given working conditions this algorithm obtains maximum o power at the output of PV panel.

Operation of the efficiency controller in the applied boost DC/DC converter in the PV system has been tested through simulations. Obtained results are presented in Figs. 9 and 10.

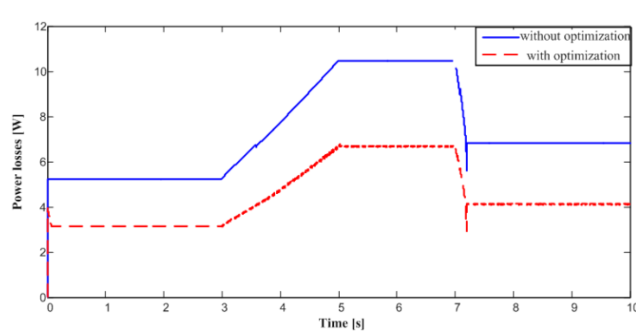

Fig. 9. Power losses for constant switching frequency and with applied efficiency optimization algorithm.

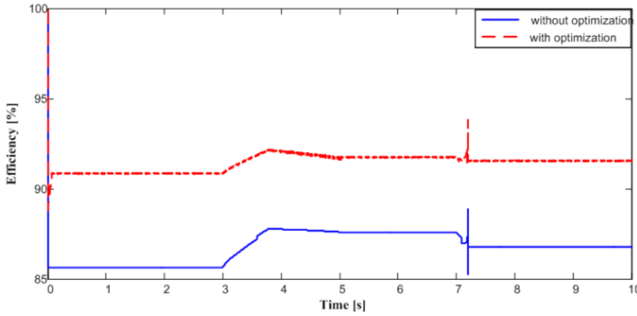

Fig. 10. Boost converter efficiency in observed PV system for constant switching frequency and with applied efficiency optimization algorithm.

Based on the results (Figs. 9 and 10), it can be concluded that the algorithm adjusts the switching frequency to the load. In this way switching losses are reduced and efficiency increased.

V. EXPERIMENTAL TESTS

Laboratory setup for experimental tests is shown in Fig. 11. It consists of:

- Autotransformer,
- Rectifier,
- Boost converter,
- MF624 acquisition card, connectors and interface board,
- Electronic load.

This laboratory setup is used to test algorithm for efficiency optimization the efficiency of the DC/DC converter. Autotransformer regulates amplitude of ac voltage on the rectifier input. This voltage is rectified and led to the input of DC/DC converter. Value of this voltage can be changed. Output of DC/DC converter has constant voltage and variable load so the output power is changeable. For input power from 10W to 80W losses and efficiency of the converter are measured when the switching frequency is constant and equal 100kHz. For the same input voltage and output power, losses and efficiency are measured when efficiency optimization algorithm with fuzzy controller is applied. Lower limit of the switching frequency is 20kHz. It is defined by the system constraints related to the maximum current ripple in the inductance and the maximum ripple of the output voltage. Also, the frequency for which the converter has the minimal losses and for given working conditions is measured. For higher input power this frequency is on the lower limit. Only, for less input power frequencies, which gives the minimum switching loss, increase above the lower limit. Results are presented in the Table II and in the Fig. 12. Applied algorithm for efficiency optimization gives a significant efficiency improvement of the converter.

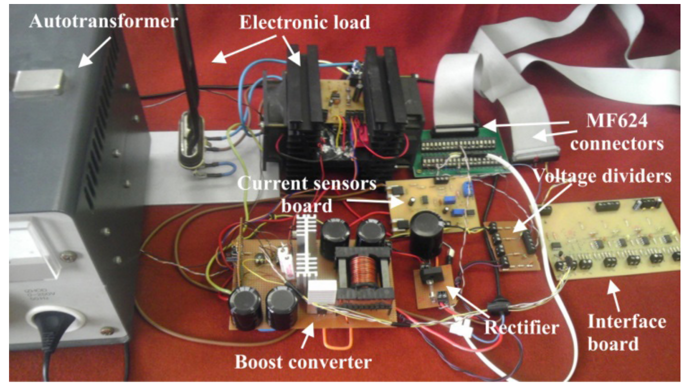

Fig. 11. Laboratory setup for experimental test.

The efficiency of the DC/DC converter in this application is somewhat lower than expected. The reason is that an available converter was used for the experimental test. This converter is not specially designed for this application.

Table II.
Power Losses and Efficiency for Constant Switching Frequency and for applied Algorithm for Efficiency Optimization

P_{in}	80	70	60	50	40	30	20	10
P_{loss} [W] const. f_{sw}	11.6	10.1	8.6	7.15	5.85	4.55	3.25	2.05
η (%) const. f_{sw}	87.3	87.4	87.5	87.5	87.2	86.75	86	83.1
P_{loss} [W] var. f_{sw}	7.3	6.25	5.25	4.33	3.52	2.72	1.95	1.27
η (%) var. f_{sw}	91.6	91.8	91.9	92	91.9	91.6	91	88.7
Optimal f_{sw} [kHz]	20	20	20	20	20	20	20.5	27

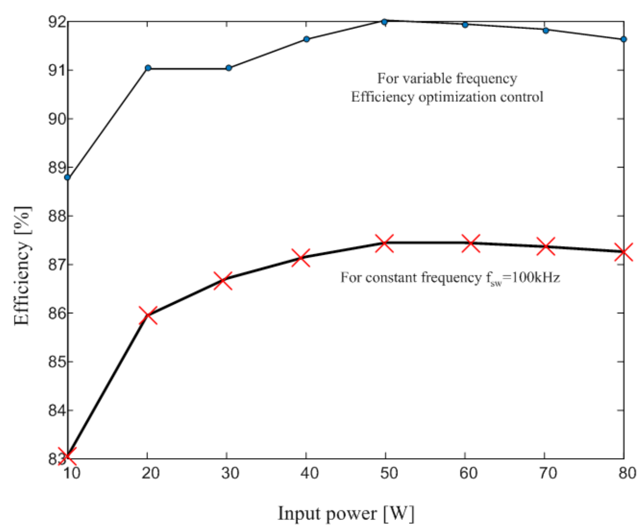

Fig. 12. Converter efficiency for constant switching frequency f=100kHz and for applied efficiency optimization algorithm.

VI. Conclusions

In this paper is presented a system with PV panel, DC/DC boost converter and a variable load.

The control system is realized with fuzzy controller which controls duty factor and a switching frequency of the converter control signal so the MPPT algorithm and efficiency optimization of boost converter are obtained. In this way two significant functions are realized with one fuzzy controller. In both cases, adaptive search techniques have been applied which provide fast convergence to the voltage which gives maximum output power from the panel and the switching frequency for which the power losses in the converter are the lowest. Applied techniques are robust and independent of the parameter changes in the PV panel model, or converter loss model. Results are confirmed through simulations and experimental tests:

1. Maximum utilization of available power from the PV panels. (Fig. 7 and 8)

2. Operation of the DC / DC converter with a switching frequency which provides maximum efficiency for a given working condition. (Figs 9, 10,12 and Table II).

Similar control concept based on fuzzy controller can be used for more complex PV systems.

References

[1] Jianpo Zhang, Tao Wang, Huijuan Ran: A Maximum Power Point Tracking Algorithm Based On Gradient Descent Method, IEEE Power & Energy Society General Meeting, PES '09, Calgary, AB, pp. 1-5, 2009.

[2] M. A. Elgendy, B. Zahawi, and D. J. Atkinson, "Assessment of perturb and observe MPPT algorithm implementation techniques for PV pumping applications," IEEE Transactions on Sustainable Energy, vol. 3, no.1, pp. 21–33, 2012.

[3] H. Kumar and R. K. Tripathi, "Simulation of variable incremental conductance method with direct control method using boost converter," in Proceedings of the Students Conference on Engineering and Systems (SCES '12), pp. 1–5 March 2012.

[4] D. Casadei, G. Grandi, and C. Rossi, "Single-phase single-stage photovoltaic generation system based on a ripple correlation control maximum power point tracking," IEEE Transactions on Energy Conversion, vol. 21, no. 2, pp. 562–568, 2006.

[5] A. Reza Reisi, M. Hassan Moradi, and S. Jamasb, "Classification and comparison of maximum power point tracking techniques for photovoltaic system: a review," Renewable and Sustainable Energy Reviews, vol. 19, pp. 433–443, 2013.

[6] R. Mahalakshmi, Aswin Kumar A. and A. Kumar, "Design of Fuzzy Logic based Maximum Power Point Tracking controller for solar array for cloudy weather conditions," *Power and Energy Systems: Towards Sustainable Energy*, pp. 1-4. 2014.

[7] Y. Soufi, M. Bechouat, S. Kahla and K. Bouallegue, "Maximum power point tracking using fuzzy logic control for photovoltaic system," *2014 International Conference on Renewable Energy Research and Application (ICRERA)*, , pp. 902-906, 2014.

[8] L. M. Elobaid, A. K. Abdelsalam, and E. E. Zakzouk, "Artificial neural network based maximum power point tracking technique for PV systems," *in Proceedings of the 38th Annual Conference on IEEE Industrial Electronics Society (IECON '12),* pp. 937–942, 2012.

[9] Adel Mellit, Soteris A.Kalogirou, MPPT-based artificial intelligence techniques for photovoltaic systems and its implementation into field programmable gate array chips: Review of current status and future perspectives Elsevier, Energy, Volume 70, Pages 1-21, 2014.

[10] Radhia Garraoui; Mouna Ben Hamed; Lassaad Sbita, "Comparison of MPPT algorithms for DC-DC boost converters based PV systems using robust control technique and artificial intelligence algorithm", *12th International Multi-Conference on Systems, Signals & Devices (SSD15)-,* pp 1-6, 2015.

[11] J. Chauhan, P. Chauhan, T. Maniar and A. Joshi, "Comparison of MPPT algorithms for DC-DC converters based photovoltaic systems," *2013 International Conference on Energy Efficient Technologies for Sustainability*, 2013, pp. 476-481., 2013

[12] Frede Blaabjerg, Zhe Chen, and Soeren Baekhoej Kjaer: Power Electronics as Efficient Interface in Dispersed Power Generation Systems, IEEE Transactions on Power Electronics, Vol. 19, No. 5, 2004.

[13] Barry, A., Robert, E., Dagan, M.: DC-DC Converter Design for Battery-Operated Systems, IEEE Power Electronics Specialists Conference, Atlanta, GA, June 18-22, 1995, pp. 103-109, 1995.

[14] Zeljko Ivanovic, Branko Blanusa, Mladen Knezic: Power Loss Model for Efficiency Improvement of Boost Converter, 23rd International Symposium on Information, Communication and Automation Technologies, pp. 1–6, 2011.

[15] Jon, K.: *Synchronous buck MOSFET loss calculation with Excel Model*, Fairchild Semiconductor Publication, 2006.

[16] Wilson, E.: *MOSFET Current Source Gate Drivers, Switching Loss Modeling and Frequency Dithering Control for MHz Switching Frequency DC-DC Converters*, PhD thesis, Queen's University Kingston, Ontario, Canada, February, 2008.

[17] Robert, E., and Dragan, M.: Fundamentals of Power Electronics, (Kluwer Academic Publishers, 912 pages, 2nd edn. 2001).

[18] Van den Bossche, A., Valchev, V. C.: Modeling Ferrite Core Losses in Power Electronics, International Reveiw of Electrical Engineering, pp. 14-22., 2006.

[19] K Benlarbi, A Mokrani, M.S. Nait-Said, A Fuzzy Global Efficiency Optimization of Photovoltaic Water Pumping System, Elesevier, Solar Energy, Volume 77, Issue 2, pp. 203-216, 2004.

[20] Ahmad Al Nabulsi, Ammar El Nosh, Abdulrahman Ahli, Mohamed Sulaiman, Rached Dhaouadi, Efficiency Optimization of 150W PV system dual axis tracking and MPPT, IEEE International Energy Conference, pp. 400-405, 2010.

Challenges and Opportunities in Applying Semantics to Improve Access Control in the Field of Internet of Things

Riste Stojanov, Vladimir Zdraveski and Dimitar Trajanov

Abstract— The increased number of IoT devices results in continuously generated massive amounts of raw data. Parts of this data are private and highly sensitive as they reflect owner's behavior, obligations, habits, and preferences. In this paper, we point out that flexible and comprehensive access control policies are "a must" in the IoT domain. The Semantic Web technologies can address many of the challenges that the IoT access control is facing with today. Therefore, we analyze the current state of the art in this area and identify the challenges and opportunities for improved access control in a semantically enriched IoT environment. Applying semantics to IoT access control opens a lot of opportunities, such as semantic inference and reasoning, easy data sharing, data trading, new approaches to authentication, security policies based on a natural language and enhances the interoperability using a common ontology.

***Index Terms* — IoT, Semantic Web, Access Control.**

Review Paper
DOI: 10.7251/ELS1721066S

I. Introduction

Internet of Things (IoT) is rapidly growing and it is expected that there will be around 30 billion devices deployed by 2020 [1]. Gartner [2] estimates that almost 60% of the available IoT devices were owned by regular people in 2014, and this percentage is expected to increase up to 65% by 2020. At this scale and impact, the need for protecting the data produced by the IoT devices is evident, since most of the IoT devices are tightly connected to their owners and can expose their privacy. The significance of the privacy is becoming crucial in the digital world, so one of the most important aspects here is the ability to control the data access, i.e. to define who can obtain the data and which part of the data is available. Indeed, this is the definition for the authorization that is well-studied discipline in the enterprise environments. However, the IoT devices and architectures impose new challenges and needs for completely new approaches in the authorization process.

In the near future, everything will be connected. Starting from our phones that access the Internet; continuing with our light bulbs, front doors, microwaves, comforters, blenders etc. One can drive some of these devices with an universal remote control, and pretty much all of them with a mobile phone or a web application. Some of the protocols overlap and support each other; whereas others are more exclusive. Currently there is no simple plug-and-play option to connect all of them and even less, to control the access to all of them and share or reuse the data they produce. The IoT expansion forecast means that there will be multiple devices that will generate a different kind of data, and owned by regular people, without technical skills [75][3]. Thus, the authorization process must provide a decentralized policy language in which each device owner can easily configure who can have access to which of his/hers devices, and what part of the data is available through the policy. The policy languages also have to overcome the heterogeneity of the devices and the data they generate, regarding precision, measurement unit and different serialization formats. It is not acceptable to have separate permissions for each device since it will be difficult to merge them for all different devices.

Unlike the traditional authorization approach, in the IoT domain, the data is not static. It is in the form of a stream that has temporal and spatial features. Therefore, the policies must support stream protection, in terms of who gets the data, as it is being generated. Moreover, the IoT has no sense without Machine-to-Machine (M2M) communication, where one device can trigger an action to another. In [5] the authors present a scenario in which an attacker causes a blackout to a smart lighting system by masquerading as a user device. Thus, it is crucial to protect the inter-device communication, so that the device corruption will be omitted.

A privacy disrupt by a "smart" baby monitor device that is controlled by an iOS application is presented in [6]. The problem appears due to the ability of each instance of the iOS application to pair with the baby monitor, even though the owner of the app is not a family member. Furthermore, once the pairing is done, the baby monitor signal can be obtained from anywhere, imposing a serious privacy leak. Thus, convenient policies should be able to limit the devices discoverability.

Manuscript received: May 18th, 2017
Received in revised form: December 26th, 2017

Riste Stojanov is with the Faculty of Computer Science and Engineering, University of Cyril and Methodius, Skopje, Macedonia (e-mail: riste.stojanov@finki.ukim.mk).

Vladimir Zdraveski is with the Faculty of Computer Science and Engineering, University of Cyril and Methodius, Skopje, Macedonia (e-mail: vladimir.zdraveski@finki.ukim.mk).

Dimitar Trajanov is with the Faculty of Computer Science and Engineering, University of Cyril and Methodius, Skopje, Macedonia (e-mail: dimitar.trajanov@finki.ukim.mk).

A smart health wearable IoT system is presented in [7] and it is pointed out that there is a need for so-called "Break the glass" or "emergency" policies so that in a case of a collapse of the wearables' owner, the private data will be available for the medical stuff. This scenario points out the indecipherable connection between the IoT systems and the surrounding context that they operate in. Thus, context- aware policies must be defined, to provide proper authorization for the IoT systems.

In this paper, we first introduce the related work in the area of IoT, in Section II, with a focus on the access control. Then, Section III provides an overview of the semantic technologies, applicable to overcome the heterogeneity problem in the IoT systems together with the state of the art approaches for Semantic Web authorization. We discuss the open challenges for access control in the IoT domain in Section IV and Section V explores the opportunities for access control implementation in the IoT domain.

II. Related Work

A. IoT Standardization

Many initiatives are focused on standardization and protocols for the IoT, including W3C, IEEE, and IETF. The authors in [8] categorize the standardization efforts in groups of application protocols, service discovery, infrastructure protocols and other influential protocols. Here we will shortly describe the most important application layer protocols.

The application protocols define the architecture and the way devices communicate with each other. The most popular protocols in this group are the IETF's Constrained Application Protocol (CoAP) [9] and the OASIS's Message Queue Telemetry Transport (MQTT) protocol [10]. The survey on application layer protocols for IoT [9] points out that REST Services and Web Sockets are commonly used protocols for consuming the data generated from the IoT devices. However, these protocols are rarely used on the devices themselves, since they use the TCP transport layer protocol and are not optimized for resource constrained environments. Furthermore, even though at the beginnings the Extensible Messaging and Presence Protocol (XMPP) was considered suitable for communication in the IoT domain due to its publish/subscribe architecture, it is now abandoned because of the overhead introduced by its XML messages. Nowadays, the most widespread protocols in the IoT domain are CoAP and MQTT because they are specially designed for resource constrained environments, and we will describe them in more details in this section.

The CoAP is is a request/response protocol based on REpresentational State Transfer (REST) architecture, which utilizes both synchronous and asynchronous responses. It reuses the HTTP methods, such as GET, POST, PUT and DELETE to define the interactions among the devices, which are identified using URIs. In order to be better suited for resource constrained sensor netwoks, this protocol removes the TCP overhead and reduces bandwidth requirements by utilizing the UDP transport layer protocol. When a secure communication is needed, the Datagram Transport Layer Security (DTLS) [11] can provide authentication, data integrity, confidentiality, automatic key management, and cryptographic algorithms.

The CoAP protocol exposes the devices as resources using the CoAP protocol URIs. The device state and observations can be accessed by using synchronous request/responses or by subscribing for asynchronous responses when new observation is available.

The device URIs are globally accessible thanks to the CoAP HTTP proxies, which handle the message translation between CoAP and HTTP.

As shown in Figure 1, the devices can communicate among each other using the CoAP protocol messages, which support the standard HTTP verbs (GET, POST, DELETE), while the communication to the outer world is translated by the CoAP proxy instance which translate the messages to HTTP and vice versa.

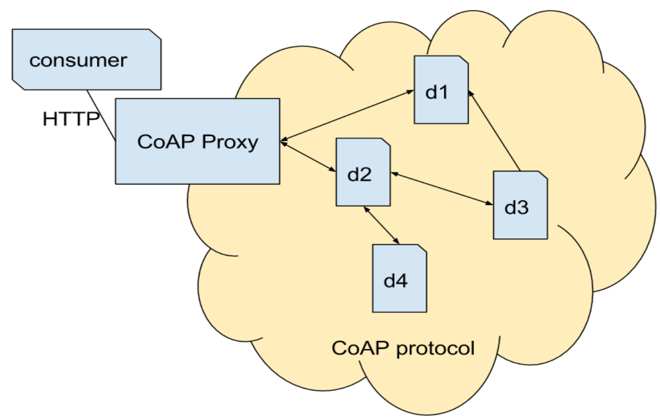

Fig. 1 CoAP Architecture

The MQTT protocol is based on the publish/subscribe mechanism, where a centralized broker distributes the messages. The broker empowers a routing in order to decide who will get the message, which makes it suitable form of M2M communication. The MQTT specification defines tree components: publisher, subscriber, and broker. The subscribers can register on the desired topics, and when the publishers send messages to those topics, the broker routes them to the subscribers. In this process, the broker is able to introduce authorization filtering, as described in [12]. Figure 2 shows the MQTT architecture where devices can publish to more than one topic on different brokers (solid lines), and subscribe for consuming the data from other topics (dashed lines). In this architecture, there is no service invocation concept, and the only way to send a command to an individual device is through a separate topic for this purpose.

The MQTT protocol is designed to use bandwidth and battery more carefully. Even though MQTT runs on TCP, it is designed to have a lower overhead compared to other TCP-based application layer protocols. MQTT does not incorporate authentication and authorization in its messages, and when a secure communication is needed, it relies on the TLS/SSL (Secure Sockets Layer), which is the same mechanism used to ensure privacy for the HTTP protocol.

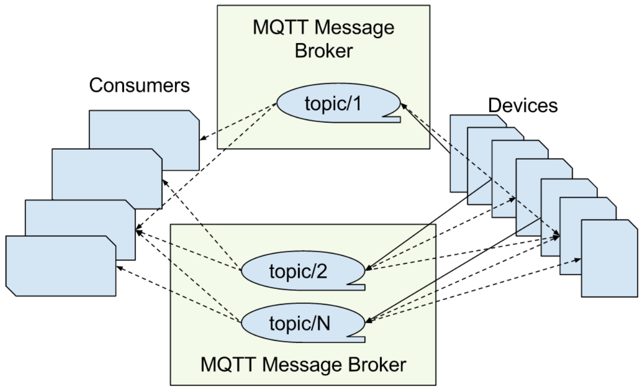

Fig. 2 MQTT Architecture

According to the study in [12], MQTT has lower delays than CoAP for low packet losses, but CoAP generates less additional traffic for reliability. However, results can vary depending on the network conditions and the QoS of the messages.

B. IoT Access Control

Most of the work in the field of IoT authorization relies on the concept of securing the communication channel with Transport Layer Security (TLS) or DTLS, through various ways of keys definition and distribution [13]-[16]. These approaches implement the authorization using shared keys for the involved devices and users in order to securely authorize their communication. They do not provide an option for filtering out the pieces of data that are prohibited in the exchange process. Thus, it can result in unwanted information sharing. This approach is partially extended by the use of OAuth protocol, where the authorization is determined based on scopes and available resources. Few implementations of this approach are available in the IoT domain, some for the MQTT protocol [15] [16], and other for the CoAP protocol [17]. The work in [18] describes how to secure the web APIs for the IoT infrastructures using the OAuth protocol for authorization.

In [19] the authors discuss that the IoT system protection should provide support for dynamic context, trust management, information flow control and actions for actuator control as well as data anonymization. In order to provide these functionalities, they implement the SecKit toolkit, which enables multiple models management, such as data, behavioral, context, and rule model, among the others. These models have a graph structure that is managed through a tree view component, which makes this process ambiguous. A model definition in their system requires a lot of technical knowledge and modeling skills. This imposes that well-trained security specialists are required to maintain the protection of the IoT systems with this toolkit. The protection is defined through an Event-Condition-Action form of rules, which provides a flexible policy definition. However, the use of the concepts from the other models makes the maintenance more difficult. This policy model is used in [12] for the MQTT application layer protocol. The authors define a policy enforcement point component, embedded in the MQTT message broker, which enforces the defined protection rules.

The IoT system authorization also depends on context in which the device operates [19]-[21]. In [21] is introduced a concept for identity-based personal location system, where the location is shared only in case of emergency. The policies proposed in this work define “a level of emergency”, which is the condition under which the policy is activated, and the location is provided. However, the authors only provide one policy example in human readable form and do not provide any further formalism. In [20] the authors describe the need for emergency policies through a use case in the health care domain, but the way of context information management and the policy format is not presented.

The data from the IoT devices can be logically represented as a stream, so there is a need for streaming data authorization. The work in [22] provides a theoretical base for streaming data protection. The authors focus on the authenticity and the completeness of the data results. In [23] and [24] the authors define a secure view, read, aggregate and join operations for stream protection with authorization filtering. The secure operations use expressions with logical and set operators, in combination with data filtering expressions, in order to define the data that should be available in the stream for the consumer. The policies are stored and processed by the Data Stream Management System. These systems require high theoretical knowledge from the system administrators in order to define the policies. There is no option for decentralized policy management, leaving the device owners without option to define how their data will be protected. This problem is solved in [25], where the data owner embeds the policies in the generated stream, and the stream processors or brokers can decide to whom to distribute the information. This work defines a policy format based on tuples and filtering, where the owner defines which roles can receive which types of the data.

The machine to machine communication protection is analyzed in [26][27] for cloud managed IoT devices with the use of an extended Information Flow Control model based on [28]. The authors point out the significance of the flow control in the IoT domain and define a formal model for their policies in the form of attaching security labels to data and processes (services or devices), and then enforce the security based on these labels. In [29] is presented a context-aware capability-based security model where the policies define a capability to each user role, and the access rights are obtained based on the available capability for the user. The context provides information that is used for capability determination.

Even though there are papers that model different aspects of the IoT authorization, such as stream protection, context awareness, information flow control and identity providing (with certificates or OAuth), there is no complete solution that provides policies that cover all these features together. None of the analyzed solutions provides overcoming the heterogeneity in the IoT domain in the process of data protection. Among these challenges, a complete policy model should also cover all the features from the traditional enterprise (API based) systems, since the IoT devices are coordinated and consumed by this kind of applications, and the policies should provide distributed and complete protection of the whole infrastructure.

III. Semantics in IoT

One of the main challenges in the IoT domain is the heterogeneity of the devices, the way they communicate among each other and how to share their data. In the IoT field, many protocols and standards are developed, and their integration in one system requires protocol mapping, which is $O(N^2)$ problem, where N is the number of mapping protocols. The data representation format is another mapping dimension, since it depends on the implemented scenario. Additionally, the sensor observations can be expressed in different measurement units, so they need to be standardized in order to be further processed and used.

All those considerations introduce a need for unified data representation, in order to enable easier device integration. The Semantic Web technologies [30] are already well-known for providing standards for machine-readable and technology agnostic description of real world concepts, together with their relations and features. They enable knowledge modeling through the graph structure, by defining it as triples: <*Subject, Property, Object*>. The Subject is a resource that represents the concept that is being defined, the Property represents an attribute or a feature of the Subject, and the Object is the value assigned to the attribute. The properties can refer to a primitive value, such as a number, a string or a date in the case of simple features, but they can also reference another resource. The RDF standard uses Internationalized Resource Identifiers (IRI) in order to represent all concepts (resources) and their properties uniquely. There are multiple serialization formats, among which the Resource Definition Framework (RDF) [31], N3 [32], turtle [33] and jsonLD [34] are most widely used. All these standards allow knowledge representation that is self-explanatory and easy to consume.

The concepts' knowledge is usually defined in ontologies that are developed using the RDF Schema (RDFS)[35] and Ontology Web Language (OWL)[36]. The RDFS standard extends the RDF specification with the ability to assign resources into classes (rdfs:in the form ofClass), defining new properties and hierarchies of classes, whereas OWL provides a functional description of the properties and classes, such as symmetric, transitive or functional properties, disjoint classes, and many other features.

One of the downsides of Semantic Web technologies' applicability in IoT domain is that it takes more space to represent the sensory information, due to the self-explanatory form of the Semantic Web knowledge. In [37], the authors examine the impact of the different semantic formats regarding CPU cycles, power consumption, and packet size. The overall conclusion from their work is that the short form of the Entity Notation is the most optimal for semantic data representation in resource-constrained environments, while the next options are the N3 format and the jsonLD format with context references. However, even though the semantically represented data introduces some performance drawbacks, it provides an abstraction for the data being transferred and provides easier combination of the raw sensory data, which leads toward smarter and better observations.

A. IoT abstraction using semantic web

One of the most influential work in the IoT domain is the Semantic Sensor Networks (SSN) ontology [38][39]. It provides abstraction of the IoT devices, represented as *ssn:Sensor*, that observe a property (*ssn:Property*) of some feature of interest (*ssn:FeatureOfInterest*). The actual devices in this ontology are represented through *ssn:SensorDevice*, and it allows to define the platform and the deployment characteristics of the device. The measured data from the sensors are represented through the *ssn:Observation* instances. Even though this ontology is widely accepted, it does not model the different units of data representation and the domain knowledge of the device context, but it allows integration with domain ontologies for this purpose [40]-[42].

According to the survey [43], the ultimate goal of the IoT devices is to provide a perception from the raw sensory data. The raw sensory data does not have any deeper meaning for the humans, but when the abstraction is added to the sensory data, it becomes more suitable for the reasoning process that is used to produce the perceptions. The Semantic Web technologies provide a solid ground for an abstraction of real world processes and knowledge, and this is already accepted in the IoT community. The authors in [40] discuss that the IoT devices generate data streams that are time and location dependent, i.e., there is a large number of row data entities with a small size and a short lifespan. Thus, the authors propose an abstraction that extends the Observation and Measurement ontology with a connection to the Units ontology [44] for unifying the results. The meta-data they define also models the location and time of occurrence of the information and provide connection to the domain dependent ontologies. Since there are different types of devices (for example moving or static), and the stream is generated from one device, most of the data entities share the common attributes, and thus overwhelming the stream with redundant information. In [40] authors propose two stream compression techniques: (1) with grouping the entities with common attributes in a sequence, where the sequence contains the common attributes, and the elements contain the dynamic measurements; and (2) each element is using stream reference to other previous data element from which it inherits the common attributes. A discussion of the resource constrained IoT devices may not be the only place for data annotation and enrichment is presented in [45]. The authors propose that the Gateway devices, that have more resources, should be the one doing the semantic annotation, in their example with the SNN Ontology.

Unlike the previously described approaches, which represent the devices as resources that generate a stream of annotated data, the work in [41][42][46]-[48] represents the devices as sensor services. This way of treatment of the devices is started by the definition of the SemSOS ontology [46] that enables service level integration. The authors in [48] introduce the term "sensor as a service" and extend the SSN and SemSOS ontologies for better description and abstraction of the sensory systems.

B. Integrating IoT devices and streams

The authors in [49] define that the devices are creating continuous streams, and in their follow up work [50] they use a semantic annotation to overcome the heterogeneous data and provide seamless integration. The integration of multiple annotated and integrated data streams can provide fused knowledge that is more valuable to the humans and closer to a perception [43][52].

When the devices are represented as a services, the integration process that leads toward perception extraction is implemented through service composition [42][47][41]. In [42] the authors propose semantic middleware for the IoT that provides composition of multiple services through their OWL-S definition [51]. OWL-S is an OWL extension for describing semantic web services, composed of the following tree main parts: (1) profile, (2) process and (3) grounding. The authors in [42] provide a tool for service discovery, composition, and execution in the IoT domain. A similar approach is presented in [47], where the authors provide business level integration with the help of a lightweight semantic model. In [41] the semantic model is additionally extended to define Quality of Service and Quality of Information, IoT service testing for device availability and other modules that enrich the IoT environment description. The authors in their work propose service composition based on probabilistic and logic filtering of the available devices, after which the results are ranked in order to produce results that outperform all previous work in respect to the precision at N measure.

The service composition and stream data fusion cannot occur if there is no way of device registration and discovery. The authors in [42] and [54] define middleware in which the different devices are semantically abstracted using an extension of the SSN ontology, and they register themselves to a centralized point through custom services. As [40] describes, the need for scalable solution for the IoT systems requires decentralized registration and discovery of the IoT devices. They propose to use device registries in each gateway and SPARQL[1] queries for discovering devices, with the use of the geospatial location information for narrowing down the gateways that should be queried. Simplified version of this discovery method is used in [55][41].

Autonomous perception and the actuation are the final refined products that should be provided by the sophisticated IoT systems. Furthermore, the actuation depends on perception, since when some perception occurs, some action should be taken. The process of obtaining a perception is an abductive process that produces inference to the best explanation in scenarios with incomplete information [52]. As explained in [52], efficient abstraction and semantic integration will significantly improve the perception inference through the process of reasoning. In [54] the authors propose aggregation and combination of semantically annotated data streams in each "virtual sensor"[2] in order to provide perceptions as an output.

C. Semantic security policies

In the field of Semantic Web, the problem of access control and authorization is a topic of interest of dozen research papers. The following text gives a survey of methods and techniques used for access control and authorization in Semantic Web, that we identified in our previous work [53].

According to [56] the policies for access control can be formally defined as

$< Subject, Resources, AccessRight >$

The *subject* represents how the policy defines the eligible users or agents, while the *resources* element defines which portion of the data is protected. Most of the current approaches define the subjects and the resources with a direct IRI referencing, or by grouping of the subjects according to their *class* or *role*. This way of policy declaring is not maintainable in large-scale scenarios, since the number of the policies will be substantially large. Thus, resource and subject grouping (using *role* properties [57]-[59], by *class* [60]-[63], or some other property [59][61]-[65]) provides more flexible way of policy definition, but it does not have the option for filtering values of the primitive properties. Data selection trough SPARQL query construct [64][66][67][58][68][69] or with rules [70] is the most flexible way for policy *subject* and *resources* definition, because they are designed for data selection with finest granularity.

Most of the related work does not consider the *context* in the policy format or only use temporal and spatial attributes for this purpose. A *context* is used in few approaches for selecting the active polices for the authorizing *subject* [71][67]. In [70] the authors define dynamic context definition with rules. As discussed in [68], a dynamic context is necessary for the protection of IoT data streams.

The access right defines whether the policy allows or denies access to the resources by the *subject* through some *action*. When only one option is available (either allow, or deny), the enforcement process is simpler, since there are no conflicts and need for their resolution. In this case, when client tries to protect the opposite scenario, the requirement must be translated with negation, which often is error prone. If both access and deny policies are available, there is no need for statement negation in the process of policy definition, but conflicts may occur, and there is a need for their resolution and detection. The access right also defines which actions will be allowed or denied by the policy. Most of the approaches available in the literature support some of the CRUD (Create, Retrieve, Update, Delete) operations for protection.

[1] SPARQL is a query language for semantic web represented resources

[2] The devices and the humans are generalized together and abstracted as virtual sensors.

The policy format is responsible for the ease of maintenance of the system security, as well as for its understandability and flexibility. The ease of maintenance is generally defined by the required time and effort for policy design and writing. Generally, the policy format and language should provide easy transformation of the user authorization requirements into policies. This means that in an ideal case there will be only one policy. Regarding understandability, the policy definition should be close to the human language, or at least managed through an interface that is intuitive. The flexibility for policy definition covers the ability to select the finest portion of the data in correlation with the context and subject, and provide them for every required action.

However, there is a trade-off between these aspects. The SPARQL and the rule-based language provide the finest granularity in terms of *resource* and *subject* selection, but they require high technical knowledge for policies definition. The flexibility, in this case, provides easier maintenance, while sacrificing the understandability.

In addition, the context definition is crucial for the policies in the IoT domain. However, for the human users, this is not very clear, since they perceive the context implicitly, and it is difficult to define it formally. For instance, it is clear for the users what is an emergency situation [75], but a formal definition for this contextual state is not a simple task.

IV. Using semantics to enhance and simplify security policies in IoT domain

The available protection systems described in Section II-B are addressing the features of the IoT devices, such as the streaming nature of their data, their inseparable connection to the context in which they operate and the need for their communication in order to provide autonomous functioning of the system. However, the work in this field does not address the heterogeneity issue introduced by the multiple device platforms, protocols and data formats. Also, the access control approaches analyzed here does not take into account that most of the users of the IoT systems will be regular people without any technical knowledge of the underlying technologies, and unaware of the security risks imposed by the smart IoT environment around them.The semantic web provides standards that overcome the heterogeneity problems in the IoT domain and enable easier integration of domain-centric abstractions, thus tracing the road toward better perceptions and more precise actuation. Even though there is a substantial work for access control in the semantic web, the aspects of managing the device discovery and information flow control are not covered. Also, even though there are work that include the streaming data in the semantic web [72][73], there are still challenges that need to be addressed regarding access control over semantic streams.

The use of semantic web can enable better IoT perception and actuation if it provides flexible, and manageable access control for the devices and their data. The people are recently becoming more aware of the value of their data and the privacy risks it imposes whether someone uses it without authorization. Thus, there is a need for unified policies that are easy to manage and understand, but flexible enough to protect the tiniest part of the data streams, together with the discoverability of their devices.

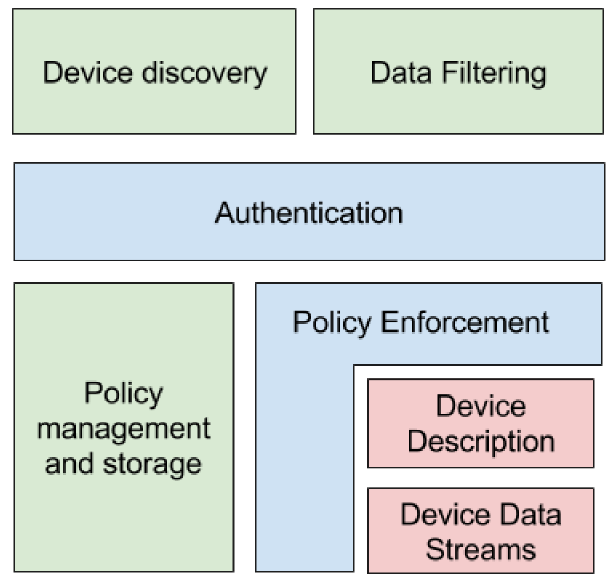

Fig. 3 Access Control modules dependency

Figure 3 provides a general overview of the components required for IoT authorization. The end-users and devices are most-often required to discover the devices and to filter the data. In order to do so, they need to authenticate their self. The policy enforcement component plays the key role in the authorization process. It uses policies, managed and stored by the policy management, and a storage module in order to define which part of the requested data should be allowed for the authenticated subject. The policy enforcement module defines the algorithms used to protect the device description in the discovery process, and to ensure that only the allowed data is returned from the devices' data streams. In this section, we will provide a further description of the components in Figure 3, with more details about the approaches that appear to be promising.

A. Device discovery

Using the semantic web abstractions and the system architecture described in [40] the data and the device discovery information are represented in the same way, enabling the same policy to protect the device discovery and data by filtering the exposure of the corresponding semantical relations. Thus, the discovery process can be achieved by adoption of the techniques for SPARQL endpoints access control. As described in Section III-C, there are multiple approaches for protection of SPARQL endpoints, but only a few of them support context awareness. The distributed nature of the IoT environment is also not considered there. The main challenges for semantically annotated device discovery protection are:

- Protection for decentralized semantics storage (multiple endpoints)
- Context support in policy definition and enforcement

B. Filtering semantic data streams

The protection of the IoT data streams defines which part of the data stream is visible to which subject. Another aspect is the protection and authorization of stream processing subscription. It can be solved by allowing subscription to everyone, but filtering everything for them when they do not have access to the data. This significantly simplifies the policies but increase the processing and complexity of the underlying system.

The main open challenges here are:

- Protecting semantically annotated data streams
- Protecting data combined from multiple streams
- Including the subject's graph in the process of policy enforcement

C. Policy storage and management

The IoT interoperability and scalability requirements impose that the access control policies should be stored in distributed manner.

A comprehensive policy model will enable easy maintenance of the policies [68]. One example is the architecture defined in [40] that allows policies to be stored and retrieved by each gateway using the SPARQL endpoints.

Since we described that there would be protected contextual data stream, the most flexible way to protect it is by defining queries that allow or deny access to some portion of the data. Since SPARQL is a formal language and most of the regular users are not familiar with it, we propose that a simple query-building interface can enable the users to use it, without sacrificing the flexibility [76]. An even better solution can be the use of guided natural language interface such as [74]. The module for Policy management from Figure 3 should provide an intuitive interface and model for policy definition. This module also provides policy storage and defines the way policies are stored and retrieved.

Additionally, incorrect policy configuration can lead to a scenario that would jeopardize the privacy and security of the IoT devices' owners. Therefore, it is important to provide design time policy validation and testing. In our previous work [67], we have designed a tool that addresses the design time policy validation through extraction of the data protected by the policy and the possible requesters that can access that data. Furthermore, we provide a design time conflict detection among the policies, together with overall unprotected data extraction. Figure 4 shows our policy management tool in action, where it extracts the protected data for a given policy and enables testing of the protected data in a given context through the generated Simulate intent form.

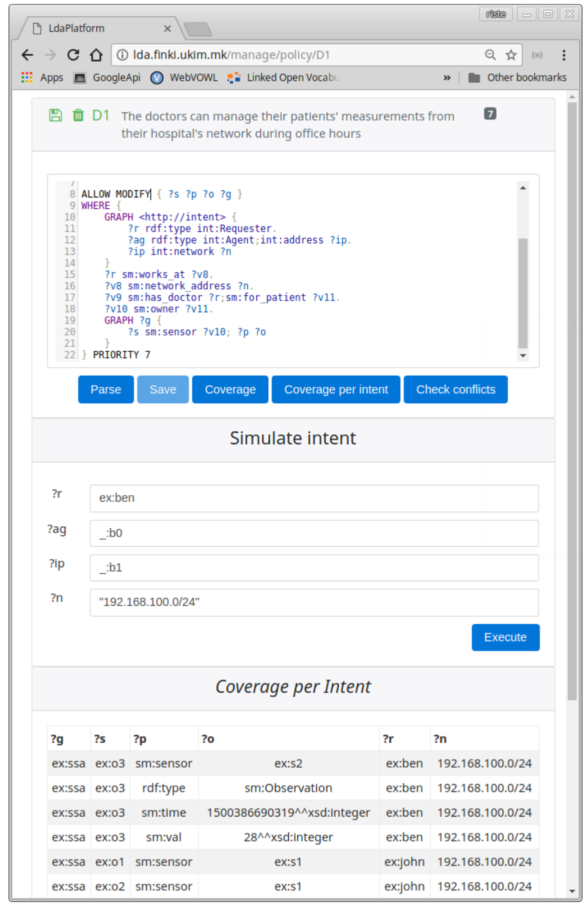

Fig. 4 Policy management console [67]

D. Authentication

In order to identify the subject that wants to consume the stream or discover the device, the WebID protocol [77][78] can be adapted for the IoT domain. This protocol transfers the subject description as a semantic graph in the headers of the HTTP message, and the protocol provides validation mechanisms using X509 public and private keys. The principle of this protocol should be reused and adapted for the IoT semantic messages. Since this protocol is based on X509 certificates for trust maintenance, the same certificates can be reused for communication protection at the transport layer, either through the TLS or DTLS protocols.

The authentication module in Figure 3 provides the information about the subject that is trying to consume the data or discover the device attributes or services. As suggested here, if an adoption of the WebID protocol is used, a semantic graph that describes the subject can be provided to the Device Discovery and Data filtering modules, which will enable them to decide about device and data availability.

E. Policy enforcement

Since the environment is provided during the device registration, data stream and the consuming subjects are represented in a semantic form, they all form the overall context graph that should be protected. The policy engine has all the required information to decide which policies are applicable and to decide which part of this graph will be allowed for the subject. In the case of stream queries, the query engine will obtain only the portion of the stream that is allowed for the *subject*, and in the discovery case, only the allowed environment and device attributes will be exposed. The main challenge here is to provide simultaneous support on streaming data and standard queries for device and service discovery, without imposing significant performance penalties.

V. Opportunities

The semantic web technologies provide an abstraction level that opens new opportunities in the IoT technology. Their main advantage is the abstraction level they introduce, which is the main enabler for integration of multiple devices and opens the way toward better perceptions.

A. Semantic inference and reasoning

The first opportunity they open is the possibility for reasoning over the semantic data. This way, new knowledge, and perceptions can be inferred, opening opportunities for exposure to previously unknown security threats. Such example is discussed in [79], where a security threat is introduced when face recognition information is combined with the location of the person.

B. Data sharing and data trading

The unified description of sensory data with Semantic Web technologies opens an opportunity for trading with sensory information, where the device holder can "sell" the data to the consumers that can benefit from it or to expose it for the common goods. The example for the later can be publishing information such as pollution values or location for city traffic optimization (the example with Google Traffic) [80]. In these cases, it is challenging to filter or aggregate only the data that is useful for the common purpose, while hiding and protecting the personal info.

C. New approaches to authentication

In most of the current approaches, the authentication process is based on private or public keys, where their distribution is a complex process, and they do not provide any additional information about who the subject is. Thus, adoption of the webID protocol for the IoT devices can simplify the process of identification of the devices and can increase the trust among them.

D. Security policies writing using natural language

One of the biggest challenges in the access control, in general, is design and implementation of comprehensive policies. In most cases, the policy languages are hard to learn and understand, due to the use of languages that increase their flexibility and maintainability. In other cases, user interfaces are designed for convenient usage but limiting the flexibility. The natural human language is the most flexible tool through which all access control constraints can be expressed and easily understood. The semantic abstractions provide an opportunity for building guided natural language interface that will significantly simplify the process of policy design and definition.

E. Interoperability enhancing using common ontology

A standardized policy model, in the form of ontology, is also required, so that the different systems can leverage the shared domain knowledge. The schema.org is currently the most popular repository, so publication of standardized policy ontology here is a real opportunity that has potential to be widely used.

VI. Conclusion

The Semantic Web provides powerful mechanisms for knowledge representation and abstraction and this paper reviewed how the IoT systems can benefit from it. The semantic annotations can be used for device registration and discovery, whereas the semantic data streams enrich the observations and bring them closer to the desired perceptions. The interoperable nature of the semantic data, together with the reasoning techniques offer data fusion and perception inference.

The unified representation of the devices' meta-data and their observations opens new access control challenges that are not modeled by neither the IoT nor the Semantic Web research community. In this paper, we identified the potential modules that should be extended in order to solve these challenges, together with the opened opportunities for access control research. Among the most important challenges are enabling context-aware policy language that offers flexibility to protect the devices' data at a various granularity levels, and providing tools that will simplify the policy maintenance in a way that will minimize the configuration mistakes.

References

[1] A. Nordrum, "Popular internet of things forecast of 50 billion devices by 2020 is outdated," IEEE Spectrum, 18 Aug. 2016.
[2] GARTNER, "Gartner says 6.4 billion connected things will be in use in 2016, up 30 percent from 2015," Online http://www.gartner.com/newsroom/id/3165317, November 10, 2015.
[3] Stojanov R., Georgiev M., Zdraveski V., Jovanovik M., and Trajanov D.. Live objects-collaborative window in the corporate documents. In New Trends in Database and Information Systems II , pages 71–81. Cham, 2015. Springer International Publishing. AISC, volume 312
[4] Trajanov D., Stojanov R., Jovanovik M., Zdraveski V., Ristoski P., Georgiev M., and Filiposka S.. Semantic sky: a platform for cloud service integration based on semantic web technologies. In Proceedings of the 8th International Conference on Semantic Systems, ISBN: 978-1-4503-1112-0, pages 109–116. ACM, 2012. DOI: 10.1145/2362499.2362515)
[5] N. Dhanjani, "Hacking lightbulbs: Security evaluation of the philips hue personal wireless lighting system," 2013.
[6] N. Dhanjani, "Reconsidering the perimeter security argument," 2013.
[7] J. Singh and J. M. Bacon, "On middleware for emerging health services,"

Journal of Internet Services and Applications, vol. 5, no. 1, pp. 1–19, 2014.

[8] A. Al-Fuqaha, M. Guizani, M. Mohammadi, M. Aledhari, and M. Ayyash, “Internet of things: A survey on enabling technologies, protocols, and applications,” IEEE Communications Surveys & Tutorials, vol. 17, no. 4, pp. 2347–2376, 2015.

[9] C. Bormann, A. P. Castellani, and Z. Shelby, “Coap: An application protocol for billions of tiny internet nodes,” IEEE Internet Computing, vol. 16, no. 2, pp. 62–67, 2012.

[10] D. Locke, “Mq telemetry transport (mqtt) v3. 1 protocol specification,” IBM developerWorks Technical Library, 2010.

[11] E. Rescorla and N. Modadugu, “Datagram transport layer security version 1.2,” 2012.

[12] R. Neisse, G. Steri, and G. Baldini, “Enforcement of security policy rules for the internet of things,” in Wireless and Mobile Computing, Networking and Communications (WiMob), 2014 IEEE 10th International Conference on, pp. 165–172, IEEE, 2014.

[13] A. Alcaide, E. Palomar, J. Montero-Castillo, and A. Ribagorda, “Anonymous authentication for privacy-preserving iot target-driven applications,” Computers & Security, vol. 37, pp. 111–123, 2013.

[14] C. Hu, J. Zhang, and Q. Wen, “An identity-based personal location system with protected privacy in iot,” in Broadband Network and Multimedia Technology (IC-BNMT), 2011 4th IEEE International Conference on, pp. 192–195, IEEE, 2011.

[15] A. Niruntasukrat, C. Issariyapat, P. Pongpaibool, K. Meesublak, P. Aiumsupucgul, and A. Panya, “Authorization mechanism for mqtt-based internet of things,” in Communications Workshops (ICC), 2016 IEEE International Conference on, pp. 290–295, IEEE, 2016.

[16] P. Fremantle and B. Aziz, “Oauthing: privacy-enhancing federation for the internet of things,” 2016.

[17] S. Cirani, M. Picone, P. Gonizzi, L. Veltri, and G. Ferrari, “Iot-oas: An oauth-based authorization service architecture for secure services in iot scenarios,” IEEE sensors journal, vol. 15, no. 2, pp. 1224–1234, 2015.

[18] P. Fremantle, J. Kopecky` , and B. Aziz, “Web api management meets the internet of things,” in European Semantic Web Conference, pp. 367–375, Springer, 2015.

[19] R. Neisse, G. Steri, I. N. Fovino, and G. Baldini, “Seckit: a model-based security toolkit for the internet of things,” Computers & Security, vol. 54, pp. 60–76, 2015.

[20] J. Singh and J. M. Bacon, “On middleware for emerging health services,” Journal of Internet Services and Applications, vol. 5, no. 1, pp. 1–19, 2014.

[21] R. M. Savola and H. Abie, “Metrics-driven security objective decomposition for an e-health application with adaptive security management,” in Proceedings of the International Workshop on Adaptive Security, p. 6, ACM, 2013.

[22] S. Papadopoulos, Y. Yang, and D. Papadias, “Cads: Continuous authentication on data streams,” in Proceedings of the 33rd international conference on Very large data bases, pp. 135–146, VLDB Endowment, 2007.

[23] B. Carminati, E. Ferrari, and K. L. Tan, “Enforcing access control over data streams,” in Proceedings of the 12th ACM symposium on Access control models and technologies, pp. 21–30, ACM, 2007.

[24] B. Carminati, E. Ferrari, J. Cao, and K. L. Tan, “A framework to enforce access control over data streams,” ACM Transactions on Information and System Security (TISSEC), vol. 13, no. 3, p. 28, 2010.

[25] R. V. Nehme, E. A. Rundensteiner, and E. Bertino, “A security punctuation framework for enforcing access control on streaming data,” in Data Engineering, 2008. ICDE 2008. IEEE 24th International Conference on, pp. 406–415, IEEE, 2008.

[26] J. Bacon, D. Eyers, T. F.-M. Pasquier, J. Singh, I. Papagiannis, and P. Pietzuch, “Information flow control for secure cloud computing,” IEEE Transactions on Network and Service Management, vol. 11, no. 1, pp. 76–89, 2014.

[27] J. Singh, T. F.-M. Pasquier, J. Bacon, and D. Eyers, “Integrating messaging middleware and information flow control,” in Cloud Engineering (IC2E), 2015 IEEE International Conference on, pp. 54–59, IEEE, 2015.

[28] D. E. Denning, “A lattice model of secure information flow,” Communications of the ACM, vol. 19, no. 5, pp. 236–243, 1976.

[29] S. Gusmeroli, S. Piccione, and D. Rotondi, “A capability-based security approach to manage access control in the internet of things,” Mathematical and Computer Modelling, vol. 58, no. 5, pp. 1189–1205, 2013.

[30] T. Berners-Lee, J. Hendler, O. Lassila, et al., “The semantic web,” Scientific american, vol. 284, no. 5, pp. 28–37, 2001.

[31] G. Klyne and J. J. Carroll, “Resource description framework (rdf): Concepts and abstract syntax,” 2006.

[32] T. Berners-Lee and D. Connoll, “Notation3 (N3): A readable RDF syntax” W3C Team Submission, W3C, mar 2011, http://www.w3.org/TeamSubmission/2011/SUBM-n3-20110328/

[33] G. Carothers and E. Prud’hommeaux, “RDF 1.1 Turtle” W3C recommendation, W3C, feb 2014. http://www.w3.org/TR/2014/REC-turtle-20140225/

[34] M. Lanthaler, M. Sporny and G. Kellogg, “JSON-LD 1.0” W3C recommendation, W3C, jan 2014. http://www.w3.org/TR/2014/REC-json-ld-20140116/.

[35] R. Guha and D. Brickley , “RDF schema 1.1” W3C recommendation, W3C, feb 2014. http://www.w3.org/TR/2014/REC-rdf-schema-20140225/.

[36] F. Harmelen and D. McGuinness , “OWL Web Ontology Language Overview” W3C recommendation, W3C, feb 2004. http://www.w3.org/TR/2004/REC-owl-features-20040210/.

[37] X. Su, J. Riekki, J. K. Nurminen, J. Nieminen, and M. Koskimies, “Adding semantics to internet of things,” Concurrency and Computation: Practice and Experience, vol. 27, no. 8, pp. 1844–1860, 2015.

[38] L. Lefort, C. Henson, K. Taylor, P. Barnaghi, M. Compton, O. Corcho, R. Garcia-Castro, J. Graybeal, A. Herzog, K. Janowicz, et al., “Semantic sensor network xg final report,” W3C Incubator Group Report, vol. 28, 2011.

[39] M. Compton, P. Barnaghi, L. Bermudez, R. Garc´ıA-Castro, O. Corcho, S. Cox, J. Graybeal, M. Hauswirth, C. Henson, A. Herzog, et al., “The ssn ontology of the w3c semantic sensor network incubator group,” Web semantics: science, services and agents on the World Wide Web, vol. 17, pp. 25–32, 2012.

[40] P. Barnaghi, W. Wang, L. Dong, and C. Wang, “A linked-data model for semantic sensor streams,” pp. 468–475, 2013.

[41] W. Wang, S. De, G. Cassar, and K. Moessner, “Knowledge representation in the internet of things: semantic modelling and its applications,” automatika, vol. 54, no. 4, pp. 388–400, 2013.

[42] Z. Song, A. A. Ca´rdenas, and R. Masuoka, “Semantic middleware for the internet of things,” pp. 1–8, 2010.

[43] P. Barnaghi, W. Wang, C. Henson, and K. Taylor, “Semantics for the internet of things: early progress and back to the future,” International Journal on Semantic Web and Information Systems (IJSWIS), vol. 8, no. 1, pp. 1–21, 2012.

[44] L. Lefort, “Ontology for Quantity Kinds and Units: units and quantities definitions”, W3 Semantic Sensor Network Incubator Activity, 2005. http://www.w3.org/2005/Incubator/ssn/ssnx/qu/qu-rec20.html

[45] F. Ganz, P. Barnaghi, F. Carrez, and K. Moessner, “Context-aware management for sensor networks,” p. 6, 2011.

[46] C. A. Henson, J. K. Pschorr, A. P. Sheth, and K. Thirunarayan, “Semsos: Semantic sensor observation service,” pp. 44–53, 2009.

[47] D. Guinard, V. Trifa, S. Karnouskos, P. Spiess, and D. Savio, “Interacting with the soa-based internet of things: Discovery, query, selection, and on-demand provisioning of web services,” IEEE transactions on Services Computing, vol. 3, no. 3, pp. 223–235, 2010.

[48] S. De, P. Barnaghi, M. Bauer, and S. Meissner, “Service modelling for the internet of things,” pp. 949–955, 2011.

[49] A. Sheth, C. Thomas, and P. Mehra, “Continuous semantics to analyze real-time data,” IEEE Internet Computing, vol. 14, no. 6, pp. 84–89, 2010.

[50] A. P. Sheth, “Computing for human experience: Semantics empowered cyber-physical, social and ubiquitous computing beyond the web,” 2011.

[51] D. Martin, M. Burstein, J. Hobbs, O. Lassila, D. McDermott, S. McIlraith, S. Narayanan, M. Paolucci, B. Parsia, T. Payne and E. Sirin, “OWL-S: Semantic markup for web services”. W3C member submission, nov 2004. http://www.w3.org/Submission/2004/SUBM-OWL-S-20041122/.

[52] C. Henson, A. Sheth, and K. Thirunarayan, "Semantic perception: Converting sensory observations to abstractions," IEEE Internet Computing, vol. 16, no. 2, pp. 26–34, 2012.
[53] Trajkova S., Stojanov R., and Trajanov D.. Semantic Web Access Control Aspects. In The 12th International Conference on Informatics and Information Technologies , pages 243-245, 2015.
[54] J.-P. Calbimonte, S. Sarni, J. Eberle, and K. Aberer, "Xgsn: An open-source semantic sensing middleware for the web of things.," pp. 51–66, 2014.
[55] S. De, T. Elsaleh, P. Barnaghi, and S. Meissner, "An internet of things platform for real-world and digital objects," Scalable Computing: Practice and Experience, vol. 13, no. 1, pp. 45–58, 2012.
[56] N. Lopes, S. Kirrane, A. Zimmermann, A. Polleres, and A. Mileo, "A Logic Programming approach for Access Control over RDF". PhD thesis, Dagstuhl, Germany, 2012.
[57] S. Kirrane, Linked data with access control. PhD thesis, 2015.
[58] S. Dietzold and S. Auer, "Access control on rdf triple stores from a semantic wiki perspective," in ESWC Workshop on Scripting for the Semantic Web, Citeseer, 2006.
[59] W. Chen and H. Stuckenschmidt, "A model-driven approach to enable access control for ontologies.," in Wirtschaftsinformatik (1), pp. 663–672, 2009.
[60] J. Hollenbach, J. Presbrey, and T. Berners-Lee, "Using rdf metadata to enable access control on the social semantic web," in Proceedings of the Workshop on Collaborative Construction, Management and Linking of Structured Knowledge (CK2009), vol. 514, 2009.
[61] S. Kirrane, A. Abdelrahman, A. Mileo and S. Decker, "Secure manipulation of linked data" in International Semantic Web Conference, pp. 248-263, 2013.
[62] H. Muhleisen, M. Kost, and J.-C. Freytag, "Swrl-based access policies for linked data," Procs of SPOT, vol. 80, 2010.
[63] S. Franzoni, P. Mazzoleni, S. Valtolina, and E. Bertino, "Towards a fine-grained access control model and mechanisms for semantic databases," in IEEE International Conference on Web Services (ICWS 2007), pp. 993–1000, IEEE, 2007.
[64] O. Sacco and J. G. Breslin, "Ppo & ppm 2.0: Extending the privacy preference framework to provide finer-grained access control for the web of data," in Proceedings of the 8th International Conference on Semantic Systems, pp. 80–87, ACM, 2012.
[65] S. Oulmakhzoune, N. Cuppens-Boulahia, F. Cuppens, and S. Morucci, "fquery: Sparql query rewriting to enforce data confidentiality," in IFIP Annual Conference on Data and Applications Security and Privacy, pp. 146–161, Springer, 2010.
[66] G. Flouris, I. Fundulaki, M. Michou, and G. Antoniou, "Controlling access to rdf graphs," in Future Internet Symposium, pp. 107–117, Springer, 2010.
[67] F. Abel, J. L. De Coi, N. Henze, A. W. Koesling, D. Krause, and D. Olmedilla, "Enabling advanced and context-dependent access control in rdf stores," in The Semantic Web, pp. 1–14, Springer, 2007.
[68] Stojanov R., Gramatikov, S., Mishkovski, I. and Trajanov, D.. Linked data authorization platform. IEEE Access, Issue 99. 2017. DOI: 10.1109/ACCESS.2017.2778029
[69] Stojanov R. and Jovanovik M.. Authorization proxy for sparql endpoints. In ICT Innovations 2017, pages 205–218, Cham, 2017. Springer International Publishing. CCIS, volume 778
[70] A. Toninelli, R. Montanari, L. Kagal, and O. Lassila, "A semantic context-aware access control framework for secure collaborations in pervasive computing environments," in International semantic web conference, pp. 473–486, Springer, 2006.
[71] L. Costabello, S. Villata, and F. Gandon, "Context-aware access control for rdf graph stores.," in ECAI, vol. 242, pp. 282–287, 2012.
[72] M. Koubarakis and K. Kyzirakos, "Modeling and querying metadata in the semantic sensor web: The model strdf and the query language stsparql," pp. 425–439, 2010.
[73] D. F. Barbieri, D. Braga, S. Ceri, E. Della Valle, and M. Grossniklaus, "C-sparql: Sparql for continuous querying," pp. 1061–1062, 2009.
[74] E. Kaufmann and A. Bernstein, "Evaluating the usability of natural language query languages and interfaces to semantic web knowledge bases," Web Semantics: Science, Services and Agents on the World Wide Web, vol. 8, no. 4, pp. 377–393, 2010.
[75] Popovski V., Kostadinov B., Stojanov R., Mishkovski I., and Trajanov D.. Web-based disaster and crisis management system. 2013.
[76] Andreevski A., Stojanov R., Jovanovik M., and Trajanov D.. Semantic web integration with sparql autocomplete. In The 12th International Conference on Informatics and Information Technologies , pages 1–4, 2015.
[77] M. Sporny, T. Inkster, H. Story, B. Harbulot, and R. Bachmann-Gmu¨ r, "Webid 1.0: Web identification and discovery," Editor's draft, W3C, 2011.
[78] H. Story, B. Harbulot, I. Jacobi, and M. Jones, "Foaf+ ssl: Restful authentication for the social web," in Proceedings of the First Workshop on Trust and Privacy on the Social and Semantic Web (SPOT2009), 2009.
[79] J. Singh, T. Pasquier, J. Bacon, H. Ko, and D. Eyers, "Twenty security considerations for cloud-supported internet of things," IEEE Internet of Things Journal, vol. 3, no. 3, pp. 269–284, 2016.
[80] Najdenov B., Petkovski G., Jovanovik M., Stojanov R., and Trajanov D.. Automated linked data generation from the transport administration domain. In Telecommunications Forum Telfor (TELFOR), 2015, pages 827–830. IEEE, 2015.

Bode Plots Revisited: a Software System for Automated Generation od Piecewise Linear Frequency Response Plots

Predrag Pejović and Amela Zeković

***Abstract*—The paper presents an algorithm for automatic generation of piecewise linear Bode plots. The algorithm is complete in the sense it covers for all posible locations of poles and zeros of transfer functions, including unstable poles and poles and zeroes at the imaginary axis. The starting transfer function is factored into a canonical form, and thirteen elementary transfer function types are defined by their canonical forms. The thirteen elementary transfer function types are shown to be derived from just five generic transfer function types, and piecewise linear Bode plots are defined and depicted for all five of the generic types. For all thirteen elementary transfer function types the nodes they introduce in the piecewise linear plots are specified, as well as the algorithms how they affect the node altitudes. Finally, a three stage algorithm that produces both the Bode plots and the exact numerically computed frequency response plots is described. The algorithm is implemented in a command line based program, illustrated in a filter example, and future work directions are indicated, aiming a graphical user interface and integration of the program to a linear system symbolic analysis software suite.**

Original Research Paper
DOI: 10.7251/ELS1721076P

I. Introduction

Electric circuit design was the first discipline where computer aided analysis became widely spread. Pioneering work of [1], expanded and updated in [2], is still a foundation stone upon which the analysis tools were built. In its basis, the approach of [1], [2] is numerical, which results in reduced efforts to build circuit and the cost of playing with their parameters. Frequency response plots, which are focused in this paper, are covered in [1], [2] within the AC analysis, and frequency response of linear or linearized circuits is readily obtained as the program output. In the control systems area, which applies Bode plots [3] in the frequency response method to design control loops [4], [5], computer aided design tools provide amplitude and phase plots through various packages, like the control package for GNU Octave [6]. Both of the approaches result in smooth numerically computed curves, corresponding to exact frequency response equations. The results are accurate, but they lack clear information needed for the design: which parameters to tune to obtain desired response?

The design oriented analysis is pioneered by R. D. Middlebrook [7], [8], where presentation of mathematically obtained data in a convenient and intuitive manner is focused in order to facilitate effective and creative system synthesis. The approach is expanded and documented in [9], [10], and [11]. Aim of this paper is to follow this path, and to formalize and completely cover the Bode plots in an algorithmic manner. Under the term "Bode plots" so called "asymptotic" plots are assumed. Although the authors agree that the terminological issues are less relevant, we must state that "asymptotic plot" is the term accurate only for some of the "elementary transfer functions", that are going to be defined formally somewhat later. In some of the cases, the linear plot is exact, and there are no asymptotes there. On the other hand, in some other cases asymptotes constitute only a part of the corresponding Bode plot for the elementary transfer function. However, in all of the cases, the resulting Bode plot is piecewise linear. Thus, under "Bode plot" we will assume piecewise linear approximation of the amplitude and phase response of a considered transfer function or an impedance. The term "transfer function" will be used both for actual transfer functions of linear systems or for the network impedances [9], [10] and admittances.

Classical circuit theory textbooks [12], [13] address Bode plots, but primarily in examples and in a rather intuitive fashion, focusing to cases frequently encountered in practice. Some other textbook examples, not to be cited here, provide either incomplete, either incomplete and overly simplified coverage of the topic. Some of the approaches are so rough to prevent estimating the phase margin, which is essential in the control loop design. Aim of this paper is to provide complete algorithmic approach to creating piecewise linear approximations of the amplitude and phase frequency response, understood under the term "Bode plots". The approach is algorithmic enough and complete only when it can be programmed and when all possible situations are covered, including unstable transfer functions, which do exist in control systems and need to be stabilized, and resonant cases with poles on the imaginary axis, resulting in infinite values in the logarithmic amplitude response plot. To program the proposed algorithm, Python programming language [14] will be used, accompanied by PyLab modules NumPy [15], SciPy [16], and matplotlib [17]. The choice is made due to high level programming capabilities of Python and its modules, with advanced data types and powerful list processing methods, additionally requiring all of the used software tools to be free software.

To summarize, aim of the paper is to provide an algorithm to generate piecewise linear frequency response Bode plots for amplitude and phase of linear systems with lumped parameters. The algorithm is required to be complete, to cover all possible locations of poles and zeros. Motivation to design such algorithm is in the design oriented analysis, to provide simplified and clear information how specific discrete values

Manuscript received: May 18th, 2017
Received in revised form: December 31st, 2017

of design variables affect the frequency response, in order to facilitate efficient frequency response shaping during the design process.

II. Problem Statement

Let us consider a transfer function $H(s)$ of a linear lumped parameter system. Its frequency response is a complex function $H(j\omega)$ for $\omega \geq 0$, representing values of $H(s)$ at the upper ray of the imaginary axis. As the system being considered is a lumped parameter one, $H(s)$ is a rational function of complex frequency s, and it can be factored and written in a canonical form

$$H(s) = K \prod_{i=1}^{k_z} \left(H_{z,i}(s)\right)^{l_{z,i}} \prod_{i=1}^{k_p} \left(H_{p,i}(s)\right)^{l_{p,i}} \tag{1}$$

where $K \in \mathbb{R}$ and k_z, k_p, $l_{z,i}$, $l_{p,i} \in \mathbb{N}$. The factorization into a canonical form is algorithmic, though the choice of the canonical form is somewhat arbitrary, and the choice criterion applied in this paper is that the canonical form should be intuitive. All aspects of the canonical form are going to be formally specified somewhat later, and at this point it is sufficient to note that the factorization is performed into a constant K, zero producing elementary transfer functions $H_{z,i}(s)$, and pole producing elementary transfer functions $H_{p,i}(s)$. Each of the zero producing and pole producing elementary functions produces either one zero or pole, either a pair of complex conjugate zeros or poles.

Aim of the algorithm is to generate piecewise linear approximations of the amplitude response

$$a(\omega) = 20 \log |H(j\omega)| \tag{2}$$

and the phase response

$$\varphi(\omega) = \arg\left(H(j\omega)\right) \tag{3}$$

For phase response plots of the elementary transfer functions we generally assume $\varphi \in [-180°, 180°)$, with some exceptions introduced by mirroring of elementary transfer functions containing pole or zero pairs. For the entire transfer function phase response plot, the curve has not been reduced to this range for the sake of its readability, though the reduction could be easily performed in a straightforward manner.

Substituting (1) into (2) in order to get the logarithmic amplitude response, the products of elementary transfer functions transform to sums of their logarithmic equivalents

$$\begin{aligned} a(\omega) = \quad & 20 \log |K| + \\ & \textstyle\sum_{i=1}^{k_z} l_{z,i}\, 20 \log |H_{z,i}(s)| + \\ & \textstyle\sum_{i=1}^{k_p} l_{p,i}\, 20 \log |H_{p,i}(s)| \end{aligned} \tag{4}$$

and substituting (1) into (3) transforms the products to sums of phase responses of elementary transfer functions

$$\begin{aligned} \varphi(\omega) = \quad & \arg(K) + \\ & \textstyle\sum_{i=1}^{k_z} l_{z,i} \arg\left(H_{z,i}(s)\right) + \\ & \textstyle\sum_{i=1}^{k_p} l_{p,i} \arg\left(H_{p,i}(s)\right). \end{aligned} \tag{5}$$

Thus, the task of creating amplitude and phase plot of the frequency response is reduced to summing frequency responses of elementary transfer functions.

The choice of elementary transfer functions is somewhat arbitrary. Some textbooks do not provide complete coverage of the complex plane by allowed places of poles and zeros, focusing to frequently encountered responses only, like restricting the attention to stable poles, or even to real axis only. In this paper, to provide complete coverage and an intuitive set of elementary transfer functions for the canonical form, the following list of elementary transfer functions is proposed:

1) constant, $H_a(s)$
2) pole at the origin, $H_b(s)$
3) zero at the origin, $H_c(s)$
4) stable real pole, $H_d(s)$
5) left half plane real zero, $H_e(s)$
6) unstable real pole, $H_f(s)$
7) right half plane real zero, $H_g(s)$
8) stable pair of poles, $H_h(s)$
9) left half plane pair of zeros, $H_i(s)$
10) unstable pair of poles, $H_j(s)$
11) right half plane pair of zeros, $H_k(s)$
12) pair of poles at the imaginary axis, $H_l(s)$
13) pair of zeros at the imaginary axis, $H_m(s)$.

The set of elementary transfer functions is not minimal. Allowing negative exponents $l_{z,i}$ and $l_{p,i}$ would reduce the set from thirteen elementary transfer functions to seven. Furthermore, allowing $\pm$ sign in some of the elementary transfer functions would further reduce the set to only five transfer functions, which is the minimal set if we exclude infinite Q-factors as an option (otherwise the set would be reduced to only four transfer functions, but numerical computation problems with infinite Q-factor values would emerge). The choice is made following the logic of the design oriented analysis, to provide an intuitive set, and to provide information how each elementary transfer function affects the frequency response.

III. Frequency Responses of Elementary Transfer Functions

In this section, thirteen elementary transfer functions will be defined by specifying their canonical forms and their frequency responses in terms of piecewise linear approximation, which sometimes really is asymptotic, but sometimes not only asymptotic. For the five "really elementary" transfer functions, the plots will be provided, while for the others appropriate sign changing relations, i.e. mirroring, will be indicated, being sufficient to provide complete description of the plots. Critical points of the elementary transfer functions, named nodes, in which line segments of the the piecewise linear curves change their directions, will be defined, as well as the effects they cause to other nodes, both in the amplitude and in the phase response.

A. Constant

The first elementary transfer function is a constant,

$$H_a(a) = K \tag{6}$$

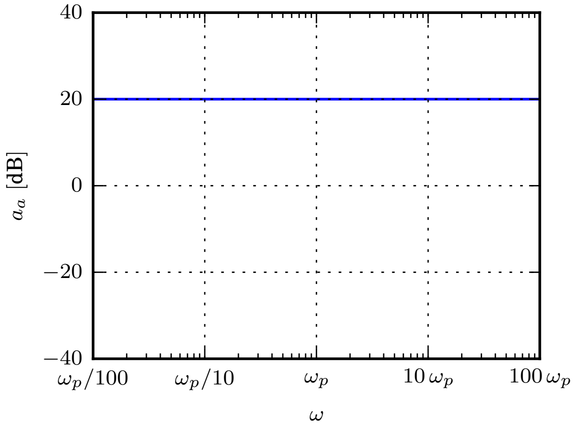

Fig. 1. $H_a(s)$, amplitude response.

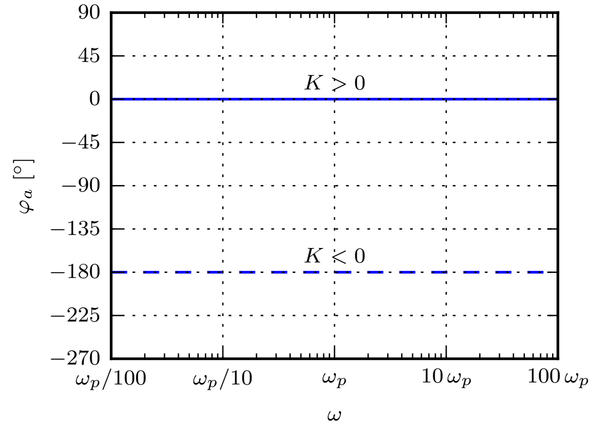

Fig. 2. $H_a(s)$, phase response.

where $K \in \mathbb{R}$. For linear lumped parameter systems the constant is necessarily real, and it could be either positive or negative. For the constant equal to zero there is not much to plot, thus this case is excluded from the analysis. Also, in the case $K = 1$ it would be assumed that this elementary transfer function is not present in the product of elementary transfer functions (1), since it would not produce any change in the frequency response plots.

Amplitude response of the constant is

$$a_a(\omega) = 20\,\log|K| \tag{7}$$

and it only shifts all of the amplitude response nodes in the vertical direction (modifies so called "altitudes"), not introducing any nodes of its own. The response is depicted in Fig. 1.

The phase response of the constant depends on its sign, and it is

$$\varphi_a(\omega) = \begin{cases} 0, & \text{for } K > 0 \\ -\pi, & \text{for } K < 0. \end{cases} \tag{8}$$

Again, new nodes are not introduced, and the phase response is either not affected, for $K > 0$, either is shifted down for $180°$ for $K < 0$ for all of the phase response nodes. The phase response for both of the cases is depicted in Fig. 2.

It is worth to mention that in this case the plot is exact, there are no approximations being introduced, there are no asymptotes.

B. Pole at the origin

A frequent case encountered in practice is to have a pole at the origin. The elementary transfer function is specified by its canonical form

$$H_b(s) = \frac{\omega_p}{s} \tag{9}$$

where $\omega_p > 0$, resulting in the amplitude response

$$a_b(\omega) = -20\,\log\frac{\omega}{\omega_p} \tag{10}$$

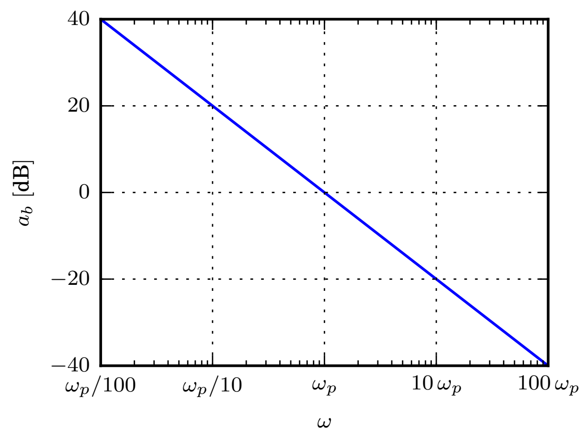

Fig. 3. $H_b(s)$, amplitude response.

and the phase response

$$\varphi_b(\omega) = -\frac{\pi}{2}. \tag{11}$$

As for the constant, in this case both the amplitude and the phase response are exact, there are no approximations being introduced. Besides, they are linear, there are no changes in the piecewise linear curve direction, and new nodes do not have to be introduced. The amplitude response of this elementary transfer function is depicted in Fig. 3, while the phase response is depicted in Fig. 4.

For the amplitude response, this elementary transfer function increases the level of the amplitude response at each node for $20\,\text{dB}\,\log\frac{\omega_p}{\omega}$, where ω is the angular frequency of the node. The overall phase response is affected by this elementary transfer function such that for all nodes the phase is reduced by $90°$.

In this case, the piecewise linear plot, which happened to be linear, is exact, approximations are not required.

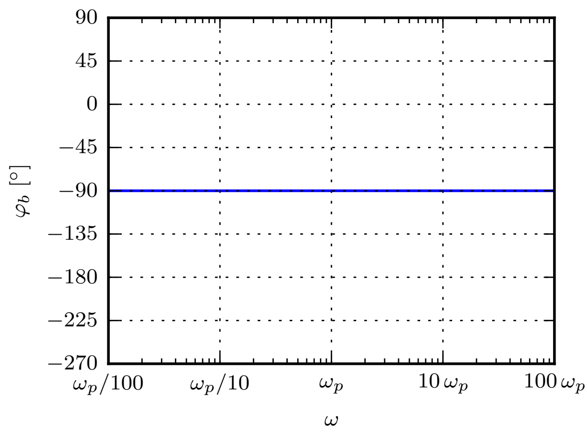

Fig. 4. $H_b(s)$, phase response.

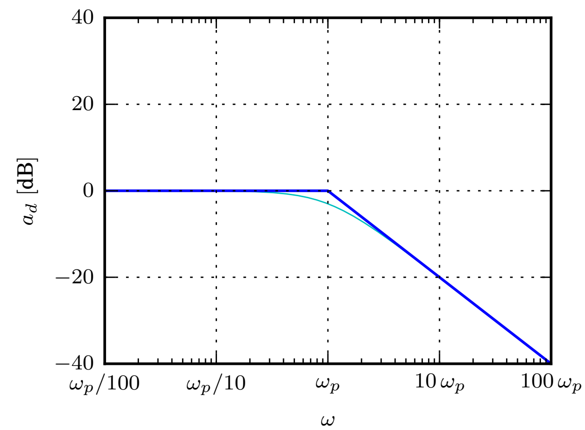

Fig. 5. $H_d(s)$, amplitude response.

C. Zero at the origin

The next elementary transfer function is zero at the origin, specified by its canonical form

$$H_c(s) = \frac{s}{\omega_z} \tag{12}$$

where $\omega_z > 0$, which results in the amplitude response

$$a_c(\omega) = 20\,\log\frac{\omega}{\omega_z} \tag{13}$$

and the phase response

$$\varphi_c(\omega) = \frac{\pi}{2}. \tag{14}$$

Again, the piecewise linear plot is exact and purely linear. This elementary transfer function does not introduce any nodes. To implement automatic adjustment of node amplitudes and phases, it is worth to note that $a_c(\omega) = -a_b(\omega)$ and $\varphi_c(\omega) = -\varphi_b(\omega)$ assuming parameter ω_z of $H_c(s)$ having value equal to the value of the parameter ω_p of $H_b(s)$.

D. Stable real pole

The next elementary transfer function to be considers is the stable real pole, i.e. the pole in the left half plane. This elementary transfer function is characterized by

$$H_d(s) = \frac{1}{1+\frac{s}{\omega_p}} \tag{15}$$

where $\omega_p > 0$, which results in the amplitude response of

$$a_d(\omega) = -10\,\log\left(1+\left(\frac{\omega}{\omega_p}\right)^2\right) \tag{16}$$

and the phase response of

$$\varphi_d(\omega) = -\arctan\left(\frac{\omega}{\omega_p}\right). \tag{17}$$

In this case, the piecewise linear representation is approximate. For the amplitude response, it is entirely asymptotic, as depicted in Fig. 5. For the phase response, the piecewise linear representation is asymptotic in two out of three segments, as depicted in Fig. 6, while the third segment is somewhat arbitrary, to connect the parallel asymptotes, as detailed in [9], connecting the asymptotes by a line segment from $\omega_p/10$ to $10\,\omega_p$.

Regarding the nodes, the amplitude response adds a node at ω_p. Before that frequency, for $\omega \le \omega_p$, this elementary transfer function does not affect the overall amplitude response. After that frequency, for $\omega_p < \omega$, the nodes are shifted down for $20\,\text{dB}\,\log\frac{\omega}{\omega_p}$.

The phase response adds nodes at $\omega_p/10$ and at $10\,\omega_p$. For $\omega \le \omega_p/10$, the overall phase response is not affected. For $\omega_p/10 \le \omega < 10\,\omega_p$, the overall phase response is affected such that the phase is reduced by $45^\circ\,\log\frac{10\,\omega}{\omega_p}$. For $10\,\omega_p \le \omega$, the overall phase response is affected such that the phase is shifted down for 90°. Contributions of this elementary transfer function to overall amplitude and phase response are depicted in Figs. 5 and 6.

The piecewise linear representation of this elementary transfer function is approximate. As detailed in [9], the maximum of the error caused by the approximation is $3\,\text{dB}$ for the amplitude response, at ω_p, while the maximum of the error for the phase response is about 6°. In Figs. 5 and 6 the exact responses are plotted in thin lines.

approximate

E. Left half plane real zero

Opposite type of the elementary transfer function to the stable real pole is the left half plane real zero, caused by a zero of the transfer function (1) at $s = -\omega_z$. For ω_p of $H_d(s)$ being equal to ω_z of $H_e(s)$, the two elementary transfer functions would cancel out, thus they are the opposites. The elementary transfer function $H_e(s)$ in its canonical form is

$$H_e(s) = 1 + \frac{s}{\omega_z} \tag{18}$$

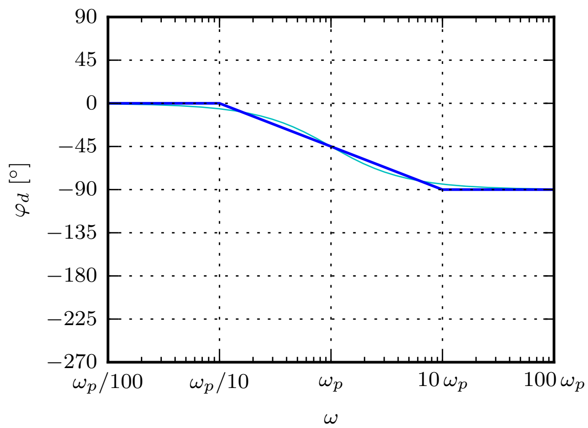

Fig. 6. $H_d(s)$, phase response.

where $\omega_z > 0$, resulting in the amplitude response of

$$a_e(\omega) = 10\,\log\left(1 + \left(\frac{\omega}{\omega_z}\right)^2\right) \tag{19}$$

and the phase response of

$$\varphi_e(\omega) = \arctan\left(\frac{\omega}{\omega_z}\right). \tag{20}$$

Relations of this elementary transfer function responses to the responses of $H_d(s)$ are given by $a_e(\omega) = -a_d(\omega)$ and $\varphi_e(\omega) = -\varphi_d(\omega)$, for the parameter values $\omega_z = \omega_p$. Thus, these responses need not to be plotted here, they are just mirrored responses shown in Figs. 5 and 6. This elementary transfer function adds nodes at ω_z for the amplitude response and $\omega_z/10$ and $10\,\omega_z$ for the phase response. The responses are approximate in the same manner as the responses of $H_d(s)$.

F. Unstable real pole

This elementary transfer function is frequently omitted from consideration in popular textbooks, since stable open loop systems are focused. However, such response is possible in real systems, an example of such is the peak limiting current mode controlled buck converter in the discontinuous conduction mode for the steady state duty ratio of $D > \frac{1}{2}$. The canonical form of the elementary transfer function is

$$H_f(s) = \frac{1}{1 - \frac{s}{\omega_p}} \tag{21}$$

where $\omega_p > 0$, resulting in the amplitude response of

$$a_f(\omega) = -10\,\log\left(1 + \left(\frac{\omega}{\omega_p}\right)^2\right) \tag{22}$$

and the phase response of

$$\varphi_f(\omega) = \arctan\left(\frac{\omega}{\omega_p}\right). \tag{23}$$

Relation of $H_f(s)$ to $H_d(s)$ is $a_f(\omega) = a_d(\omega)$ and $\varphi_f(\omega) = -\varphi_d(\omega)$, meaning that the amplitude responses are equal, while the phase responses are mirrored. The elementary transfer function $H_f(s)$ introduces the same critical points as $H_d(s)$, and introduces the same level of approximation.

G. Right half plane real zero

A complement of unstable real pole is the left half plane real zero elementary transfer function, specified by the transfer function canonical form

$$H_g(s) = 1 - \frac{s}{\omega_z} \tag{24}$$

where $\omega_z > 0$, which results in the amplitude response of

$$a_g(\omega) = 10\,\log\left(1 + \left(\frac{\omega}{\omega_z}\right)^2\right) \tag{25}$$

and the phase response of

$$\varphi_g(\omega) = -\arctan\left(\frac{\omega}{\omega_z}\right). \tag{26}$$

For parameter values $\omega_z = \omega_p$, relation of the responses of $H_g(s)$ to the responses of $H_d(s)$ are given by $a_g(\omega) = -a_d(\omega)$, $\varphi_g(\omega) = \varphi_d(\omega)$. The elementary transfer function adds the same nodes as $H_d(s)$, and introduces the same level of approximation.

Elementary transfer functions $H_d(s)$, $H_e(s)$, $H_f(s)$, and $H_g(s)$ form a group of real axis excluding origin poles and zeros, sharing the same nodes and similar amplitude and phase responses. They could have been treated as a single response type, but in this approach they are treated as four distinct elementary transfer functions to underline different effects they cause to the frequency response.

H. Stable pair of poles

The next group containing four elementary transfer functions starts with the pair of complex conjugate poles, specified by a canonical form of the elementary transfer function

$$H_h(s) = \frac{1}{1 + \frac{s}{Q_p\,\omega_p} + \frac{s^2}{\omega_p^2}} \tag{27}$$

where $\omega_p > 0$ and $Q_p > 0$. The assumption that the elementary transfer function represents a complex conjugate pair of poles results in $Q_p > \frac{1}{2}$. This elementary transfer function results in the amplitude response

$$a_h(\omega) = -10\,\log\left(\left(1 - \left(\frac{\omega}{\omega_p}\right)^2\right)^2 + \left(\frac{\omega}{Q_p\,\omega_p}\right)^2\right) \tag{28}$$

and the phase response

$$\varphi_h(\omega) = -\arctan\left(\frac{1}{Q_p}\,\frac{\omega\,\omega_p}{\omega_p^2 - \omega^2}\right). \tag{29}$$

The responses are dependent on two parameters, ω_p and Q_p, resulting in somewhat more complex piecewise linear plotting rules. The rules are detailed in [9], and the resulting plots are depicted in Figs. 7 and 9.

For the amplitude response, the elementary transfer function introduces a node at ω_p. For $\omega \leq \omega_p$, the overall amplitude

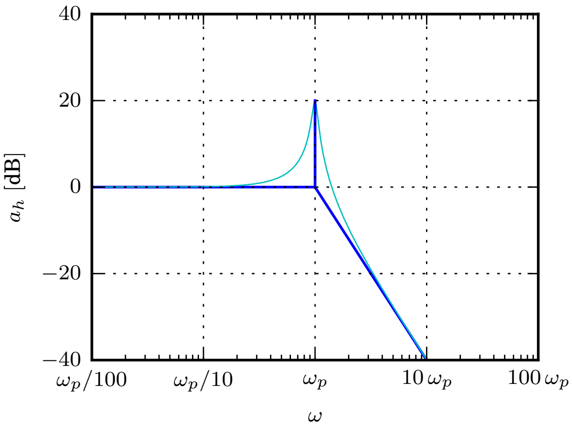

Fig. 7. $H_h(s)$, $Q_p = 10$, amplitude response.

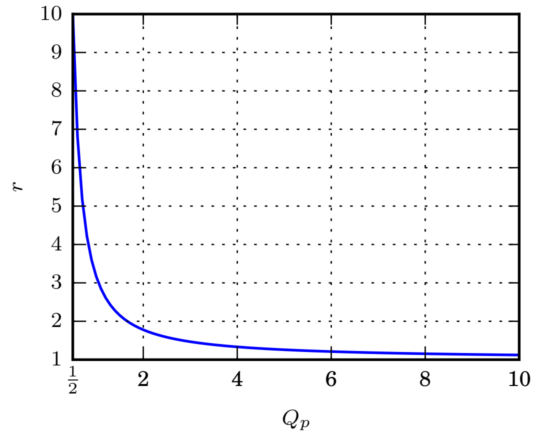

Fig. 8. Dependence of r on Q_p.

response is not affected. For $\omega_p < \omega$, the amplitude response is reduced by $40\,\text{dB}\,\log\frac{\omega}{\omega_p}$. Besides that, the amplitude response includes an overshoot which at $\omega = \omega_p$ equals $q_p = 20\,\log Q_p$. In the piecewise linear representation, this overshoot is represented by a vertical line segment at ω_p of q_p in height, as depicted in Fig. 7.

For the phase response, let us introduce the transition zone parameter according to [9] first, as

$$r = 10^{\frac{1}{2\,Q_p}}. \tag{30}$$

This parameter is dependent on the Q-factor Q_p and specifies the nodes and thus the phase response transition zone. The dependence of r on Q_p is depicted in Fig. 8, and it sharply decreases from $r = 10$ for $Q_p = \frac{1}{2}$ to its asymptotic value of 1 as Q_p increases. The nodes are introduced at ω_p/r and at $r\,\omega_p$. For $\omega \leq \omega_p/r$ the overall phase response is not affected. For $\omega_p/r < \omega \leq r\,\omega_p$ the phase response is reduced by $\frac{90^\circ}{\log r}\,\log\frac{r\,\omega}{\omega_p}$. For $r\,\omega_p < \omega$ the overall phase response is reduced by 180°. The phase response of this elementary transfer function is shown in Fig. 9.

For $Q_p = \frac{1}{2}$, the complex conjugate pair reduces to a repeated pole at the real axis, and both the amplitude and the phase response of the piecewise linear Bode plot are equal for both of the approaches, providing consistency of the approximate analysis.

As already indicated, both the amplitude response and the phase response are approximate, and the error is dependent on Q_p. In Figs. 7 and 9 the exact responses are plotted in thin lines.

I. Left half plane pair of zeros

As already indicated, the elementary transfer function $H_h(s)$ is a basis for a group of four elementary transfer functions, like $H_d(s)$ is the basis for the group that also involves $H_e(s)$, $H_f(s)$, and $H_g(s)$. The first of the elementary transfer functions based upon $H_h(s)$ is its opposite

$$H_i(s) = 1 + \frac{s}{Q_z\,\omega_z} + \frac{s^2}{\omega_z^2} \tag{31}$$

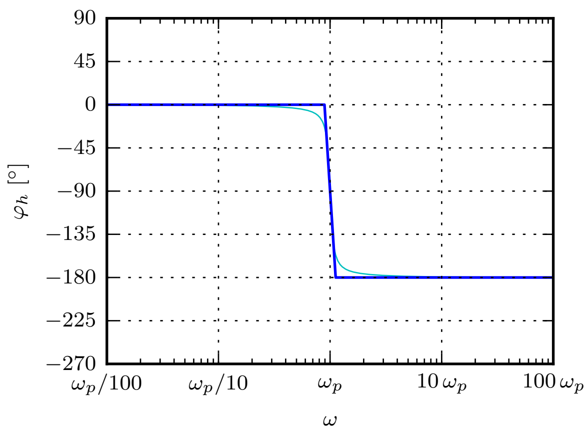

Fig. 9. $H_h(s)$, $Q_p = 10$, phase response.

where $\omega_z > 0$ and $Q_z > 0$, resulting in the amplitude response

$$a_i(\omega) = 10\,\log\left(\left(1 - \left(\frac{\omega}{\omega_z}\right)^2\right)^2 + \left(\frac{\omega}{Q_z\,\omega_z}\right)^2\right) \tag{32}$$

and the phase response

$$\varphi_i(\omega) = \arctan\left(\frac{1}{Q_z}\,\frac{\omega\,\omega_z}{\omega_z^2 - \omega^2}\right). \tag{33}$$

Assuming the parameter values $\omega_z = \omega_p$ and $Q_z = Q_p$, relation of the responses of $H_i(s)$ to the responses of $H_h(s)$ are $a_i(\omega) = -a_h(\omega)$, and $\varphi_i(\omega) = -\varphi_h(\omega)$. The nodes are the same as for $H_h(s)$, and both the amplitude and the phase responses are mirrored.

J. Unstable pair of poles

The next in this group of elementary transfer functions is caused by an unstable pair of complex conjugate poles, specified by its canonical form

$$H_j(s) = \frac{1}{1 - \frac{s}{Q_p\,\omega_p} + \frac{s^2}{\omega_p^2}} \tag{34}$$

where $\omega_p > 0$ and $Q_p > 0$. This elementary transfer function results in the amplitude response

$$a_j(\omega) = -10\,\log\left(\left(1-\left(\tfrac{\omega}{\omega_p}\right)^2\right)^2+\left(\tfrac{\omega}{Q_p\,\omega_p}\right)^2\right) \quad (35)$$

and the phase response

$$\varphi_j(\omega) = \arctan\left(\frac{1}{Q_p}\,\frac{\omega\,\omega_p}{\omega_p^2-\omega^2}\right). \quad (36)$$

The responses are related to the responses of $H_h(s)$ by $a_j(\omega) = a_h(\omega)$ and $\varphi_j(\omega) = -\varphi_h(\omega)$, sharing the same nodes, the same amplitude responses, and mirrored phase responses.

K. Right half plane pair of zeros

The last in this group of elementary transfer functions is specified by its canonical form

$$H_k(s) = 1-\frac{s}{Q_z\,\omega_z}+\frac{s^2}{\omega_z^2} \quad (37)$$

where $\omega_z > 0$ and $Q_z > 0$, and results in the amplitude response of

$$a_k(\omega) = 10\,\log\left(\left(1-\left(\tfrac{\omega}{\omega_z}\right)^2\right)^2+\left(\tfrac{\omega}{Q_z\,\omega_z}\right)^2\right) \quad (38)$$

and the phase response of

$$\varphi_k(\omega) = -\arctan\left(\frac{1}{Q_z}\,\frac{\omega\,\omega_z}{\omega_z^2-\omega^2}\right). \quad (39)$$

Assuming parameter values $\omega_z = \omega_p$ and $Q_z = Q_p$, the responses are related to the responses of $H_h(s)$ such that $a_k(\omega) = -a_h(\omega)$, $\varphi_k(\omega) = \varphi_h(\omega)$. The nodes are the same as for $H_h(s)$, the amplitude response is mirrored, while the phase responses are the same.

L. Pair of poles at the imaginary axis

The last group of elementary transfer functions considers two elementary transfer functions: pair of poles at the imaginary axis and pair of zeros at the imaginary axis. This group of elementary transfer functions had to be separated to avoid numerical problems that would be caused by the infinite value of corresponding Q-factors.

Pair of poles at the imaginary axis is specified by the elementary transfer function in its canonical form

$$H_l(s) = \frac{1}{1+\frac{s^2}{\omega_p^2}} \quad (40)$$

where $\omega_p > 0$, resulting in the amplitude response of

$$a_l(\omega) = -10\,\log\left(1-\left(\tfrac{\omega}{\omega_p}\right)^2\right)^2 \quad (41)$$

and the phase response of

$$\varphi_l(\omega) = \begin{cases} 0, & \omega < \omega_p \\ -\pi, & \omega_p < \omega. \end{cases} \quad (42)$$

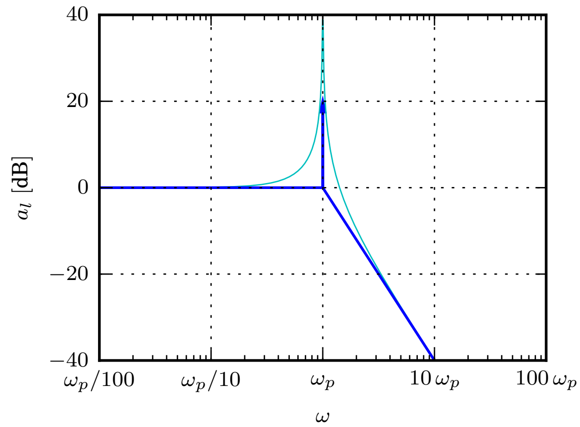

Fig. 10. $H_l(s)$, amplitude response.

The amplitude response is specific in the sense it contains a singularity for a finite value of ω, for $\omega = \omega_p$, which is the node for the amplitude response. The piecewise linear representation of the amplitude response is depicted in Fig. 10, and it contains two asymptotes, for $\omega \to 0$ and for $\omega \to \infty$. The asymptotes intersect at ω_p, which is the node. The piecewise linear representation of this elementary transfer function does not affect the overall amplitude response for $\omega \le \omega_p$, while for $\omega_p < \omega$ it decreases the amplitude nodes for $40\,\log\frac{\omega}{\omega_p}$. At $\omega = \omega_p$ the elementary transfer function has a pole, resulting in the amplitude response singularity, which is indicated by an arrow in Fig. 10, since there is no other way to indicate infinity in the response. The exact amplitude response is indicated by the thin line. The piecewise linear representation is approximate, having significant error at some values of ω.

Contrary to the piecewise linear representation of the amplitude response, the piecewise linear representation of the phase response is exact, as depicted in Fig. 11. For $\omega \le \omega_p$ the overall phase response is not affected by this elementary transfer function. For $\omega_p < \omega$, the overall phase response is affected such the phases for all nodes are decreased for $180°$. This response is somewhat peculiar in the sense it is discontinuous. This requires two nodes for the phase response at the same frequency, ω_p. At the first of these nodes, in terms of the node index, not frequency, the phase response is not affected; at the second, it is reduced by $180°$.

M. Pair of zeros at the imaginary axis

The last of the elementary transfer functions considers the pair of zeros at the imaginary axis, represented by the elementary transfer function canonical form

$$H_m(s) = 1+\frac{s^2}{\omega_z^2} \quad (43)$$

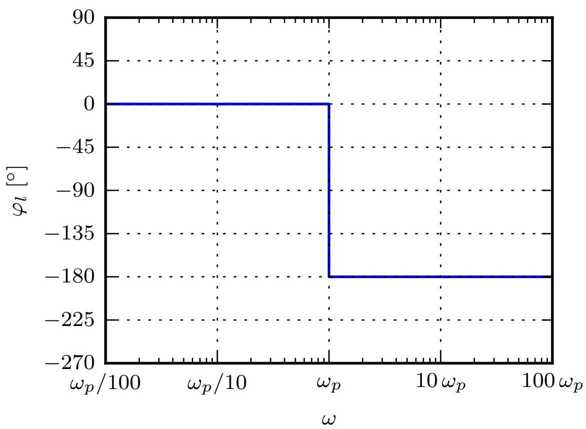

Fig. 11. $H_l(s)$, phase response.

where $\omega_z > 0$, and it is the opposite of $H_l(s)$, having the amplitude response

$$a_m(\omega) = 10\,\log\left(1-\left(\frac{\omega}{\omega_z}\right)^2\right)^2 \tag{44}$$

and the phase response

$$\varphi_m(\omega) = \left\{\begin{array}{ll} 0, & \omega < \omega_z \\ -\pi, & \omega_z < \omega. \end{array}\right. \tag{45}$$

Assuming the parameter value $\omega_z = \omega_p$, relation of the frequency responses of $H_m(s)$ to the responses of $H_l(s)$ are $a_m(\omega) = -a_l(\omega)$ and $\varphi_m(\omega) = \varphi_l(\omega)$. The responses of the two elementary transfer functions share the same nodes. The amplitude response is mirrored, while the phase response is the same. Actually, it is mirrored, but restriction that the phase response of elementary transfer functions is within $[-180°, 180°)$ reduced the phase response to be the same, by shifting down for $360°$ at $\omega > \omega_p$.

N. A constraint

After the elementary transfer functions have been defined, in order to provide unique factorization let us introduce a constraint here: in the factorization of (1) only one of the elementary transfer functions $H_a(s)$, $H_b(s)$, and $H_c(s)$ is present.

IV. The Algorithm for Creating the Bode Plots

The algorithm described in this paper starts with the transfer function factored into canonical form of (1). To achieve the factorization, either exact factorization may be applied using computer algebra tools, like Maxima [18] or SymPy [19], either approximate methods described in [9], [10], [11] might be used. This task is planned to be automated in near future. The factored transfer function of (1) is specified in an input file, where a line corresponds to an elementary transfer function. The elementary transfer functions are specified by several fields. The first field specifies the type of elementary transfer function, and it is followed by one or two fields that specify the elementary transfer function parameters: K for $H_a(s)$, ω_p or ω_z for $H_b(s)$ to $H_g(s)$, and for $H_l(s)$ and $H_m(s)$, while for $H_h(s)$ to $H_k(s)$ ω_p or ω_z and Q_p or Q_z are specified. The next field contains exponent of the elementary transfer function, labeled by $l_{p,i}$ and by $l_{z,i}$ in (1). A frequent value of this parameter is 1. The following field contains a label assigned to the elementary transfer function. Finally, the last two fields contain flags indicating whether the final diagram will contain Bode plot of the elementary transfer function besides the plot of (1) and whether the final plot will contain exact plot of the elementary transfer function.

Besides the lines that specify elementary transfer functions, the input file contains two additional lines to specify values of ω_{min} and ω_{max} that define the frequency range in which the frequency response is plotted. The final line specifies flags whether the Bode plot and/or the exact plot are included in the final diagram. As a matter of fact, the final diagram needs not to be generated at all: the program might be run just to generate and save the data that the user might use later to create his/her own diagrams.

A. Parsing

The first part of the program is a parser, which is considered as an auxiliary part, not the part of the algorithm itself. The parser initialized the data structures and goes through the input file, firstly trying to parse the lines that specify elementary transfer functions. This step involves identifying elementary transfer function type and checking the parameter values such that all ω_p and ω_z values are positive floats, that Q_p and Q_z values are floats greater that $\frac{1}{2}$, and that exponents are positive integers. If an elementary function specifying line does not pass a parsing requirements, the program quits and the user is informed about the problem. Similar procedure applies for the final three lines that specify ω_{min}, ω_{max}, and the diagram plotting flags. Also there are some auxiliary topics: following the conventions set in [1], the first line of the file contains the transfer function name; comment lines might be added and they are indicated by starting the comment line with #, as in Python and some other programming languages.

The data structure provided by the parser contain lists of parameter values, including the labels and the flags, for each of the elementary transfer function types, as well as the display values of ω_{min} and ω_{max}, and the diagram plotting flags.

B. Setting the nodes

The first pass of the algorithm sets the nodes for the amplitude and the phase response and the frequency ranges both for computing the plot and for displaying the plot. The display range is always a subset of the computing range. To achieve this goal, the program initializes lists of amplitude nodes and phase nodes as empty lists, and passing through the data structure adds the nodes as specified by the elementary transfer function descriptions given in Section III.

After the lists of nodes required by the elementary transfer functions is generated, the task is to determine frequency range for computing the plot. For the union of the node frequencies for the amplitude plot and the phase plot the minimum and the maximum are determined. To avoid exceptions, it is worth to mention that in the case the only elementary transfer function in (1) is either $H_a(s)$, $H_b(s)$, or $H_c(s)$, the initial set of node frequencies, before adding the border frequencies, is an empty set; this should be handled by the program smoothly, just by skipping the search and by taking the display border frequencies as the computational border frequencies. Possible candidates for the computing range limits ω_{min} and ω_{max} are determined as one tenth of the minimal node frequency and ten times the maximal node frequency. If the display frequency range is wider than the range required by the nodes, the values of ω_{min} and ω_{max} are adjusted to cover the entire display range. Finally, the values of ω_{min} and ω_{max} are added as the nodes both for the amplitude response and for the phase response. When the values of ω_{min} and ω_{max} are determined, an array object of frequency values to determine the exact amplitude and phase response is created using the logspace function. The number of data points is determined automatically, depending on ω_{min} and ω_{max}, to provide about 100 data points per decade.

After the node frequency values are set, the lists of node frequencies are converted to array data type of the NumPy module [15], and associated arrays of the amplitude response values and the phase response values are initialized as objects of the matching length containing zeros. The second pass of the algorithm is required to adjust these values, which essentially creates the piecewise linear Bode plot. The third pass sets the vertical line segments and/or the arrows that correspond to infinite resonant responses.

C. Adjusting the nodes

The second pass of the algorithm adjusts the nodes, both for the amplitude and the phase response. The algorithm is described in Section III for each of the elementary transfer functions. The program passes through the data structure created by the parser for each of the elementary transfer function types and adjusts the node altitudes as required.

Besides adjusting the node altitudes, the second pass of the algorithm possesses information about ω_{min} and ω_{max}, thus able to create the database of Bode plots for each of the elementary transfer functions contained in (1), the exact frequency responses for all of the elementary transfer functions, and the exact frequency response of (1) according to (2) and (3).

D. Resolving resonances

The third pass of the algorithm starts at the point when the Bode plots are almost finished, and only "resonant responses" caused by Q_p and Q_z values should be indicated, as well as the infinite values in the logarithmic plots of the amplitude responses caused by $H_l(s)$ and $H_m(s)$. It should be noted that this phase of the algorithm involves amplitude response only. The third pass of the algorithm starts by initializing the lists of line segment patches and the list of arrow patches as empty lists.

The first part of "resolving resonances" considers elementary transfer functions $H_h(s)$ to $H_k(s)$ that contribute to the line segment patches. Values of the amplitude response at corresponding value of ω_p or ω_z are read from the piecewise linear Bode plot of the amplitude response, and having these values and the value of corresponding q_p or q_z, the vertical line segment patch is created.

The second part of "resolving resonances" considers elementary transfer functions $H_l(s)$ and $H_m(s)$ that create arrow patches. Values of the amplitude response at corresponding value of ω_p or ω_z are read from the piecewise linear Bode plot of the amplitude response, and these values are used as starting points for the arrows. The arrows point upwards for $H_l(s)$ and downwards for $H_m(s)$. The length of the arrow that indicates infinite response is chosen to be standardized to equivalent 20 dB.

This concludes the algorithm, and all the data that specify both the exact plots and the piecewise linear Bode plots are constructed. If the user requires, an informative plot is created, containing curves specified by the flags. This is convenient in the control loop design process, but publication quality graphs usually require access to the created database of plots, to adjust ticks and grids, and to add some labeling manually, according to the user wishes.

V. An Example

To illustrate application of the described algorithm, an equiripple group delay filter with amplitude corrector, inspired by [20], [21] is selected. The filter contains 14 poles and 12 zeros. Filter applications are not particularly suited for Bode piecewise linear approximation, since both the poles and zeros are closely grouped in the complex plane, resulting in tendency of the approximation error to accumulate. Thus, the example should be considered as a particularly hard test for the method.

Transfer function of the considered filter $H_{vbl}(s)$ is factored according to (1) into the following list of elementary transfer functions

1) $H_a(s)$, $K = 1$
2) $H_h(s)$, $\omega_p = 1.15148675$, $Q_p = 0.61625492$
3) $H_h(s)$, $\omega_p = 0.95360261$, $Q_p = 0.51157670$
4) $H_h(s)$, $\omega_p = 0.98559505$, $Q_p = 0.53174411$
5) $H_h(s)$, $\omega_p = 1.02900047$, $Q_p = 0.56136078$
6) $H_h(s)$, $\omega_p = 1.07702300$, $Q_p = 0.60099034$
7) $H_h(s)$, $\omega_p = 1.11337090$, $Q_p = 0.65696211$
8) $H_h(s)$, $\omega_p = 1.07821613$, $Q_p = 0.79159298$
9) $H_m(s)$, $\omega_z = 3.1335590$
10) $H_m(s)$, $\omega_z = 3.7630714$
11) $H_m(s)$, $\omega_z = 4.7859023$
12) $H_m(s)$, $\omega_z = 6.0011218$
13) $H_m(s)$, $\omega_z = 7.3087231$
14) $H_m(s)$, $\omega_z = 8.6935655$

where each elementary function type is followed by its parameters.

Diagrams containing piecewise linear Bode plots accompanied by the exact plots are given in Figs. 12 and 13 for the amplitude and the phase response, respectively. Value

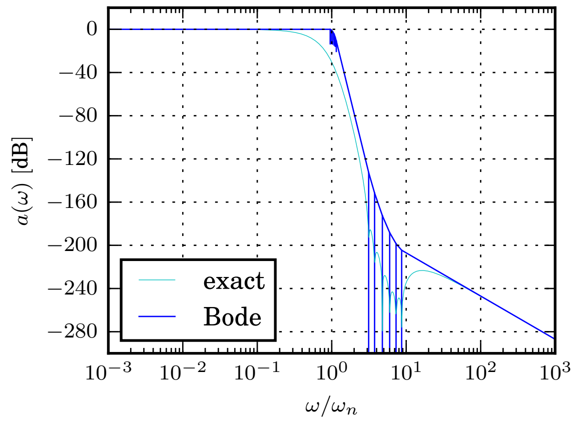

Fig. 12. $H_{vbl}(s)$, amplitude response.

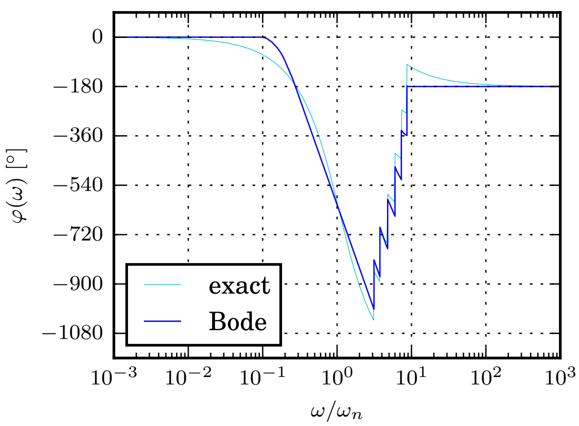

Fig. 13. $H_{vbl}(s)$, phase response.

ω_n in the diagrams indicates the normalization frequency. In the amplitude response, the diagram is polished manually, such that the arrows that would indicate the infinite response are replaced by the lines that spread to the diagram border. Regardless the fact that the poles and zeros are close, the approximation is acceptable. Numerous undershoots caused by low Q factor values of the pole are observed around $\omega \approx \omega_n$. Infinite response caused by zero pairs on the imaginary axes are correctly handled. In phase response, correct handling of discontinuities caused by the imaginary axis zero pairs could be observed.

VI. Future Work

At present stage, the described algorithm is implemented in a command line interface based program. The use of such program requires some sort of computer usage competence, which is not common to the majority of users nowadays. Thus, to increase availability, a graphical user interface is planned to be created. Another direction of program development is to provide automatic creation of the canonical form of (1) on the basis of the transfer function specified as a rational function of s. Finally, the algorithm is intended to be included in a comprehensive symbolic analysis software suite for linear systems.

VII. Conclusion

In this paper, an algorithm for creating piecewise linear Bode plots of amplitude and phase frequency responses of lumped parameter linear systems is proposed. The algorithm is complete in the sense that it covers for poles and zeros placed at arbitrary locations in the entire complex plane.

The transfer function is factored into a specified canonical form, as products of elementary transfer functions. Thirteen elementary transfer functions are defined, and plotting piecewise linear amplitude and phase Bode plots is defined for each of them. It is shown that the thirteen elementary transfer functions have their roots in only five generic transfer function types. Piecewise linear Bode plots are depicted for all of these five generic types, and specified for other elementary transfer functions by appropriate mirroring.

The algorithm to generate piecewise linear Bode plots is based upon introducing nodes in both the amplitude and the phase frequency response. The nodes are defined as points where the response, either amplitude or phase, changes its slope. For each of the elementary functions the list of nodes it introduces both in the amplitude and in the phase response is presented, as well as the algorithm how to modify the node altitudes according to the effects caused by the elementary transfer function.

Finally, the algorithm to generate the Bode plots is described as a three stage algorithm. In the fist stage, just after the input file parsing, frequencies of the nodes specified by the elementary functions of the transfer function factorization into canonical form are collected, and the border frequencies for the plots are included in the list of node frequencies. In the second stage, node altitudes are updated according to specifications given for each of the elementary transfer function types. In the third stage, overshoots and undershoots in the amplitude response created by complex conjugate pairs of pole or zeros are resolved, separately for the pairs outside the imaginary axis, and for the pairs located on the imaginary axis, creating linear segment patches for the overshoots or undershoots or arrow patches that indicate infinite logarithmic amplitude response, respectively. Output of the program is a diagram and a data structure that allows the user to create own diagrams to tweak the appearance if required.

An issue worth addressing is computational complexity of the proposed algorithm in comparison with standard general purpose tools that might provide Bode plots. The first difference to be underlined is in the size of the data set that describes the plot: in the case of piecewise linear Bode plot the size is related to the number of poles and zeros, and it is much smaller than the data sets that characterize standard smooth frequency response plots. Actually, this is the main reason that Bode plots are still in use today: the reduced data set is much easier to handle by human cognitive capacities in the design process. In smooth frequency response plots, the number of poles and zeros of the transfer function is not related to the data set size, instead it is determined by the number of data points required to provide the diagram detailed enough, frequently containing excessive number of points covering parts of the frequency response where not much happens. Assuming that computational complexity to generate one data point is about the same in both approaches, the conclusion is that the asymptotic Bode plot approach requires significantly reduced computational effort. Furthermore, smooth phase response plots require numerous arctangent (actually, `atan2`) computations, which are computationally more demanding than the arithmetic required by the asymptotic plots. However, it is worth to note that asymptotic Bode plots require transfer function factorization, which standard approach does not. However, factorization is required in the design process anyhow, to properly understand dynamics and to adequately place poles and zeros of the compensating regulator. Finally, with modern computers computational efficiency in creating the frequency response plot should not be a critical issue nowadays, and the main reason for using the asymptotic Bode plot approach is in its cognitive value, clear and concise presentation of the system dynamics.

REFERENCES

[1] L. W. Nagel, *SPICE2: A computer program to simulate semiconductor circuits*, ERL Memo ERL-M520, 1975.
[2] A. Vladimirescu, *The SPICE book*. John Wiley & Sons, Inc., 1994.
[3] Wikipedia contributors, "Bode plot," [Online]. Available: https://en.wikipedia.org/wiki/Bode_plot
[4] G. F. Franklin, J. D. Powell, A. Emami-Naeini, *Feedback control of dynamic systems*, 3rd ed., Addison-Wesley, 1994
[5] K. Ogata, *Modern control engineering*, 5th ed., Pearson Education, 2010
[6] GNU Octave, [Online]. Available: https://www.gnu.org/software/octave/
[7] R. D. Middlebrook, "Low Entropy Expressions: The Key to Design-Oriented Analysis," IEEE Frontiers in Education Conference, 1991 Proceedings, pp. 399–403, Sept. 1991.
[8] R. D. Middlebrook, "Methods of Design-Oriented Analysis: The Quadratic Equation Revisited," IEEE Frontiers in Education Conference, 1992 Proceedings, pp. 95–102, Nov. 1991.
[9] R. W. Erickson, *Bode Diagrams of Transfer Functions and Impedances*, ECEN 2260 Supplementary Notes, [Online]. Available: http://ecee.colorado.edu/ecen2270/materials/Bodenotes.pdf
[10] R. W. Erickson and D. Maksimović, *Fundamentals of power electronics*, 2nd ed., Kluwer Academic Publishers, 2001
[11] V. Vorperian, *Fast analytical techniques for electrical and electronic circuits*, Cambridge University Press, 2002.
[12] C. K. Alexander and M. N. O. Sadiku, *Fundamentals of electric circuits*, 2nd ed., McGraw-Hill, 2004.
[13] A. Agarwal, J. H. Lang *Foundations of analog and digital electronic circuits*, Elsevier, 2005.
[14] Python Programming Language — Official Website, [Online]. Available: http://www.python.org/.
[15] NumPy [Online]. Available: http://www.numpy.org/
[16] SciPy [Online]. Available: https://www.scipy.org/
[17] matplotlib, [Online]. Available: http://matplotlib.org/
[18] Maxima, a Computer Algebra System, [Online]. Available: http://maxima.sourceforge.net/
[19] SymPy, [Online]. Available: http://www.sympy.org/en/index.html
[20] V. B. Litovski, "Synthesis of Monotonic Passband Sharp Cutoff Filters with Constant Group Delay Response," *IEEE Transactions on Circuits and Systems*, vol. CAS-26, no. 8, pp. 597–602, Aug. 1979.
[21] V. B. Litovski, D. P. Milovanović, "New solution for the ideal filter approximation problem," *IEE Proceedings G (Electronic Circuits and Systems)*, vol. 130, no. 4, pp. 161–163, Aug. 1983.

Applications of Artificial Neural Networks in Electronics

Miona Andrejević Stošović and Vančo Litovski

Abstract—**In this paper we will give short overview of different applications of artificial neural networks in electronics. Artificial neural networks are shown to be universal approximators, so they were successfully used in applications in modelling of electronic circuits, as well as in fault diagnosis and classification.**

Index Terms— **artificial neural networks, diagnosis, modelling, simulation.**

Review Paper
DOI: 10.7251/ELS1721087A

I. Introduction

Artificial neural networks (ANNs) were shown to be an excellent candidate for the approximant needed in the black-box modelling. Also, they are universal approximators so they can be used in the best way both to capture the mapping, and to search through the dictionary, thereby to perform diagnosis.

We will give in this paper an overview of numerous applications of ANNs both in modelling in diagnosis. There are also many more applications of artificial neural networks that we performed, but they cannot be presented here. We will abstract only the ones we consider most important.

We will start from the first example of application of ANNs in modelling, when characteristics of MOS transistor were modelled and implemented in behavioral simulator. Then, a micro-electro-magneto-mechanical actuator was modelled but the modelling was in fact quasi-dynamic. The motivation for modeling of non-linear dynamic networks appeared with the problem of modeling implanted hearing aids, so this example is followed by different instances of modelling nonlinear dynamic circuits. Modelling of the A/D and D/A interfaces in mixed-mode simulation is one of the most published examples.

Another aspect of our application of artificial neural network is defects diagnosis. Here, we started from analogue electronic circuits, which are difficult to be diagnosed due to huge number of possible faults, and inherent nonlinearity of these circuits. This concept is also shown in a complex system that can be decomposed in order to simplify the process of diagnosis. This is followed by few examples where ANNs are used to capture mappings in different fault dictionaries.

Manuscript received: May 18th, 2017
Received in revised form: May 18th, 2017

This research was partly funded by The Ministry of Education and Science of Republic of Serbia under contract No.TR32004.

Miona Andrejević Stošović is with the University of Niš, Faculty of Electronic Engineering, Niš, Serbia (+381-18-529-208; e-mail: miona.andrejevic@elfak.ni.ac.rs).

Vančo Litovski is an independent researcher, e-mail: vanco.litovski@elfak.ni.ac.rs.

II. Application of ANNs in Modelling

There are two basic approaches to the modelling of electronic components: the physical and the black-box approach. When the physical laws undergoing the component's behavior are known one may create a set of expressions (usually by solving differential equations) relating the terminals excitations and responses. The obtained current-voltage relations are referred to as *physical model* of the component. Main advantage of this concept may be devoted to the existence of physical meaning of the coefficients arising in the modelling expressions. There are, however, many difficulties in the implementation of such models [1]. Firstly, one rarely knows the physics of the components in such a detail that enables to establish the mutual dominance of all physical and technological parameters. Further, in most cases it is not possible to describe the complete behavior by one equation only having in mind different working regimes of the component [2]. The equations describing parts of the model, frequently become incompatible leading to non-analytical overall approximating function.

When no full knowledge of the physics of the device is available one uses the so-called black-box approach. The behavior is captured by measurements of input (signal) and output (response) quantities. After that an approximation procedure is performed over the set of measured data in order to get an analytical expression convenient for equation formulation in the circuit-simulation process. The question of the choice of adequate approximant is crucial for this type of modelling. In some cases polynomial interpolation is used in between two measured points [3]. In other cases the complete measurement is described by linear segments leading to piece-wise linear models [1], [4]. To our knowledge there is no general receipt for the choice of an analytical function for this approximation. Main advantage of the black-box approach is related to the fact that one doesn't need to have full knowledge on the physics of the device being modelled. In general there are no limitations about the choice of the approximants, most frequently, the main restriction is that they need to be analytical function. From the other side, main problem encountered during use of this approach is modelling simultaneously of the non-linear and dynamic behavior of the device.

Artificial Neural Networks (ANN) were shown to be an excellent candidate for the approximant needed in the black-box modelling. The first example of application of an ANN for modelling an electronic device was given in [5]. Fig. 1. contains reproduction of the first modelling results. There the output characteristics of a MOS transistor are approximated by a feed-forward three layer ANN. The implementation of such model was limited by the need of existence of behavioral simulator being able to formulate circuit equations for system containing simultaneously component described by electrical equations and others described by functions (i.e. ANNs) [6, 7].

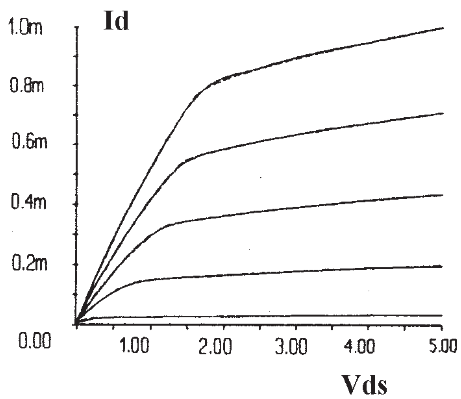

Fig. 1. MOS transistor characteristics and approximation

After publication of the first results in [5], ANNs were successfully applied in electronic modelling several times [8]. In all these applications feed-forward networks were used meaning that only resistive properties of the devices were captured. The first attempt of modelling dynamic behavior was described in [9]. A micro-electro-magneto-mechanical actuator was modelled but the modelling was in fact quasi-dynamic. Namely, by its virtue it was possible to separate the resistive and the dynamic part of the model. The ANN was applied for the resistive part but strongly connected to the rest of the model. This is illustrated in Fig. 2. Fig. 2a represents the electrical schematic of the model of a non-linear magnet, while Fig. 2.b represents the characteristics of the non-linear-inductor both original and approximated. Note the magnet has a moving armature hence the dependence of the characteristics on the displacement x. These drawings were taken from [9] without changes so one should note that Φ and Ψ stand for the same variable: the magnetic flux.

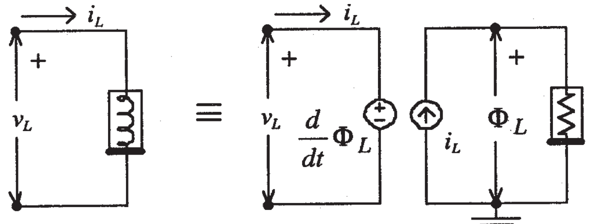

a)

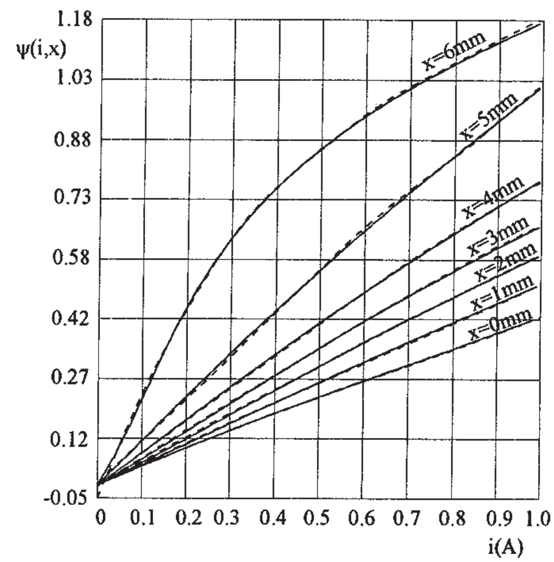

b)

Fig. 2. Modelling of an electro-magnet with moving armature

ANNs are then used for modelling of non-linear dynamic networks. The motivation for modeling of this kind of circuits appeared with the problem of modeling implanted hearing aids [10], [11]. Here, however, in order to present reproducible results the nonlinear circuit, Fig. 3, containing quartz crystal, Fig. 4, will be considered for modeling. The schematic symbol for a quartz crystal is shown in Fig. 4a. The equivalent circuit for a quartz crystal near fundamental resonance is shown in Fig. 4b. The equivalent circuit is an electrical representation of the quartz crystal's mechanical and electrical behavior. The components C_1, L_1, r_1, are called the motional arm that represents the mechanical behavior of the crystal element. C_0 represents the electrical behavior of the crystal element and holder [12].

C_1 is motional arm capacitance representing the elasticity of the quartz, the area of the electrodes on the face, thickness and shape of the quartz wafer. Values range in femtofarads.

L_1 is motional arm inductance representing the vibrating mechanical mass of the quartz in motion. Low frequency crystals have thicker and larger quartz wafers and range in a few Henrys. High frequency crystals have thinner and smaller quartz wafers and range in few millihenrys.

r_1 represents the real resistive losses within the crystal.

C_0 is shunt capacitance representing the sum of capacitance due to the electrodes of the crystal plate plus stray capacitances due to the crystal holder and enclosure.

Crystal has two resonant frequencies characterized by a zero phase shift. The first is the series resonant, f_s frequency. The second resonant frequency is the anti-resonant f_a, frequency.

As an example of modeling of nonlinear dynamic circuits [13], [14] the electronic circuit depicted in Fig. 3. will be modeled. The pair of branches containing diodes is introduced enabling the nonlinearity of the circuit to be accounted for. Resonant frequency of the crystal oscillator is 8MHz, meaning that both f_s and f_a are close to that value. So, a chirp $i(t)$ signal is needed to cover the frequency band around 8MHz. Recurrent time delay neural network with five input, four hidden and one output neuron is used, because the structure from Fig. 3. is highly nonlinear.

The response of this circuit excited by a chirp signal with the change of frequency from 7.997÷8.03MHz is given in Fig. 5. Series resonant frequency can be noticed first, and then, anti-resonant frequency.

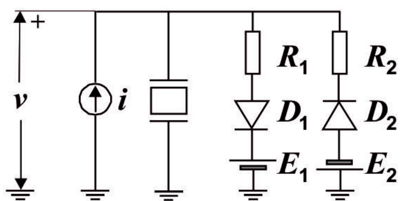

Fig. 3. Nonlinear dynamic circuit chosen for modeling

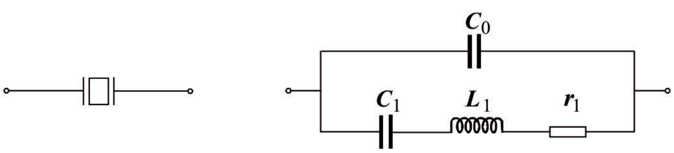

Fig. 4. a) Crystal equivalent circuit and b) its symbol

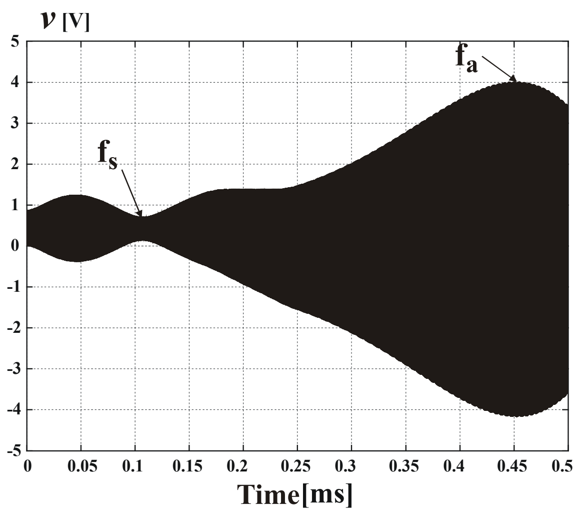

Fig. 5. Response of the circuit, Fig. 4, excited by a chirp signal

The responses of the modeled circuit and the model are shown in Fig. 6. It is obtained as an envelope of the time domain response [15].

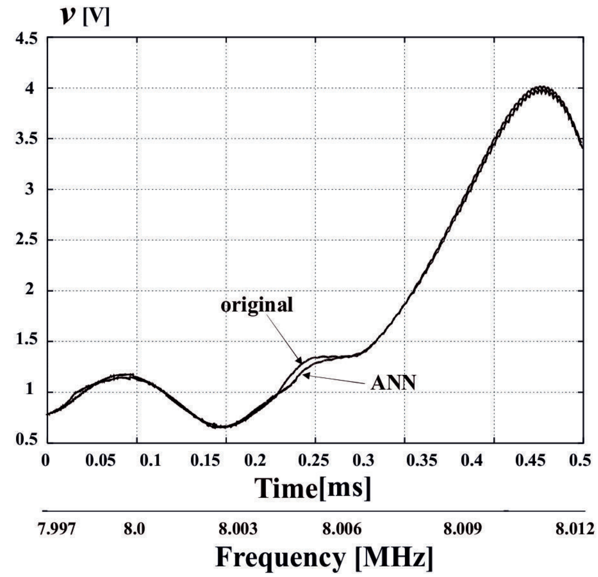

Fig. 6. Responses of the original circuit (Fig. 4) and the model (only the envelopes of the positive periods are shown)

The next example of ANNs implementation for behavioral modelling of nonlinear dynamic circuits is modelling of the A/D and D/A interfaces in mixed-mode simulation. We will here present only modelling of D/A interface. Modelling of A/D interface is explained in detail in [16], [17].

For modelling of the D/A interface [16], [17], [18] the output circuit of the digital part is represented by a circuit that is supposed to drive an analog load. Note that mixed-mode simulation is considered. This means that an event scheduler is active, marking the controlling input of the digital circuit. The event scheduler does not allow for two inputs to be active simultaneously because that is considered as a hazard. Hence, modelling the output of an inverter is general enough for verification of the modelling procedure.

The topology of the new model is depicted in Fig. 7a. In the figure, v_{in} stands for a controlling ramp-shaped voltage-waveform:

$$i(v_{in}) = I_{max}\left[1 - \tanh(v_{in} - v_T)\right] \tag{1}$$

and Z is a recurrent time-delay neural network approximating the function:

$$v_{out} = Z(i)\,. \tag{2}$$

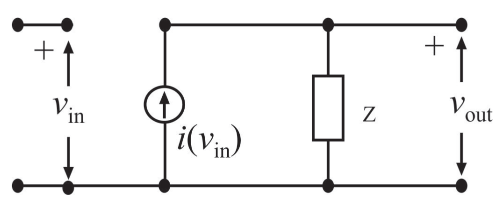

a)

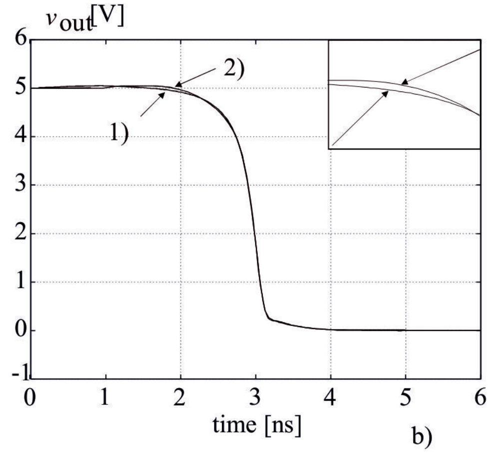

Fig.7. a) Circuit representation of the model and b) responses: 1) unloaded CMOS inverter (considered as digital output) and 2) of the new model.

Here, I_{max} is the maximum supply current during the transition in the inverter, and v_T is (usually) equal to $V_{DD}/2$, V_{DD} being the supply voltage. Obviously, the ANN model of Z has one input (current) and one output (voltage) terminal. The network is trained using input-output pairs $[i(t), v_{out}(t)]$, where $i(t)$ is calculated from (1) while $v_{out}(t)$ is obtained from simulation by the *Alecsis* simulator of the circuit to be modelled (here an inverter). Note that we need the electrical schematic of the digital part during the modelling phase.

First results are shown in Fig. 7b. Here output waveforms of the original inverter and the model are shown to illustrate the quality of the approximation procedure. Unloaded circuits are simulated. The ANN has five input units, three hidden units, and one output unit.

The following three examples are intended to check the modelling procedure based on situations not present during training. The first trace (marked 1)) in Fig. 8a is the output voltage of an inverter being loaded by an inverter, all modelled by regular transistor models, i.e., obtained by regular circuit simulation. The second one (marked 2)) represents the response of the same circuit with the ANN model used for the driving part and circuit model for the loading. This situation was not encountered in the training process. Excellent agreement was obtained, especially in the steepest part of the response that defines both the gain and the delay of the loaded inverter.

Further, Fig. 8b gives a similar comparison the loading element here being a transmission line modelled by a π-RC network. Finally, a TTL load (diode), Fig. 9, was used to demonstrate the success of the ANN model in the case of a 'large' non-linear dynamic load. Note the average value of the output voltage is less than 0.5 V while the difference is still smaller than 10 mV. Once again, the ANN model was developed using an unloaded inverter.

Our next usage of artificial neural networks in modelling is producing a small signal linear dynamic model of the solar cell that may be used for characterization of the interface and in the whole PV system in the frequency domain [19]. This idea is based on the experience that the output voltage and the output current of a PV panel are not pure DC constant due to the inevitable connection to a converter (or inverter) which is working as a switching system, so we came to a conclusion that interest exists for the behavior of the solar cell at the frequencies of the harmonics of the converters switching frequency which is subject of change according to the maximum-power-point tracking.

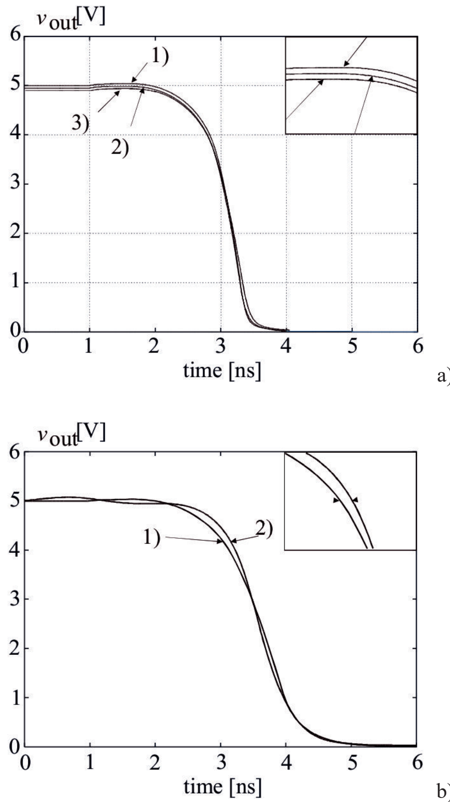

Fig. 8. a) Responses of 1) inverter loaded by inverter, 2) a model loaded by inverter, and 3) an ANN (modelling the output) loaded by an ANN modelling the input of an inverter. b) Responses of 1) an inverter loaded by RC ð -network and 2) a model loaded by RC ð -network.

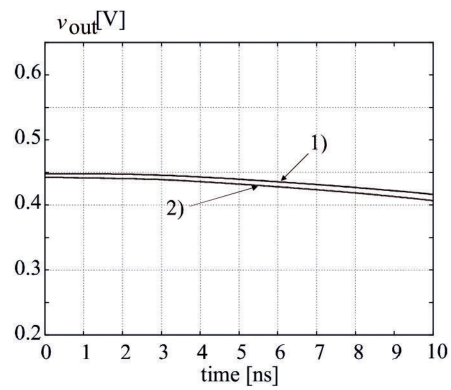

Fig. 9. Responses of a) inverter loaded by a diode and b) ANN model loaded by a diode.

To extract the small signal model the usual one-diode large signal dynamic model is used with known parameter values. The modeling process is conceived to be performed in two steps. In the first one, for a given cell, measurements are performed in order to produce the element values and proper parameters for the one-diode nonlinear model. In the second step the nonlinear model obtained so far is exploited for generation of the linear one. The element values versus photocurrent and cell-voltage dependences are captured by feed-forward artificial neural networks, one per element. The ANNs serves as a mapping algorithm capturing the "look-up" tables with the dependences of the model elements on the illumination and cell voltage. Verification of the model is performed by comparisons of the small signal frequency domain responses of the original nonlinear dynamic model and of the new linear RC model. We expect implementation of these results to find place not only in modeling for energy conversion applications but also for modeling devices that are capturing light as signal carrying information.

III. Application of ANNs in Diagnosis

Whenever we think about why something does not behave, as it should, we are starting the process of diagnosis. Diagnosis is therefore a common activity in our everyday lives [20]. Every system is liable to faults or failures. In the most general terms, a fault is any change in a system that prevents it from operating in the proper manner. We define diagnosis as the task of identifying the cause and location of a fault manifested by some observed behaviour. This is often considered to be a two-stage process: first the fact that fault has occurred must be recognized – this is referred to as *fault detection*. Secondly, the nature and location should be determined such that appropriate remedial action may be initiated.

The general structure of a diagnostic system is shown in Fig. 10. Signals $u(t)$ and $y(t)$ are input and output to the system, respectively. Faults and disturbances (here measurement errors) also influence the system under test, here denoted as the "Process", but there is no information about the values of these errors. The task of the diagnostic system is to generate a diagnostic statement $\boldsymbol{S}$, which contains information about fault modes that can explain the behaviour of the Process. Note that the diagnostic system is assumed to be passive i.e. it cannot affect the Process itself.

The whole diagnostic system can be divided into smaller parts referred here to as tests. These tests are also diagnostic systems, DS_i. It is assumed that each of them generates diagnostic statement S_i. The purpose of the decision logic (voting system) is then to combine this information in order to form the diagnostic statement S.

Analogue electronic circuits are known to be difficult to test and diagnose. Apart from the huge number of possible faults, this difficulty is a consequence of the inherent nonlinearity of these circuits. Even linear circuits (having linear input-output signal interdependence) exhibit nonlinear relations between circuit parameters and the output response. There are no linear active networks. Active networks are nonlinear with nonlinear reactive elements. They may be linearized and thought of as such in situations where signal and parameter changes are small in comparison to nominal values. When large parameter changes or even catastrophic faults occur (affecting the DC state), however, one must distinguish between linear and analogue circuits.

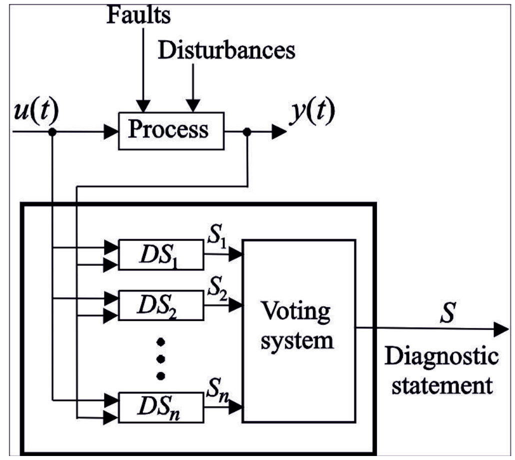

Fig. 10. A general diagnostic system

Here we describe the results of applying feed-forward ANNs to the diagnosis of non-linear dynamic electronic circuits with no restriction on the number and type of faults. This method is based on fault dictionary creation and using an ANN for data compression by memorizing the table representing the fault dictionary. Only DC and small signal sinusoidal excitations are applied, so preserving the usual measurement procedure for generating the data given in a component's and/or a circuit's data-sheets. The ANN so created is, consequently, used for diagnosis by applying to it the signals obtained by measuring the faulty network. This process may be considered as looking-up a fault in the fault dictionary. The ANN finds the most probable *fault code* that corresponds to the measured signals.

The network used for this diagnostic example is a feed-forward neural network structured in three layers. It has only one hidden layer, which has been proved sufficient for this kind of problem [21]. The neurons in the hidden layer are activated by a sigmoidal function, while the neurons in the output layer are activated by a linear function. The learning algorithm used for training this network is a version of the steepest-descent minimization algorithm [22].

In order to describe the way in which the fault dictionary was created, the circuit in Fig. 11. is used as an application example [23]. This is a CMOS operational amplifier consisting of seven transistors. To our knowledge this example belongs to the category of the most complex ones reported, both from the number of circuit elements point of view and the number of faults inserted. Three (nonlinear) capacitors are associated with every transistor totalling the number of nonlinear circuit elements to 28 but, for the sake of simplicity, are not shown in the figure. In order to emphasize the method as such, while not offering a full solution of the diagnostic problem for this circuit, having in mind abundance of possible faults, a reduced set of faults was considered. To this end only single transistor faults are sought. That, of course will not affect the generality of the ideas implemented in the next.

Ten faults per transistor, six catastrophic and four parametric were added to the dictionary. As shown in the figure (using T_7 as an example) there exist three open-circuit faults (OC) and three short-circuit faults (SC) per transistor. In addition, two faulty values for every channel length (±20%), and two for every channel width (±20%) were introduced, totalling 10 faults per transistor.

The DC output values were first obtained by simulation. In addition, the frequency response of the circuit (the non-inverting input terminal was excited by a signal of amplitude 1mV) was obtained by simulation over a fixed frequency range in order to extract two response parameters: the nominal gain (A_m) and the 3-dB cut-off frequency ($f_{3\text{ dB }m}$). Note that, for the DC supply current point of view, the fault effects of most open faults at sources and drains in series connected transistors may have equivalent signatures.

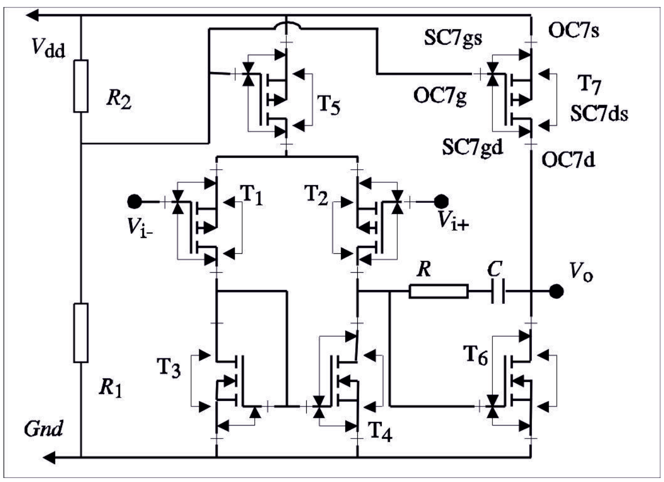

Fig. 11. The operational amplifier circuit. SC = short circuit, OC=open circuit

There are several important issues that need to be considered in this diagnosis process. The fault coding is one of them. In fact, some defects exhibit very similar effects. So, input data can have very close numerical values, and if the output values (defect codes) were also similar, the network could not always be trained successfully. Thus, faults are coded randomly, so that faults with similar effects are unlikely to have similar codes. This approach is proven to be good, because the way of coding influences the training time, and also, the training error.

Another issue is existing of the *ambiguity groups* or the groups of equivalent faults. Here, we can say that an ambiguity group consists of a set of *faults* that propagate identical signatures to the output, making the faults detectable and the circuit testable, but no distinction between the individual faults is possible making them un-diagnosable. In this example, we formed 10 ambiguity groups, so only one representative of each ambiguity group is included in the fault dictionary. We found that the complete fault dictionary in this case had 55 elements.

With three pieces of data for each fault, the neural network input structure was restricted to three input terminals. The ANN diagnoses the fault by outputting the fault-code (m) as a signal level, so we needed only one output neuron. The number of hidden neurons, n, was found by trial and error after several iterations starting with an estimation based on that in [24]. The goal was to find the optimum n leading to a satisfactory classification even with noisy excitations. Using too many neurons would increase the training time, but using too few would starve the network of the resources needed to solve the problem. In practice, 30 hidden neurons were used. After successful training, no mistakes were observed for all 55 faults.

The generalization property of the network was verified by supplying noisy data to its inputs. Thirty samples were examined. For each sample, one input is incremented by +5% or -5%, representing noise generated during the measurement process. The ANN response was considered to be correct (i.e. acceptable) when its value was in the range [(m-0.5), (m+0.5)]. All faults were diagnosed, though few of them with some difficulties.

Next application of feed-forward artificial neural networks to the diagnosis of mixed-mode electronic circuit is in a more complex system that can be decomposed in order to simplify the process of diagnosis [25]. Actually, in order to tackle the circuit complexity and to reduce the number of test points, we implemented hierarchical approach to the diagnosis generation with two levels of decision: the system level and the circuit level. For every level, using the simulation-before-test (SBT) approach, fault dictionary was created first, containing data relating the fault code and the circuit response for a given input signal. ANNs were used to model the fault dictionaries. During the learning phase, the ANNs were considered as an approximation algorithm to capture the mapping enclosed within the fault dictionary. Later on, in the diagnostic phase, the ANNs were used as an algorithm for mapping the measured data into fault code what is equivalent to searching the fault dictionary performed by some other diagnostic procedures. At the topmost level, the fault dictionary was split into parts simplifying the implementation of the concept. A voting system was created at the topmost level in order to distinguish which ANN's output is to be accepted as the final diagnostic statement. The approach was tested on an example of an analog-to-digital converter, and only one test point was used i.e. the digital output. Full diversity of faults was considered in both digital (stuck-at and delay faults) and analog (parametric and catastrophic faults) part of the diagnosed system. Special attention was paid to the

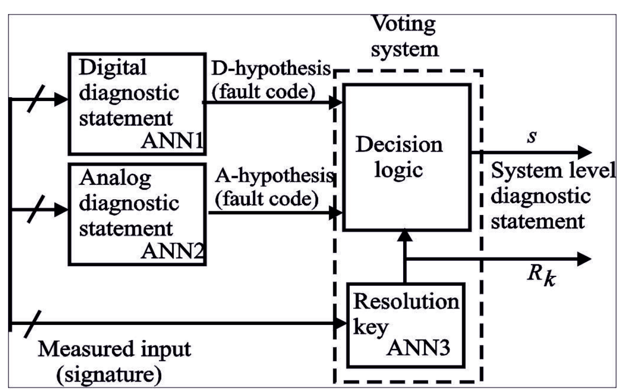

Fig. 12. The ANN based hierarchical diagnostic system

faults related to the A/D and D/A interfaces within the circuit. The example is given in Fig. 12, where a mixed-mode circuit is diagnosed.

ANN1 diagnoses defects in the digital part of the system, while *ANN2* diagnoses defects in the analog part of the system. *ANN3* gets the measured signature as an input as *ANN1* and *ANN2* do. It gets trained so that its output code takes values from the set {-1, 0, 1}. We refer to these values as to resolution key. Namely, if the defect comes from the digital part, the output code is set to 1, while if it comes from the analog, the output code is set to -1. In the special cases when ambiguity arises, that is when one has the same signature coming from faults belonging to the digital and analog part, we assign 0 to the output of *ANN3.* Generally, one can introduce as many levels of diagnosis as necessary.

The implementation of ANNs for diagnostic purposes was also performed in [26] and [27] in the same way as that described in [23], [25]. An artificial neural network (ANN) was used to capture the fault dictionary and perform the diagnosis.

Namely, oscillation-based diagnosis (OBD) was used for the first time as a systematic method for diagnosis of analog filter cells. The method was implemented on a second order Sallen and Key notch cell [28]. A minimum number of test points and, accordingly, measurements were used: just the response at the output terminal. The measured output signal was processed in order to obtain the following parameters: frequency of the first harmonic and four consecutive harmonics. This is clearly simpler than versions of oscillation-based *testing* that also require monitoring of the supply current. Single soft and catastrophic faults were considered in detail, while some double soft faults were also shown to be detectable.

For every passive element within the RC circuit, a short- or open-circuit is considered as a catastrophic fault. We found that in six out of twelve faulty cases the circuit oscillated. In all cases the fault effect is distinct from the fault-free, because the oscillation frequency is not the same as that of the fault-free circuit, or there is no oscillation. In general, therefore, we can state that by implementing OBT we got almost perfect fault coverage of catastrophic faults. We also calculated the frequency change relative to the oscillating frequency, given as a percentage.

When considering parametric (soft) defects, we decided that parametric defects were seen when the element value within the RC-circuit was changed by 20% compared to its nominal value. Both positive and negative changes are taken into account. By inspection of the obtained results, we noticed that in only two cases there was no difference between the behavior of the fault-free and the faulty circuit. In four cases, the change in the frequency value was relatively low (less than 5%) so making the decision difficult. Here again we may conclude that the fault coverage is almost perfect.

The possible number of double parametric defects is much larger than in the case of the single faults. Therefore, a reduced set of pairs of soft faults was considered. We may observe that in all cases, the faulty circuit exhibits a new value for oscillation frequency. In five cases the change in the frequency value is small.

The complete fault dictionary was memorized as parameters (weights and thresholds) of artificial neural network. Diagnosis was performed by running the neural network after measurement (here simulation) of the faulty circuit. Noise was added to the signals obtained by simulation in order to check for the robustness of the method. It was shown that OBD may be successfully used for diagnosis of the notch cell, which in our experience, is among the most difficult circuits to handle. In order to enable manipulation with an extremely large amount of data we now intend to implement a hierarchical approach, as was done for testing purposes in [25].

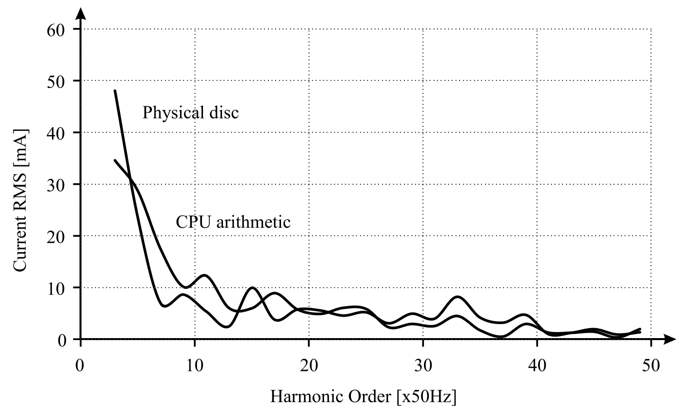

Fig. 13. Odd harmonics measured from supply current, running different benchmark tests. The first harmonic is omitted for convenience

One more example of using artificial neural networks in diagnosis is given in the next. The method we proposed [29] is based on measurement of the supply current and analysis of its harmonic content. Namely, we suppose that different activities happening within a computer map themselves into the supply current waveform in a different way and consequently may be recognized by analysis of the harmonic content. To demonstrate the method we selected a set of software packages with the goal to develop a tool that will recognize every one of them when running within the computer. For each of them we measured the supply current and computed the harmonics generated by one personal computer (DELL Optiplex 980, Intel Core i7 CPU @ 2.8GHz, 4GB RAM, 500GB HDD) under different working conditions i.e. by different benchmark tests running.

Approximately 50 harmonics were observed in a sample (200 ms, 10000 samples) of a grid current. Fig. 13. illustrates two (out of eight) different states of the workstation. Since even-harmonics have incomparably smaller values than the odd ones, only the DC, the main, and the odd harmonics are presented.

We showed in [29], [30] how one can establish, by measurement of the supply current taken from the electricity distribution grid, which software, one out of a previously given list, is running within the computer. For that purpose artificial neural networks were used to perform the classification i.e. recognition of the state of the computer. The method was proven to be good.

IV. Conclusion

In this paper we presented numerous examples where we proved that artificial neural networks could be used in many different applications in electronics. We applied them successfully in modelling of electronic circuits, as well as in fault diagnosis and classification.

References

[1] Chua, L., and Lin, P., "Computer-Aided Analysis of Electronic circuits: Algorithms and Computational Techniques", Prentice-Hall, New Jersey, 1975

[2] Foty, D., "MOSFET Modelling Circuit Simulation", IEEE Circuits and Devices, Vol. 14, No 4, July 1998, pp. 26-31.

[3] Shahram, M., "Calibrating Simulations Tools for Nanometer Designs", IEEE Spectrum, Vol. 36, No 6, June 1999, pp 77-82.

[4] Katzenelson, J., "An Algorithm for Solving Non-linear resistive networks", Bell System Technical Journal, Vol. 44, October 1965, pp. 1605-1620.

[5] Litovski, V. B., et al., "MOS transistor modelling u-sing neural networks", Electronic Letters, Vol. 28, No. 18, 1992, pp. 1766-1768.

[6] Glozić, D., et al., "Alecsis, the Simulator", Faculty of Electronic Engineering, LEDA, Niš, Yugoslavia (internal report), 1996.

[7] Litovski, V., Maksimović, D. and Mrčarica, Ž. , "Mixed-signal modelling with AleC++: Specific features of the HDL", Simulation, Practice and Theory, Elsevier, Vol. 8, 2001, pp. 433-449.

[8] Wang, F., and Zhang, Q-j., "Knowledge-based Neural Models for Microwave Design", IEEE Trans. on MTT, Vol. 45, No. 12, December 1997, pp. 2333-2343.

[9] V.B. Litovski, Ž. Mrčarica, T. Ilić, "Simulation of non-linear magnetic circuits modelled using artificial neural network", Simulation Practice and Theory, Elsevier, No. 5, 1997, pp. 553-570, (Awarded the Savastano award by the European Federation of Simulation Societies).

[10] Ball, G., and Maxfield, B., "Floating Mass Transducer for Middle Ear Applications: An Analytical Model", private communication, 1997.

[11] Andrejević Stošović, M. , Litovski, V.: Implementation of Recurrent Artificial Neural Networks for Nonlinear Dynamic Modelling in Biomedical Applications, The International Journal of Artificial Organs, Wichtig Editore, November, 2013, Vol. 36, Issue 11, pp. 833-842, ISSN: 0391-3988, doi:10.5301/ijao.5000255.

[12] www.microchip.com/download/appnote/rfpic, Crystal Oscillator Basics and Crystal Selection for rfPIC and PICmicro Devices.

[13] Andrejević, M. , Litovski, V., *Electronic Modelling Using ANNs for Analogue and Mixed-Mode Behavioural Simulation*, NEUREL 2002, Belgrade, Serbia, September 2002, pp. 113-118.

[14] Andrejević, M., Litovski, V., *Electronic circuits modeling using artificial neural networks*, Journal of Automation Control, 2003, vol. 13(1), pp. 31-37.

[15] Andrejević, M., Milovanović, D., Petković, P., Litovski, V.: "Extraction of Frequency Characteristics of Switched-Capacitor Circuits Using Time-Domain Analysis", Proceedings of the Conference MIEL 2002, May 2002, Niš, Yugoslavia, pp. 635-638.

[16] Litovski, V., Andrejević, M. , Petković, P., Damper, R.: *ANN Application to Modelling of the D/A and A/D Interface for Mixed-Mode Behavioural Simulation*, Journal of Circuits, Systems and Computers, Volume 13, Number 1, February, 2004, pp. 181-192, ISBN 0218-1266.

[17] Andrejević, M. , Litovski, V.: *ANN Application in Modelling of A/D Interfaces for Mixed-Mode Behavioural Simulation*, Zbornik radova XLVI konferencije Etran 2002, Banja Vrućica, 3.6.-6.6., 2002, pp. Vol. I 51-54.

[18] Litovski, V., Andrejević, M. , Damper, R.: *Modeling the D/A Interface for Mixed-Mode Behavioral Simulation*, EUROCON 2003, Ljubljana, Slovenia, Septembar, 2003, A130-A133.

[19] Miona Andrejević Stošović, Ivan Litovski, Duško Lukač, Marko Dimitrijević, Vančo Litovski: *Small Signal Model of a Solar Cell*, Simulation: Transactions of the Society for Modeling and Simulation International, Sage Science Press, London, Vol. 90(11), November, 2014, pp. 1231-1243, ISSN: 0037-5497.

[20] Benjamins, R., and Jansweijer, W., "Toward a competence theory of diagnosis", IEEE Expert, Vol. 9, No. 5, October 1994, pp. 43-52.

[21] Masters, T., "Practical Neural Network Recipes in C++", Academic Press, San Diego, 1993.

[22] Zografski, Z., "A Novel Machine Learning Algorithm and Its Use in Modeling and Simulation of Dynamical Systems", Proceedings of 5th Annual European Computer Conference, COMPEURO'91, Bologna, Italy 1991, pp. 860-4.

[23] Litovski, V., Andrejević, M., Zwolinski, M.: *Analogue Electronic Circuit Diagnosis Based on ANNs*, Microelectronics Reliability, August, 2006, pp. 1382-1391, ISSN:0026-2714.

[24] Baum, E. B., and Haussler, D., "What size net gives valid generalization", Neural Computing, Vol. 1, 1989, pp. 151-60.

[25] Andrejević Stošović, M. , Milovanović, D., Litovski, V.: Hierarchical Approach to Diagnosis of Mixed-mode Circuits using Artificial Neural Networks, Neural Network World, Institute of Computer Science AS CR, v. v. i. and Faculty of Transportation Sciences, May, 2011, Vol. 2/11, pp 153-168, ISSN 1210-0552.

[26] Andrejević Stošović, M., Milić, M., Zwolinski, M., Litovski, V.: Oscillation-based analog diagnosis using artificial neural networks based inference mechanism, Computers and electrical engineering, Vol. 39, Issue 2, Elsevier, February, 2013, pp. 190-201, ISSN 0045-7906.

[27] Andrejević Stošović, M., Milić, M., Litovski, V.: Analog Filter Diagnosis Using the Oscillation Based Method, Journal of Electrical Engineering - ElektrotechnickĂ˝, Vol. 63, No. 6, 2012, pp. 349-356, ISSN 1335-3632.

[28] L. P. Huelsman, Active and Passive Analog Filter Design: An Introduction, McGraw-Hill College, 1993.

[29] Miona Andrejević Stošović, Marko Dimitrijević, Vančo Litovski: *Computer Security Vulnerability Seen From the Electricity Distribution Grid Side*, Applied Artificial Intelligence, Taylor & Francis Ltd., No 28, Vol 4, London, April 2014, pp. 323-336, ISSN 0883-9514, doi:10.1080/08839514.2014.891831.

[30] Marko Dimitrijević, Miona Andrejević Stošović, Jelena Milojković, Vančo Litovski: *Implementation of Artificial Neural Networks Based AI Concepts to the Smart Grid*, FACTA UNIVERSITATIS, Series: Electronic and Energetics, University of Niš, Vol. 27, No. 3, Niš, September, 2014, pp. 411-424, ISSN: 0353-3670, doi:10.2298/FUEE1403411D.

Simulation of a Pick-and-Place Cube Robot by Means of the Simulation Software Kuka Sim Pro

Duško Lukač and Miljana Milić

Abstract — **In this work the creation of the program code for industrial robot and the simulation of a robot cell by means of the simulation software KUKA Sim Pro in version 2.2.2, is presented. Simulated and programmed is, in reality existing KUKA-robot cell with industrial robot of the type KR6 R900 sixx (Agilus) with signal connected conveyor belt. The software KUKA Sim Pro is a program for design of 3D-layouts of a plant components including KUKA-robots. On this occasion, any layouts and concept designs can be simulated and be analysed. The used components were taken from the integrated library or were partly newly created. The industrial robot KUKA KR6 R900 sixx counts to the quickest robots of the world. In this work, the simulation of the robot cell and periphery is elaborated, as well as with it, connected practical circumstances and issues with the programming of the abovementioned robot.**

Keywords – Industrial Robot, Simulation, KUKA Sim Pro, Pick-and-Place, Cube, Education

Review Paper
DOI: 10.7251/ELS1721095L

I. Introduction

Comparing the simulation systems for robots of today with those of the 90s, it can be argued, that compared to the 90s, there are nowadays a lot of useful simulation systems which can be effortlessly used in the industrial practice and education. The rising offer of such simulation systems hangs immediately together up with the development of the IT technology and the computer engineering. As stated in [1], the middle and the end of the 90's have been marked by the use of the Java based systems. The main improvement of the robot simulation systems, has been caused by the development of the suitable simulation robot libraries, also of the libraries for older industrial robot models [2] which have been already mathematically well modelled in the 60's. There are many reasons nowadays why to use simulation systems in industrial practice. As stated by [3] by using of simulations wrong decisions can be avoided already in planning stadium and therefore they are sound decisive factor in the planning process. Furthermore they can save the costs because in the regularly case, the simulation costs are much lower as investment costs or the target cost of the real process. Behind it, simulation leads to a more quick solution than analytic procedures, detailed representation of the existing system can lead to new cognitions and often the simulation technology is generally the only analytical possibility to scrutinize the project, because a real realization of the model would not be possible in practice. All those are factors, which support the idea of the necessity of simulation systems' usage in the industry but also in the educational practices at school and/or universities. However, the successful use of such systems requires profound knowledge, not only about the simulation software itself, but also about the margin disciplines and branches of learning, which concern the real simulation problem. Especially the "3D fabric simulation is complex and its implementation requires knowledge in different fields" [4, p. 634]. In the following section, it will be, with the help of a practical problem formulation explained, how industrial robot simulation software can be used in the practical case.

Manuscript received: May 18th, 2017
Received in revised form: February 12th, 2018

Duško Lukač, Rheinische Fachhochschule Köln gGmbH, University of Applied Sciences, Vogelsanger Strasse 295, 50825 Köln, Deutschland, e-mail: dusko.lukac@rfh-koeln.de

Miljana Milić, Laboratory for Electronic Design Automation, Faculty of Electronic Engineering, University of Niš, Niš, Serbia, e-mail: miljana.milic@elfak.ni.ac.rs

II. System Components and Simulation Environment

The choose the suitable simulation software is one of the important decisions in the simulation practice. Different criteria influence this choice. Besides, is to be noted that there are, as a rule, slight decisive differences if the software is seated for industrial purposes or if it used for education purposes. The essential decisive factors for the simulation choice in the educational application are explained in [1]. At the market one can find different robot simulation systems. To find the right one for use requires the knowledge of the technical systems and also the knowledge about the industrial robot market. Some often used simulation application in robotics are presented in the following table:

Table I. Industrial Simulation Systems for Industrial Robots

Name of the application	Producer
RoboGuide	FANUC K.K.
RobotStudio	ABB AG
KUKA Sim	KUKA AG
CODESYS	3S-Smart Software Solutions GmbH

It is an interest of the university to educate students in that way that they become prepared for requirements of the industrial market. Therefore it is understandable that such robot systems and simulation applications should be used at the university, which are mostly implemented in the industrial companies. Due to those criteria and the vast amount of today's robot simulation applications today, in the following are briefly introduced four simulation applications, which are shortly mutually evaluated. These above named simulation applications of the companies FANUC K.K., ABB AG, KUKA AG and 3S-Smart-Smart Software Solutions GmbH are often used in the industrial applications. Furthermore it is to be pointed out that intermutually translation applications exist, as e.g. "SubitoRun", which enable translation of the application of the one company into other, here of FANUC GUI into KUKA GUI. Such translation modules exist also in the case of KUKA C4 interfaces which are translated into Siemens S7 GUI. Even translation of Siemens TIA portal exist, which is offered by "FTP Robotik" [9]. It indicates the necessity of the development of such specified translation-software market. Accordingly, especially hardware demands and the licensing conditions have to be taking into consideration [1, p. 1013]. Out of the different robot industrial simulation systems available on the market, as e.g. RoboGuide by FANUC or Robot Studio by ABB, the KUKA SIM Pro software has been used in the realization of the project described in this paper. The main reason for it, are the hardware demands, because simulation is applied to the existing industrial robot KUKA KR6 R900 sixx, which is also available in the library of the named simulation platform.

A. KUKA.Sim Pro

KUKA.Sim Pro is a special program for the creation of 3D-layouts of arrangements with KUKA industrial robots. Any layouts and draughts can be simulated and be examined with it. Therefore, the software system is appropriate for engineering or system integrators. The program library is extended compared with the older software versions and it disposes numerous smart components and geometries with own parametric behavior, as e.g. conveyor belts or light barriers. The software offers, also wide-ranging API and COM functionalities which allow the integration of the own plug-ins. An integration of the Python scripts is also pos-sible. Optionally are available possibilities for imports of dif-ferent CAD formats as Siemens NX, CATIA V5, STEP or Pro Engineer [5]. By using of the virtual machine, the KUKA SIM Pro software can be directly coupled with the real time programming software of KUKA, so called Office Lite application, so that simulated program application can be transferred to the real industrial robot system and can be tested under the real environmental conditions [6].

B. KR AGILUS R900 sixx

The KR AGILUS R900 sixx robot reaches maximum repeat accuracy and continuous precision thanks to his robust construction. It is known as one of the quickest robots of the world, what became successfully presented in numerous advertising campaigns of the KUKA Company [7]. At extreme speed the robot reduces the cycle times and on that way increases the manufacturing quality without getting out of the tact. The robot disposes with the highest precision characteristics on the smallest space thanks to his integrated energy supply and proven KR C4 compact control unit. Therefore this systems has been used in the following practical application, described in the next section. The main characteristics of the robot are summarized in the following table:

Table II. Main Characteristics of KR AGILUS R900 sixx

CHARACTERISTIC	VALUE
Nominal load / Maximal load	3 kg /6 Kg
Interfaces	USB, EtherNet, DVI-I
BUS connections	PROFINET, EtherNet/IP, PROFIBUS, DeviceNet, EtherCAT
Position repeat accuracy	+/- 0,03mm
Axis	6
Velocity with nominal load	300 °/s

III. Real Environment and Simulation

The real simulation environment is introduced in following block representation.

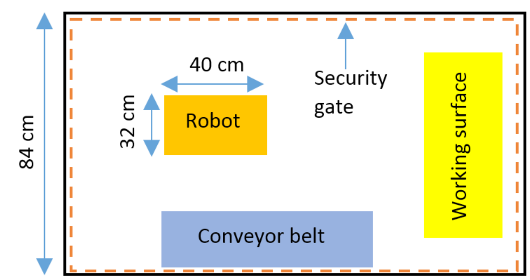

Fig. 1. Block represenataion of the real eviroment

Fig. 2. Robot system basic position

The purpose of the project is the creation of a program design in addition to the digital simulation of a really existing robot system in Sim KUKA Pro 2.2.2, using the available KUKA KR6 R900 sixx robot and conveyor belt connected with the robot control unit [8]. Once the robot and conveyor belt program are started, if not already in the basic position, the robot moves first in its basic position. This is presented in the Fig. 2. A conveyor belt, with integrated light barrier, transports an aluminium cube with the dimensions (HxWxD): 100 mm x 100 mm x 100 mm in the defined position. As soon as the conveyor belt is launched, the robot moves in the pre-position for removal of the cube and waits, till the workpiece interrupts the light barrier.

Fig. 3. Conveyor belt with aluminum cube

Then, it removes the cube from the defined position and places it, in the working surface in the form of a palletizing task.

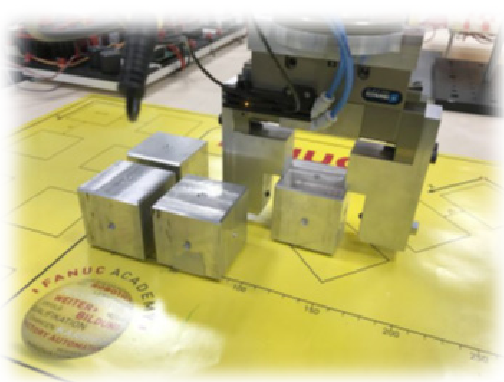

Fig. 4. Palletizing the cubes

This continuously task is repeated till all 11 cubes are palletized.

A. Control program extract

The extract of the real control program written in KUKA Robot Language used for this task and combined with the PLC control unit is presented in the following:

;1. First section
WAIT FOR (IN 7 , WORKPIECE CONVEYOR')
IF $IN [7]==TRUE THEN

WAIT Time=1 sec

PTP BAND1 Vel=100% PDAT10 Tool[1]:flange Base[0] OUT 1 'Gripper open' State=FALSE OUT 4 'Gripper closed' State=TRUE PTP UBAND1 CONT Vel=100% PDAT9 Tool[2] Base[0] PTP UP11 CONT Vel=100% PDAT6 Tool[1]:flange Base[0] PTP P11 Vel=100% PDAT8 Tool[1]:flange Base[0] OUT 4 'Gripper closed' State=FALSE OUT 1 'Gripper open' State=TRUE PTP UP11 CONT Vel=100% PDAT6 Tool[1]:flange Base[0] PTP UBAND1 Vel=100% PDAT9 Tool[2] Base[0]

ELSE END IF

The program waits on the workpiece at the removal position of the conveyer belt. This is realized with the WAIT FOR (IN 7 ‚WORKPIECE CONVEYOR‘) command. After the input signal reaches the logical TRUE condition, the robot waits one second and moves to the gripping position „PTP BAND1“. After, the grip arm is closed and with re-grinding the geometries of trajectories of the point over the decrease point of the conveyor belt, the position over the storage area of the workpiece is started up (PTP UP11). Also this point becomes again grinded, in order to form more smoothly program process. On the workpiece storage position P11 the grip arm is opened again, the workpiece is stored and the waiting position over the decrease point of the conveyor belt is started up. Now, here the robot waits again for a new workpiece. In the both next other processes the procedure is the same, merely the storage position of the workpiece changes.

B. Simulation components

This task has been simulated. In the first step of the simulation, the components of the cube robot have been defined. These are presented in the following simulation figure [9].

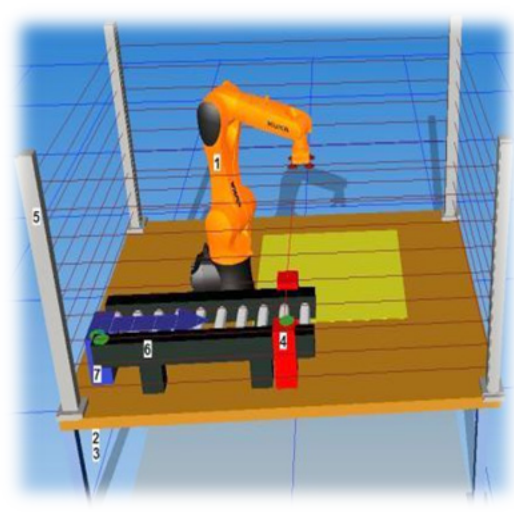

Fig. 5. Simulation components draft

The simulation components are numerated and presented in the following table.

Table III. Simulation components

POSITION	DESCRIPTION
1	Robot KR6 R900sixx
2	Control Unit
3	Peripherie
4	Sensor (H-Sensors)
5	Security Gate
6	Conveyor belt
7	Creator

All listed components are real, excluding the "Creator", which is software based simulation function for creating the cubes. All components are selected and composed from the program library of KUKA Sim Pro 2.2 Library [cf. 10]

IV. Robot programming with the Simulation software

The robot programming with the simulation software KUKA Sim Pro can be realized by using one the following approaches:

1. Programming with RSL „Robot Simple Language“
2. Programming with KUKA.Office-Lite
3. Programming with Work-Visual Software

Programming with RSL is a standard option of the KUKA Sim Pro visualization software. The Programming with KUKA. Office-Lite, requires the KUKA.Office-Lite software and realization of the connection link between KUKA.Office-Lite and KUKA Sim Pro software by virtual machine as e.g. with the VMware Workstation 12 Player [cf. 6]. Advantage of the KUKA. Office-Lite combined with the KUKA Sim Pro application is the possibility of the direct implementation of the program in the real environment because the KUKA.Office-Lite is, in fact, the HMI system for programming the KUKA robots. Programming with Work-Visual Software requires the software itself, and direct Ethernet connection to the control unit of the robot system with fitting configuration. Work-Visual Software, is the alternative programming environment offered and developed by the KUKA Company. In this project the programming has been done with RSL and KUKA.Office-Lite. Taking into account the nominal amount of the publication pages, the following description is limited to the description of the RSL programming. The detailed steps of programming are described in [10]. In order to write the program, at first the robot must be activated. For this purpose, two options are possible, activation by choice of a "sheet" on the robot foot or activation by direct choice of a robot in the tab "Teachen".

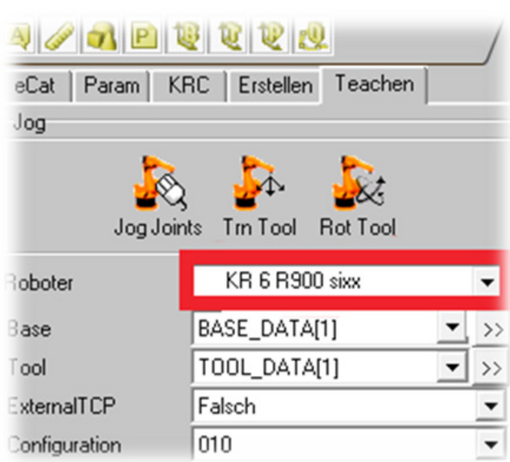

Figure 6. Activation of the robot

A. Main and subroutines

If the task is complex, it is recommended that subroutines containing similar characteristics are defined. The main sequence is already introduced by the simulation system. It is used for activation of the subroutines. For the realization of this task in total 13 subroutines have been written. Two of them, are linked with gripping functions, and two for conveyor band activation functions. The rest of the program written, is used for the positioning of the virtual cube at the defined position on the working surface. The sequences mentioned are presented in the following figure:

Fig. 7. Main and subroutines

The subroutines for gripping and release of the working piece, exist out of one instruction. The output necessary for gripping procedure and for release of the working piece, changes in this instruction the logical condition. This includes the definition of the gripping area, and becomes realized by changing the parameters of the robot. The subroutine BT1, contains the basic geometrical coordinates of the simulation space and is used for definition of the other subroutines in order to realize all gripping and release steps.

B. Signal exchange

In order to exchange the signals between robot, control unit and conveyor belt, the input and output periphery signals must be tied together. This occurs, in the so called connection editor.

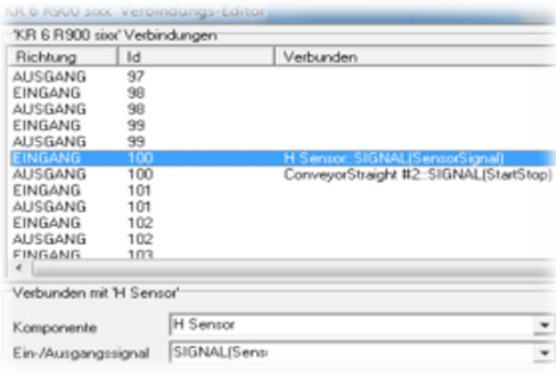

Fig. 8. Signal exchange

In the presented figure the connection between the robot and H-sensors with conveyor are presented. After following further adjustments necessary for creation of the simulation program, the final simulation has been realized. In-between, it is extend with visualization of the geometrical trajectories in order to show the differences between the movement types of the robot a for example point-to-point, cyclic or linear movement.

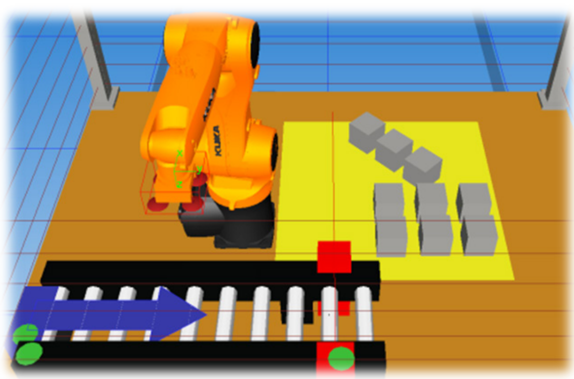

Fig. 9. Signal simulation without tracing signals

V. Conclusion

This paper presents a practical example of realization of the industrial robot simulation based on the real KUKA robot system. Furthermore, it includes initial explanation how peripheral actuators can be implemented in the process by means of the simulation software KUKA Sim Pro. The main effort in the simulation task, is related to the programming of the geometric trajectories and calculations of them. It in-cludes the transformation of the coordinates, by using of different coordination system transformation methods and including them into the program writing task. This part of the work is, by reason of the scale, not presented in this work. This is planned within the scope of next publications.

References

[1] Lukac, Dusko (2016), “Using Robot Simulation Applications at the University – Experiences with the KUKA Sim”, MIRPO IEEE Conference 2016, Opatija, Croatia, pp.1012-1016

[2] Tewkesbury, G. and Sanders,D. (1999) “A new robot command library which includes simulation”, Industrial Robot: An International Journal, Vol. 26 Iss: 1, pp.39 – 48

[3] Niessner, Helmut (2013), „Advantages of Simulations“, Simulations, available at http://simulutions.at/wp/index.php/2013/01/vorteile-von-simulationen/, 16.01.2017, 12:38h

[4] Mozafary, Vajiha and Payvandy, Pedram (2016) “Study and comparison techniques in fabric simulation using mass spring model”, International Journal of Clothing Science and Technology, Vol. 28 Iss: 5, pp.634 – 689

[5] KUKA AG (2017), „KUKA SIM Pro“, available at http://www.kuka-robotics.com/germany/de/products/software/kuka_sim/kuka_sim_detail/PS_KUKA_Sim_Pro.htm, 14.01.2017, 12:33h

[6] BBS Wolfsburg (2016), Guide for Configuration of KUKA.SimPro and KUKA.OfficeLite, Berufsbildende Schulen Wolfsburg, June 2016, pp.1.15

[7] http://www.ingenieur.de/Fachbereiche/Robotik/Tischtennis-Duell-Timo-Boll-Kuka-Roboter-PR-Ente

[8] Lukac, Dusko, Lenz,R., Siebertz, J. and Unruh, A. (2017) “Design concept for the Realization of the Cube-Robots with Simulation Software KUKA SIM Pro 2.2.2”, Project, Rheinische Fachhochschule Köln gGmbH, University of Applied Sciences, December/January 2016/17, pp.1-29

[9] Lukac, Dusko and Sperling, J. (2016), “Enhancement of the KR-Agilus robot with conveyor belt for positioning of the workpieces”, Fachhochschule Köln gGmbH, University of Applied Sciences, July - November 2016,pp.1-34

[10] KUKA College (2012), “KUKA.SIM 2.2 Pro”, KUKA Roboter AG, Version 08.06.2012,pp.1-91

Implementing Master Program on Digital Broadcasting and Broadband Technologies

Siniša Ilić, Mile Petrović, Branimir Jakšić, Slobodan Bojanić, Petar Spalević and Ranko Babić

Abstract — **The paper presents the mid-term results of the implementation of Master study program on Digital Broadcasting and Broadband Technologies in Western Balkans countries. In this period the teaching courses are developed and the corresponding laboratory equipment is acquired. The project takes part of the Erasmus+ program for Capacity Building in Higher Education. In the rest of the project lifetime the new courses will be carried out altogether with laboratory exercises.**

Index Terms — **Digital Broadcasting and Broadband Technologies, Western Balkans, Erasmus+, Capacity Building in Higher Education.**

Review Paper
DOI: 10.7251/ELS1721100I

I. Introduction

The paper presents the mid-term results of Erasmus+ project which aims to implement the modern master study programme and thus provide education for the specialists in the field of Digital Broadcasting and Broadband Technology [1]. This study profile is in line with the needs of labour market and upcoming transfer from Analogue to Digital Broadcasting in regional partner countries.

The graduated students will be capable to apply acquired knowledge in the business environment, to speed up digitising of broadcast services and to implement and maintain modern and improve existing Broadcast and Broadband Communication Systems. In this way, the long-term sustainability of the project will be achieved. To acquire theoretical and practical knowledge immediately applicable in the real circumstances, the new laboratories are created with appropriate hardware and software equipment for analysis and design of broadcasting and broadband systems with digital multimedia High-definition television (HDTV) studio and environment for implementation of digital services. This Master will improve existing state in the area of digital technologies (particularly in digitising of Radio and Television and improving of multimedia broadband services) in Western Balkans (WB) countries in accordance with the best practice [2] in European Union (EU).

The project will have an impact on the current state in the field of digital communications technologies in Kosovo (under UN resolution 1244), Bosnia and Herzegovina and Serbia due to the mandatory digitisation of broadcast services according to standards established by competent international organizations and adopted also by the EU. As a consequence, the development of digital communications technologies activates other business branches in the Western Balkans.

Therefore the project enables professional training for effective digitization of existing analogue services, maintenance, upgrading, innovation and technical sustainability of new digital services: Digital Video Broadcasting - Terrestrial (DVB-T), Digital Video Broadcasting - Handheld (DVB-H), Digital Audio Broadcasting (DAB), Digital Radio Mondiale (DRM), Digital Multimedia Broadcasting (DMB) and Hybrid Broadcast Broadband TV (HbbTV) for the region of Southeast Europe.

II. Background

International Telecommunication Union (ITU) at the Radio-Communication conference in Geneva (RRC-06) made a decision that all European countries (including countries of the former Yugoslavia) have obligation to no later than 17 June 2015 to change analogue video broadcasting with digital television and radio signals broadcasting [3].

Trough digitalization of analogue terrestrial television frequent spectrum become free for purpose of digital television and various digital services such as digital radio with supplement services, digital mobile TV and other mobile services with multimedia content.

All European and the Western Balkan countries committed to start digital terrestrial broadcasting by June 17^{th} 2015 the latest (by the acts of the Regional Radio Communication conference in Geneva RRC-06 organised by ITU) and stop with analogue broadcasting of TV signal. Many European countries have already started digital broadcasting and they already have some new digital services parallel to digital TV and Radio. The countries of south-east Europe: Serbia, Montenegro, Romania,

Manuscript received: May 18th, 2017
Received in revised form: February 7th, 2018

The paper is created within the project "Implementation of the study program – Digital Broadcasting and Broadband Technologies (Master studies)" that is co-funded by the Erasmus+ Programme of the European Union.

Siniša Ilić, Mile Petrović, Branimir Jakšić, Petar Spalević and Ranko Babić are with Faculty of Technical Sciences, University of Pristina in Kosovska Mitrovica, Serbia (phone: +381-28-425-325; fax: +381-28-425-322; e-mail: ({sinisa.ilic, mile.petrovic, branimir.jaksic, petar.spalevic, ranko.babic}@pr.ac.rs).

Slobodan Bojanić is with the ETSI Telelcomunicacion, Universidad Politecnica de Madrid, Spain (e-mail: slobodan.bojanic@upm.es).

*Kosovo under UN resolution 1244.

Albania and Greece have already started the process of transferring to digital broadcasting, but Bosnia and Herzegovina and Kosovo* have not yet [4].

According to the data of National Agencies for Radiocommunication, 21 TV and 83 Radio stations need to start digital broadcasting in Kosovo* [5], 43 TV and 141 Radio station in Bosnia and Herzegovina [6], 319 Radio stations in Serbia [7], 52 Radio stations in Montenegro [8], 79 Radio stations in Macedonia [9], and 69 Radio stations in Albania [10].

One of the reasons why digital broadcasting is not completed is the lack of experts and experience in this area. The number of specialists in WB countries is low compared to the number of needed digital services. By transferring to the digital broadcasting, the frequency range occupied by analogue broadcasting can be used for: digital TV, Radio, digital services, digital TV for mobiles and other services with multimedia content. Also, some additional broadband technologies can be used in this frequency spectrum. Broadband services (internet TV, 3G and 4G networks for mobile devices) in WB countries are implemented partially and compared to the EU countries in arrears in both: quality and quantity of services. The WB countries that aim to join EU will have to increase quality of broadcast and broadband services according to the standards of EU countries.

For the purpose of speeding up digitization of existing analogue services, maintenance, upgrading, innovation and technical sustainability of new digital services, University of Pristina - Faculty of Technical Sciences, Kosovska Mitrovica, Kosovo*, applied for Erasmus+ project under the name: Implementation of the study program Digital Broadcasting Technologies (DBBT) - Master studies. It is based on the fact that there is a lack of experts in the area of information and communication technologies (ICT) in the Western Balkan countries, especially in broadcast and broadband technologies.

The rapid increasing of the number of Radio and TV stations in transition period of WB countries and the lack of professionals resulted in lower quality of multimedia services. A large number of Broadcasting stations in Kosovo*, Serbia and Bosnia and Herzegovina do not respect quality standards for the moving images, sound and multimedia. The main reason is broadcasting of analogue signal. Transfer to the digital broadcasting will solve the problem of multimedia quality.

Therefore the project aims to introduce the new master study programmes for academic and vocational studies in the field of Digital Broadcasting and Broadband Technologies (DBBT) which is in line with the needs of business partners from the regional labour market and in line with modern study programmes from EU countries. The students will be able to apply their practical and theoretical knowledge immediately after graduation.

The graduated students will be able to develop the multimedia applications on smart phones and tablets, applications for smart TV, modelling of IP and wireless networks and wave propagation, etc. The master study programme enables formation of the specialists needed for the process of digitising, maintenance of the digital systems and introduction of new broadcast and broadband technologies in line with the needs of enterprises – potential employers.

The curricula of the study programme are implemented in master studies at universities in Kosovo (UN resolution 1244), Serbia and Bosnia and Herzegovina. The study programs are certified (accredited) by National certification bodies for Higher education. The project pursues the establishment of the infrastructure (organisational, methodological and technical) for implementation of developed study programmes (Fig. 1). It involves also the EU universities in order to transfer their experience in target area as well as certain local broadcast companies to designate the requirements for the future specialists.

III. Participating Universities

The consortium is composed of 10 Higher education institutions (HEI), 6 from WB and 4 from EU, and 3 industrial partners. Each participating WB country is presented with two Higher education institutions (HEI) interested to design the new modern curricula, and with one professional enterprise with competencies in broadcasting, multimedia creation and digital TV, available and suitable for students' internship and future employment. Also the partners from business are directly included in design of curricula specifications according to the business needs and thus have greater opportunity to find adequate future graduates.

Table I.
Course List at University of Pristina in Kosovska Mitrovica

Course	Semester	Mandatory /Elective	ECTS
Audio-Video Technologies	1	elective	6
Audio-Video Technologies	1	elective	6
Data Compression	1	elective	6
Digital TV Broadcasting	1	elective	6
IP Technologies	1	elective	6
Cable and Wireless Broadband Communications	1	elective	6
Sound Engineering	1	elective	6
Security Multimedia Systems	1	elective	6
Interactive Multimedia Applications	2	elective	6
Human and multimedia	2	mandatory	6
Student Internship	2	mandatory	2
Master thesis work	2	mandatory	16

Electives Courses – Semester 1: 5 out of 8
Electives Courses – Semester 2: 1 out of 2
Weeks in Semester: 15

University of Pristina in Kosovska Mitrovica (UPKM) is the project coordinator i.e. in charge for project management, financial management, coordination among partners and also the target user of developed study Master program. It is a higher education institution founded in 1969 and today has more than 10.000 students and 800 teachers and assistants and 350 non-teaching staff. Faculty of Technical Sciences (FTS) is one of 10 UPKM faculties, established by merging 4 technical faculties (Electrical, Mechanical, and Civil Engineering and Faculty of

Mining). Academic studies are based on Bologna education process and carried out at three levels. Faculty laboratories are carriers of practical exercises and scientific research work. Studies of electrical engineering and computer engineering are covered by departments of Power engineering, Electronics and Telecommunications, and the Computing and Informatics. Departments are specialized in digital signal processing, multimedia systems and applications, digital image processing, mobile communications, data protection, software engineering and network technology.

Higher Technical School of Professional Studies Zvečan is a state school founded in 1961, with a long tradition in education of technical personnel, as well as with developed transnational cooperation with similar institutions in the region. Throughout the school a thousands of students has passed, taught to become skilled professionals ready for all kinds of professional challenges. The goal is to maintain and improve the status of the leading high vocational school in this field in the Balkans. The evidence of quality is the license of the Ministry of Education of the Republic of Serbia. There are five study programmes in vocational studies (180 ECST): Energetic, Management in Electrical Engineering, Engineering Informatics, Production Management, Fire Protection. Also there are three study programmes in specialist studies (180+60 ECST): Energetics, Production Management, and Fire Protection. The School has a long record of engagement with industry, communities and external research partners.

Table II.
Course List at HTPSZ Zvecan

Course	Semester	Mandatory /Elective	ECTS
Multimedia systems	1	mandatory	6
Measuring in telecommunications	1	mandatory	6
Computer animation	1	elective	6
WEB programming	1	elective	6
Electric lighting design	1	mandatory	6
Human-computer interaction	1	mandatory	6
Image and sound digital editing	2	mandatory	5
Audio and video production	2	elective	5
Internet and wireless sensor networks	2	elective	5
Entrepreneurship and innovations	2	elective	5
Research marketing	2	elective	5
Professional practice	2	mandatory	5
Final thesis	2	mandatory	10

University of Banja Luka consists of 16 faculties and has 54 licensed study programs. The Faculty of Electrical Engineering (FEE) is the oldest faculty and offers 3 study programs at the 1st and 2nd study cycle. Since 2009 it has been organized the third cycle of ICT studies in collaboration with the University of Paderborn. Since the establishing of FEE, one of the main departments is the Department for telecommunications, which organized teaching in the field of radio and TV techniques. The FEE formed engineers who managed the production of analog TVs in the Cajavec factory (1966-1995). Most of the engineers who work today in the field of broadcasting, graduated at the FEE Banja Luka. Since 2014, the Institute RT-RK is established at FEE, and one of its activities is also a digital broadcasting software support.

University of Bihać was established in 1997. It has seven member units, 6 Faculties (Technical Faculty, Faculty of Pedagogy, Faculty of Law, Biotechnical Faculty, Islamic Faculty of Pedagogy and Faculty of Economy) and School of Health Studies. Total number of students is 4000. Teaching process at UNBI is organized through total 46 study programs, 27 study programs within 1st study cycle and 19 study programs within 2nd study cycle. At the Technical Faculty there are 5 Departments: Civil Engineering, Mechanical Sciences, Wood processing technology, Electromechanical Sciences, Textile Design and Technologies; the network of institutes and laboratories is wide.

Table III.
Course List at University of Bihac

Course	Semester	Mandatory /Elective	ECTS
Signall processing and Acoustics	1	mandatory	5
HD and 3D TV	1	mandatory	5
Wireless and satellite communications systems	1	mandatory	5
Multimedia TV systems	1	mandatory	5
Digital Image processing	1	elective	5
Broadcasting engineering	1	elective	5
Internet telephony and television	2	elective	5
DVB-X systems	2	elective	5
Audio-Video production	2	elective	5
Publishing research paper	2	elective	5
Master thesis	2	mandatory	20

Table IV.
Course List at University of Banja Luka

Course	Semester	Mandatory /Elective	ECTS
Digital broadcasting systems and technologies	1	mandatory	6
Digital TV receivers and DVB software	1	mandatory	6
Studio audio and video production	1	elective B1	6
Digital technologies for broadband access	1	elective B1	6
Advanced digital TV – middleware, interactive TV, IPTV	1	elective B1	6
Regulations, standards and radio monitoring	1	elective B1	6
Multimedia Web content	1	elective B2	6
Multimedia content search	1	elective B2	6
Graphics and animation	1	elective B2	6
Multimedia content security	1	elective B2	6
Modern application framework of digital TV receivers	1	elective B2	6
Human-computer interaction	1	elective B2	6
Research work	2	elective C	10
Student practice	2	elective C	10
Master thesis work	2	mandatory	20

B1, B2 – Students have to choose at least one course from the group B1.
C – Students have to choose one of two C options.

School of Electrical and Computer Engineering of Applied Studies, VISER, is the public higher education institution with more then 2500 students attending courses in seven different specializations at the first level of higher education and 5 different specializations at the second level of higher education of applied studies. VISER has particularly long tradition, as well as, well known reputation in the filed of applied studies in Telecommunications, Audio and Video Technologies and Computer Engineering. It is equipped with 24 different laboratories among which stand out Modern radiotone studio and HDTV studio. Through TEMPUS curriculum innovation project "Innovation and Implementation of the Curriculum Vocational Studies in the Field of Digital Television and Multimedia" VISER established very successful one year specialized study programme Multimedia and Digital Television.

Table V.
Course List at VISER

Course	Semester	Mandatory /Elective	ECTS
Research Methods	1	mandatory	6
Audio and video compression	1	elective	8
Digital communication systems	1	elective	8
Audio devices and systems	1	elective	8
Video devices and systems	1	elective	8
Interactive multimedia	1	elective	8
Digital radio and TV technologies	2	elective	8
Wireless systems technologies and protocols	2	elective	8
Signal processing	2	elective	8
Audio and video production systems	2	elective	8
Multimedia postproduction	2	elective	8
Student internship 1	2	mandatory	6
Broadcasting systems and technologies	3	elective	8
Multimedia internet transmission	3	elective	8
Communications standards and technologies	3	elective	8
Studio design	3	elective	8
Telecommunication measurements	3	elective	8
Student internship 2	3	mandatory	6
Entrepreneurship and Incentives in Electrical and Computer Engineering	3	elective	6
Electronic communication regulation	4	elective	6
Applied research work	4	mandatory	8
Master thesis work	4	mandatory	16

Singidunum University founded in 1999 is the first private university in the country to be awarded accreditation for the realization of bachelor's, master's and PhD degree programmes in three scientific-research fields: social sciences and humanities, technical sciences and natural sciences and mathematics. They put emphasis on the study programmes that require and support ICT implementation (Electrical Engineering and Computing, Advanced Cryptosystems, ICT, Informatics and Computing, Engineering Management). There are currently around 10 000 students enrolled. Lectures are held by over 400 eminent professors from the country and abroad. The University is also conducting undergraduate studies via distance learning platform.

Partners from the EU countries are involved to jointly and successfully develop study programme in the field od DBBT. The partners from EU have the large experience in successful education of students in the field of Information and Communication Technologies where Digital Broadcasting and Broadband Technologies are part of as well. Universities from EU countries have qualified experts, modern laboratories for studying and testing of Digital Broadcasting and Broadband Technologies, and rich experience in implementation of many projects in improving the higher education. The EU countries has successfuly transferred from analogue to digital broadcasting and they are also implementing new digital broadcasting and broadbandservices now. Also, the quality and quantity of these services are on advanced level. The EU partners have advanced knowledge of interactive multimedia applications on smart phones and tablets, networks modelling and radiocommunications engineering that is today the state of the art.

Table VI.
Course List at Singidunum University

Course	Semester	Mandatory /Elective	ECTS
Principles of digital broadcasting	1	mandatory	8
Communication networks and system design	1	mandatory	8
Principles of modern communication	1	elective	8
Digital image processing	1	elective	8
Study research work 1	1	mandatory	6
Broadband access networks	2	elective	6
Principles of wireless communication	2	elective	6
Digital TV Design	2	mandatory	10
Study research work 2	2	mandatory	4
Professional practice	2	mandatory	2
Master thesis work	2	mandatory	8

Technical University of Ostrava - Faculty of Electrical Engineering and Computer Science contributes in direction of the balanced education both theoretical and practical. They possess equipment which is very well suited for the project, such as many analysers in field of radio communications (DVB-T, PXI or USRP). More than ten years long history of study branch "Mobile Technology" in Technical University of Ostrava, results and a reputation of staff provide an essential contribution to the project.

University of Ljubljana - Laboratory for Telecommunications at the Faculty of Electrical Engineering (LTFE) team has extensive experience in development and deployment of interactive multimedia applications on a number of interactive platforms (iOS, Android, smart TV, HbbTV, etc.). Additionally, they have equipment for DVB-T broadcasting and studio production, which is being used for project development as well as for teaching purposes. In addition to student training and education, they have extensive experience in industry training and transfer of knowledge to production oriented environments.

Universidad Politecnica de Madrid and its ETSI Telecommunication (Superior Technical School of Telecommunication) extensive teaching and research facilities in courses on digital television, handling multimedia information as well as TV and HDTV signals, visual static and dynamic information encoding, etc. so it contributes fully on capacity building of the partnering universities and also on all other project activities due to previous experience in wide range of similar projects.

University of Tartu through the Institute of Technology as the part of the Faculty of Sciences and Technology of has a lot of experience in digital image and signal processing that proves with a number of scientific papers and the knowledge that can be used in this project especially in the area of efficient transmission of the signal.

TV Mreža is an association of 5 TV stations and independent production. It was established in 2009 in Priština and consists of TV Mir /Peace/ in Leposavić, TV Most /Bridge/ in Zvečan, TV Puls /Pulse/ in Šilovo, Gjilan/Gnjilane municipality, TV Herc /Hertz/ in Štrpce (regional TV station broadcasting program for viewers in the East, Central and North Kosovo), and New Press Production in Čaglavica. Programs of the TV Mreža are available for viewing to most members of the Serb ethnicity communities in Kosovo and other citizens using Serbian language. It is estimated that all members of the TV Mreža together cover more than 80 % of the territory of Kosovo*. TV Mreža is "en course" to develop its own and unique TV program, branded as "independent TV Mreža program".

JP Emisiona tehnika i veze (JP ETV) is broadcasting media network service. It is the national broadcasting operator of the Republic of Serbia whose core business is wireless telecommunications, and the main task is planning, building and maintenance of transmission infrastructure on the territory of Serbia, providing radio and television broadcasting services to the home radio and TV receivers. JP ETV established digital terestrial network for free multiplex, based on DVB-T2 system as standard for digital broadcasting and MPEG-4 version 10 (H.264/AVC) as compression standard, which consists of 208 transmitting location for first multiplex and 89 transmitting sites for second and third mux, and which covering more than 95% of population in each allotment zone for the first MUX, and more than 90% of population in the other two multiplex.

Alternativna televizija (ATV) has 17 years in business and over 110 employees. It is one of the leading broadcasters in the Republic of Srpska and the first in the Banja Luka region, and the first commercial broadcaster to build own TV home. ATV broadcasts 24 hours a day, 30% of programming is ATV produced, which includes the best rated and most influential news and current affairs shows, with terrestrial coverage with 1,5 million people in BH and neighboring countries: the Republic of Srpska, north-west of Federation BH, border areas in Croatia and Serbia. ATV can be seen also on IPTV (m:tel and BH Telecom), cable operators, satellite (Total TV) and internet (Bosnia TV). Thus the role of ATV in the project is to transfer knowledge and expirience to higher education institutions staff and students and help in designing the new curricula in the field of digital broadcasting according to the needs in labour market.

II. Developed Courses

The universities, both from EU and Western Balkan countries, analysed study programmes of counterparts, compared them and with assistance of business partners with the view from the labour market, defined the guidelines for design of new curricula (Tables I-VI).

The representatives of WB universities carried out study visits at EU partner HEIs and got trained by corresponding EU professors, getting the adequate knowledge to design the curricula for new study programmes and to start teaching newly introduced study programme after WB HEIs got accreditation from National accreditation body.

The knowledge that students gain through the studies is both theoretical and practical because the DBBT laboratory will be set up during the project. Also, the partnership protocol will be signed between HEIs and regional business partners for the students' internships and among partner HEIs for long-term cooperation on teachers' and students' mobility.

As the project develops curricula for academic and vocational master studies in the field of DBBT, the new curricula are in line with those used at the world's leading schools in the field and in concordance with the Europe 2020 strategy, the Strategic Framework for European Cooperation in Education and Training and the Bologna process.

The teaching of all courses in curricula is based on the use of contemporary teaching methods, such as problem based learning, game based learning, case study method, etc. Courses are organised using blended learning concept – a combination of traditional and e-learning concepts. All course materials and activities will be available to students through a distance learning system. During their studies, students will be involved in practical work and internships in broadcast & broadband companies that participate in the project.

After setting up methodological bases for curricula development and development of curricula for academic and vocational master studies, methodology for implementation of study programmes is set up, equipment purchase and installation in laboratoriess is carried out.

Also in the second year of project the activities concerning the introduction of study programmes like accreditation at National Accreditation offices, training of the teachers and enrolment of students are being carried out. The third project year will be dedicated to the activities of teaching and learning within innovated and designed study programmes, as well as evaluation of students' success and their feedback. All project deliverables have public acess.

III. Equipment

In order to students gain theoretical and practical knowledge that can be applied immediately after the graduation, the laboratories are set up at all universities of WB countries. The laboratories are equipped with appropriate hardware and software infrastructure for analysis of broadcasting& broadband technologies and, digital multimedia HDTV studio with appropriate equipment needed for implementation of digital multimedia services.

Since UPKM is particular target university for the implementation of the Master and setting up the laboratories, in this paper, the equipment corresponding to the HDTV studio (Fig. 1.) at UPKM is presented, although all other universities have equipped their laboratories.

Equipment purchased at UPKM is presented in the following tables:

- Video equipment (Table VII),
- Audio equipment (Table VIII),
- Computers (Table IX),
- Lighting equipment (Table X),
- Measuring equipment (Table XI), and
- Installation equipment (Table XII).

Table VII.
Video Equipment

Type	Pieces
Camcorder HD / 4K	3
Console: ATEM 1, Broadcast panel	1
Video Mixer: ATEM 2 M/E Production Studio 4K	1
Matrix: Smart Videohub 20 x 20 za 4K	1
Controls Matrix: Video-hub Master Control	1
Controls: Video-hub Smart Control	1
Conversion: Mini Converter HDMI – SDI 4K	3
Conversion: Mini Converter SDI – HDMI 4K	1
Conversion: Mini Converter SDI to Audio 4K (embeder)	1
Conversion: Mini Converter Audio to SDI 4K (deembeder)	1
Recorder: Hyper Deck Studio	1
2,5” SATA 3Gb/s 500GB	2
Communication: Data Video ITC 100	1
GPI/Tally Interface	1
LG 40UF695V LED UHD 4K Smart	5
LG 43UF680V LED UHD 4K Smart	4
Bracket LED monitor for 32” to 63”	8
HDMI extender up to 60m	8
HDMI switch 5-IN/2-OUT	1
HDMI splitter 1-IN/4-OUT	1
USB 1.1 & 2.0 extender up to 50 m	3
Computer Switch 1-IN/5 OUT	1
Encoder MSE - RS265	1
Decoder BD - RS 265	1
Camera: Canon EOS 100D 18-55IS	1
Camera: Panasonic Lumix DMC-GH4	1
4K Video Jackfields 2X26 (4K Video Patch Panels)	1
Patch Cable 0.5 m	20

Table VIII.
Audio Equipment

Type	Pieces
Digital Mixer: Behringer x32 Compact	1
Studio Monitor 5”: Fluid Audio F5	1
Studio Monitor 8”: Fluid Audio FX8	1
AKG Perception Wireless 45 Presenter Set	3
AKG Perception Wireless 45 Vokal Set	1
Microphone: Sennheiser MD-46	1
Microphone: Rode NT1-A set	1
Studio Headphones: Superlux HD-681 Evo	3
Studio Headphones: Superlux HD-669	5
Telephone Hybrid	1
Smartphone or Tablet	3
Bluetooth Headphones with Microphone for Smartphone or Tablet	3

Table IX.
Computer Equipment

Type	Pieces
Computers (destop or lap top, for the installation measuring equipment and software)	6
Computer (laptop) with Gigabit Ethernet port	1
Monitor for Computers: Samsung S 24C300HS	6
Keyboard and Mouse	6
Speakers for Computers: GENIUS SP-HF500	4
Speakers for Computers: GENIUS SP-M200	2
Speaker: Genius SW-HF5.1 4800	1
DeckLink 4K Extreme Card	1
DeckLink Studio 4K Card	1
Blackmagic UltraScope (PCIe card Mac OS X and PC hosted waveform monitoring with 6 simultaneous scopes)	1
D-LINK DES-1005D 5-Port Fast Ethernet Unmanaged Switch HDMI splitter (mini)	1
CKL HD-94M 1-IN/4-out, Fully HDMI 1.4 Complaint up to 1080p	1
Software: Elements Systems Playout 1	1
Software: V Mix 1	1
Software: Wowza Streaming Engine 1	1

Table X.
Lighting Equipment

Type	Pieces
Fluorescent softlights 4 lamps 55W, 3200K, with standard accessories	4
Fluorescent softlights 2 lamps 55W, 3200K, with standard accessories	4
Digital Luxmeter	1
Instrument for measuring the color temperature	1
DMX Controler	1
Chroma Key Green Screen 3x6 m	1

Table XI.
Measuring Equipment

Type	Pieces
DTA-2115 All-standard all-band modulator for PCIe or DTU-215-T2-SP USB-2 VHF/UHF modulator with modulation and StreamXpess	1
T2Xpress DVB-T2 signal generator software	1
DiviCatch RF-T/C T2/C2, DVB-T DVB-C DVB-T2 DVB-C2 Professional RF Analyzer	1
Meter Field and Spectrum Analyzer Televes H60	1
Professional DVB TS multiplexer ASI/TS Multiplexer 8 ASI in ASI out	1
TBS6910 DVB-S2 Dual Tuner Dual CI PCIe Card	1
INTEX TV/FM USB DVB-T/T2 HDTV PCIe Card	1
LEADTEK WinFast TV2000 XP Global TV/FM	1
DVB-S2 receiver Amiko HD8150	1
Combo Receiver DVB-T2/C Amiko Imuplse T2/C 1 Internet IPTV / DVB-S2 Combo Receiver	1
Amiko mini HD combo receiver dvb-s2 dvb-t2	1
DVB-T2 PCTV nanostick HDTV tuner SMA-BulkHeadCable	1
RTL2832U + R820T Mini DVB-T + DAB+ + FM USB Digital TV Dongle	1
Hot DVB-T2 Digital USB TV Stick Tuner Satellite receiver DVB T2 USB 2.0 TV Receiver Support DVB-T DVB-C FM DAB	1
DRM Receiver	1
DTU-245-SY-SXP FantASI USB-2 ASI/SDI, DtGrabber+, SdEye, StreamXpert and StreamXpress (adapter for analysis, generation and monitoring ASI and SD-SDI video streams and MPEG-2 transport stream)	2
SDR ETTUS Research USRP N210	2
DVB-T2 PCTV nanostick HDTV tuner	1

Type	Pieces
RTL2832U + R820T Mini DVB-T + DAB+ + FM USB Digital TV Dongle	1
Hot DVB-T2 Digital USB TV Stick Tuner Satellite receiver DVB T2 USB 2.0 TV Receiver Support DVB-T DVB-C FM DAB	1
DRM Receiver	1
DTU-245-SY-SXP FantASI USB-2 ASI/SDI, DtGrabber+, SdEye, StreamXpert and StreamXpress (adapter for analysis, generation and monitoring ASI and SD-SDI video streams and MPEG-2 transport stream)	1
SDR ETTUS Research USRP N210	1
CardSBX 400MHz-4,4GHz	1
SMA-BulkHeadCable	2
VERT900 Antenna	2

Table XII.
Installation Equipment

Type	Pieces
Rack 800x800/600	2
Shelf fixed heavy duty - for the rack depth 800 mm	8
L carriers for supporting equipment - for rack depth of 800 mm (pair)	8
Blank panel 1U/19”	4
Blank panel 2U/19”	8
220V junction boxes	6
Cable FTP kabl kat. 6 DRAKA tip UC400 S27 4P FRNC	100 m
Connector RJ-45 connector FTP/STP cat. 6 – shielded, 8P8C 8-pin	60
HD/SDI Video cable Belden 1855	100 m
HD/SDI Video cable Belden 1505 flexi 50 mConnector BNC for cable as Belden 1855	100
Connector BNC for cable as Belden 1505 flex	15
Connector XLR-F Neutrik NC3FD-LX	15
Connector XLR-M Neutrik NC3MD-LX	15
Connector XLR-F Neutrik NC5FD-LX	15
Connector HDMI Neutrik NAHDMI-W	15
Connector BNC Neutrik NBB75DFI Isolated	15
Connector XLR-F Neutrik 15	15
Connector XLR-M Neutrik 15	15
Connector XLR-M 5 pin NC5MXX 10	10
ConnectorTRS Neutrik 15	15
Connector RCA Neutrik 15	15
Audio multicore 16 line	30 m
Microphone cable	50 m

IV. Conclusion

The master study programme in the field of Digital Broadcasting and Broadband Technology is being implemented in the Western Balkans countries through the Erasmus+ project DBBT to enableeducation of specialists needed in the process of transfer of analogue to digital broadcasting, maintenance of digital systems and introducing of new broadcasting and broadband technologies. In this way, also the process of digitizing the broadcast services will be accelerated as well as the development of digital communications technologies will be followed by activation of other business opportunities in the Western Balkans. The graduated students will be able to apply acquired knowledge in the labour market since they will acquire

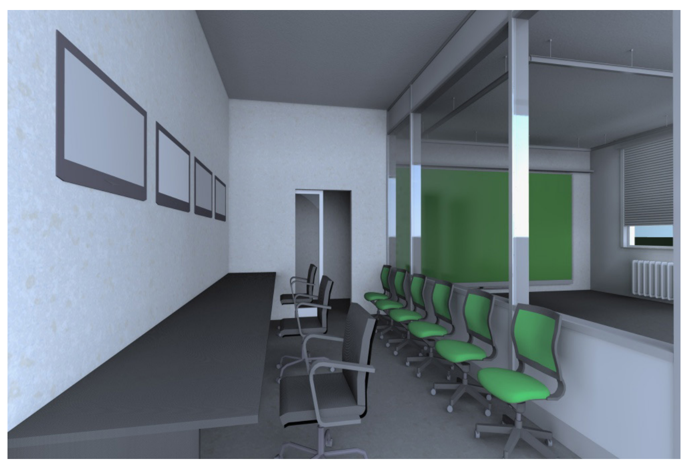

Fig. 1. HDTV studio at University of Priština in Kosovska Mitrovica

the knowledge how to introduce and maintain modern and to improve existing broadcasting and broadband communication systems, and also how to develop the multimedia applications on smart phones and tablets, applications for smart TV, modelling of IP and wireless networks and wave propagation, etc

The laboratories with appropriate hardware and software equipment for analysis and design of broadcasting and broadband systems with digital multimedia, HDTV studio and environment for implementation of digital services are being created. The formation of the experts will improve the existing state in the area of digital technologies, particularly in digitising of Radio and TV, and multimedia broadband services in WB countries in accordance with the best EU practice. The Master will impact the current state in the field of digital communications technologies in WB countries due to mandatory digitisation of broadcast services according to standards established by international organizations and adopted also by the EU.

References

[1] DBBT project: www.dbbt.pr.ac.rs.

[2] The Education, Audiovisual and Culture Executive agency EACEA: https://eacea.ec.europa.eu/erasmus-plus/funding/key-action-2-capacity-building-in-field-higher-education-2015_en.

[3] M. Petrović, B. Jakšić, I. Milošević, V. Trifunović, B. Gara, ″Pregled DVB-T u zemljama bivše Jugoslavije″, *Zbornik radova XII međunarodnog naučno-stručnog simpozijuma INFOTEH 2013*, Jahorina, Bosna i Hercegovina, 20-22 mart 2013, Vol. 12, pp. 354-359.

[4] B. Jaksic, M. Petrovic, M. Smilic, B. Gvozdic, A. Markovic, ″Terrestrial Digital Transmission of the High-Definition Television in Europe″, *Proceedings of the 23 International Electrotechnical and Computer Science Conference ERK 2014*, Portorož, Slovenia, 20-24 September 2014, pp. A: 61-64.

[5] Independent media commission: www.kpm-ks.org

[6] Communications Regulatory Agency BiH: www.rak.ba

[7] Regulatory Agency for Electronic Communications and Postal Services: www.ratel.rs

[8] Agency for Electronic Media of Montenegro: www.ardcg.org

[9] The Agency for electronic communications: www.aek.mk

[10] Authority for electronic communications and postal services: www.akep.al

[11] Budget allocation regional and national priorities protected: https://eacea.ec.europa.eu/sites/eacea-site/files/budget-allocation-regional-and-national-priorities-protected.xls

Instructions for Authors

First A. Author, Second B. Author, and Third C. Author

***Abstract*—These instructions give you guidelines for preparing papers for ELECTRONICS journal. Use this document as a template if you are using Microsoft *Word* 6.0 or later. Otherwise, use this document as an instruction set. The electronic file of your paper will be formatted further. Define all symbols used in the abstract. Do not cite references in the abstract. Do not delete the blank line immediately above the abstract; it sets the footnote at the bottom of this column.**

***Index Terms*—About four key words or phrases in alphabetical order, separated by commas.**

I. Introduction

THIS document is a template for Microsoft *Word* versions 6.0 or later.

When you open the file, select "Page Layout" from the "View" menu in the menu bar (View | Page Layout), which allows you to see the footnotes. Then, type over sections of file or cut and paste from another document and use markup styles. The pull-down style menu is at the left of the Formatting Toolbar at the top of your *Word* window (for example, the style at this point in the document is "Text"). Highlight a section that you want to designate with a certain style, then select the appropriate name on the style menu. The style will adjust your fonts and line spacing. **Do not change the font sizes or line spacing to squeeze more text into a limited number of pages.** Use italics for emphasis; do not underline. The length of the manuscript is limited to the maximum of 15 pages.

To insert images in *Word,* position the cursor at the insertion point and either use Insert | Picture | From File or copy the image to the Windows clipboard and then Edit | Paste Special | Picture (with "float over text" unchecked).

We will do the final formatting of your paper.

II. Procedure for Paper Submission

A. Review Stage

The manuscripts are to be delivered to the editor by e-mail: els-journal@etf.unibl.org. Prepare it in two-column format as shown in this template. Place all figures and tables at the end of the paper (after the references) on separate page(s). Figures and tables must have the same caption names as referenced in the text. Only PDF format of the manuscript is allowed at the review stage. Please, check if all fonts are embedded and subset and that the quality of diagrams, illustrations, and graphics is satisfactory. Failing to provide above listed requirements is a valid reason for rejection.

B. Final Stage

When you submit your final version (after your paper has been accepted), prepare it in two-column format, including figures and tables in accordance with this template. Pack all of your files (manuscript source file in *Word*, figures, and manuscript PDF form) within one archive file (you may use any of the available file compression tools: *WinZip*, *WinRAR*, *7-Zip*, etc.). Do not forget to provide the manuscript converted in PDF format that will be used as a reference for final formatting of your paper. Figures should be named as referenced in the manuscript (e.g. *fig1.eps*, *fig2.tif*, etc.)

C. Figures and Tables

Format and save your graphic images using a suitable graphics processing program and adjusts the resolution settings. We accept images in the following formats: PS, EPS, TIFF, GIF, and PNG. Additionally, it is allowed to use images generated by using one of the following software tools: Microsoft Word, Microsoft PowerPoint, or Microsoft Excel. The resolution of a RGB color file should be 400 dpi. Please note that JPG and other lossy-compressed image formats are not allowed. Use available software tools to convert these images to appropriate format.

Image quality is very important to how yours graphics will reproduce. Even though we can accept graphics in many formats, we cannot improve your graphics if they are poor quality when we receive them. If your graphic looks low in quality on your printer or monitor, please keep in mind that cannot improve the quality after submission.

Manuscript received 15 September 2011 (write the date when you have first sent the manuscript for review). Received in revised form 20 October 2011 (write the date when you have sent the manuscript in its revised form if revisions required for your paper after review).

(Place here any sponsor and financial support acknowledgments).

F. A. Author is with the Faculty of Electrical Engineering, University of Banja Luka, Banja Luka, Bosnia and Herzegovina (corresponding author to provide phone: +387-51-222-333; fax: +387-51-111-222; e-mail: author@etfbl.net).

S. B. Author was with Faculty of Technical Sciences, University of Novi Sad, Novi Sad, Serbia. He is now with the Institute "Mihailo Pupin", Belgrade, Serbia (e-mail: author@pupin.rs).

T. C. Author is with the School of Electrical Engineering, University of Belgrade, Belgrade, Serbia, on leave from the Faculty of Electronic Engineering, University of Niš, Niš, Serbia (e-mail: author@elfak.ni.ac.rs).

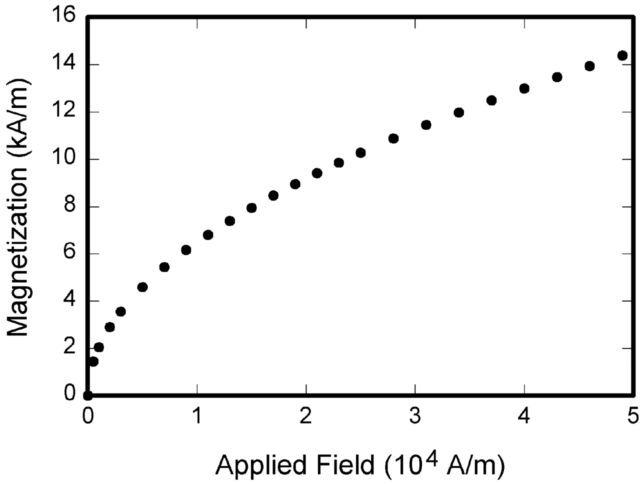

Fig. 1. Magnetization as a function of applied field. Note that "Fig." is abbreviated. There is a period after the figure number, followed by two spaces. It is good practice to explain the significance of the figure in the caption.

If you are importing your graphics into this Word template, please use the following steps:

Under the option EDIT select PASTE SPECIAL. A dialog box will open, select paste picture, then click OK. Your figure should now be in the Word Document.

If you are preparing images in TIFF, EPS, or PS format, note the following. High-contrast line figures and tables should be prepared with 600 dpi resolution and saved with no compression, 1 bit per pixel (monochrome).

Photographs and grayscale figures should be prepared with 300 dpi resolution and saved with no compression, 8 bits per pixel (grayscale).

Most charts graphs and tables are one column wide (3 1/2 inches or 21 picas) or two-column width (7 1/16 inches, 43 picas wide). We recommend that you avoid sizing figures less than one column wide, as extreme enlargements may distort your images and result in poor reproduction. Therefore, it is better if the image is slightly larger, as a minor reduction in size should not have an adverse affect the quality of the image.

III. Math

If you are using *Word,* use either the Microsoft Equation Editor or the *MathType* add-on (http://www.mathtype.com) for equations in your paper (Insert | Object | Create New | Microsoft Equation *or* MathType Equation). "Float over text" should *not* be selected.

IV. Units

Use either SI (MKS) or CGS as primary units. (SI units are strongly encouraged.) English units may be used as secondary units (in parentheses). **This applies to papers in data storage.** For example, write "15 Gb/cm^2 (100 Gb/in^2)." An exception is when English units are used as identifiers in trade, such as "3½-in disk drive." Avoid combining SI and CGS units, such as current in amperes and magnetic field in oersteds. This often leads to confusion because equations do not balance dimensionally. If you must use mixed units, clearly state the units for each quantity in an equation.

TABLE I
Units for Magnetic Properties

Symbol	Quantity	Conversion from Gaussian and CGS EMU to SI [a]
Φ	magnetic flux	1 Mx $\rightarrow 10^{-8}$ Wb $= 10^{-8}$ V·s
B	magnetic flux density, magnetic induction	1 G $\rightarrow 10^{-4}$ T $= 10^{-4}$ Wb/m^2
H	magnetic field strength	1 Oe $\rightarrow 10^3/(4\pi)$ A/m
m	magnetic moment	1 erg/G = 1 emu $\rightarrow 10^{-3}$ A·m^2 $= 10^{-3}$ J/T
M	magnetization	1 erg/(G·cm^3) = 1 emu/cm^3 $\rightarrow 10^3$ A/m
$4\pi M$	magnetization	1 G $\rightarrow 10^3/(4\pi)$ A/m
σ	specific magnetization	1 erg/(G·g) = 1 emu/g $\rightarrow$ 1 A·m^2/kg
j	magnetic dipole moment	1 erg/G = 1 emu $\rightarrow 4\pi \times 10^{-10}$ Wb·m
J	magnetic polarization	1 erg/(G·cm^3) = 1 emu/cm^3 $\rightarrow 4\pi \times 10^{-4}$ T
χ, κ	susceptibility	$1 \rightarrow 4\pi$
χ_ρ	mass susceptibility	1 cm^3/g $\rightarrow 4\pi \times 10^{-3}$ m^3/kg
μ	permeability	$1 \rightarrow 4\pi \times 10^{-7}$ H/m $= 4\pi \times 10^{-7}$ Wb/(A·m)
μ_r	relative permeability	$\mu \rightarrow \mu_r$
w, W	energy density	1 erg/cm^3 $\rightarrow 10^{-1}$ J/m^3
N, D	demagnetizing factor	$1 \rightarrow 1/(4\pi)$

Vertical lines are optional in tables. Statements that serve as captions for the entire table do not need footnote letters.

[a]Gaussian units are the same as cgs emu for magnetostatics; Mx = maxwell, G = gauss, Oe = oersted; Wb = weber, V = volt, s = second, T = tesla, m = meter, A = ampere, J = joule, kg = kilogram, H = henry.

The SI unit for magnetic field strength H is A/m. However, if you wish to use units of T, either refer to magnetic flux density B or magnetic field strength symbolized as $\mu_0 H$. Use the center dot to separate compound units, e.g., "A·m^2."

V. Helpful Hints

A. Figures and Tables

Because we will do the final formatting of your paper, you do not need to position figures and tables at the top and bottom of each column. In fact, all figures, figure captions, and tables can be at the end of the paper. Large figures and tables may span both columns. Place figure captions below the figures; place table titles above the tables. If your figure has two parts, include the labels "(a)" and "(b)" as part of the artwork. Please verify that the figures and tables you mention in the text actually exist. **Please do not include captions as part of the figures. Do not put captions in "text boxes" linked to the figures. Do not put borders around the outside of your figures.** Use the abbreviation "Fig." even at the beginning of a sentence. Do not abbreviate "Table." Tables are numbered with Roman numerals.

Color printing of figures is not available Do not use color unless it is necessary for the proper interpretation of your figures.

Figure axis labels are often a source of confusion. Use words rather than symbols. As an example, write the quantity "Magnetization," or "Magnetization *M*," not just "*M*." Put units in parentheses. Do not label axes only with units. As in Fig. 1, for example, write "Magnetization (A/m)" or "Magnetization ($A \cdot m^{-1}$)," not just "A/m." Do not label axes with a ratio of quantities and units. For example, write "Temperature (K)," not "Temperature/K."

Multipliers can be especially confusing. Write "Magnetization (kA/m)" or "Magnetization (10^3 A/m)." Do not write "Magnetization (A/m) × 1000" because the reader would not know whether the top axis label in Fig. 1 meant 16000 A/m or 0.016 A/m. Figure labels should be legible, approximately 8 to 12 point type.

B. References

Number citations consecutively in square brackets [1]. The sentence punctuation follows the brackets [2]. Multiple references [2], [3] are each numbered with separate brackets [1]–[3]. When citing a section in a book, please give the relevant page numbers [2]. In sentences, refer simply to the reference number, as in [3]. Do not use "Ref. [3]" or "reference [3]" except at the beginning of a sentence: "Reference [3] shows ... ." Please do not use automatic endnotes in *Word*, rather, type the reference list at the end of the paper using the "References" style.

Number footnotes separately in superscripts (Insert | Footnote).[1] Place the actual footnote at the bottom of the column in which it is cited; do not put footnotes in the reference list (endnotes). Use letters for table footnotes (see Table I).

Please note that the references at the end of this document are in the preferred referencing style. Give all authors' names; do not use "*et al*." unless there are six authors or more. Use a space after authors' initials. Papers that have not been published should be cited as "unpublished" [4]. Papers that have been accepted for publication, but not yet specified for an issue should be cited as "to be published" [5]. Papers that have been submitted for publication should be cited as "submitted for publication" [6]. Please give affiliations and addresses for private communications [7].

Capitalize only the first word in a paper title, except for proper nouns and element symbols. For papers published in translation journals, please give the English citation first, followed by the original foreign-language citation [8]. All references **must be** written in Roman alphabet.

C. Abbreviations and Acronyms

Define abbreviations and acronyms the first time they are used in the text, even after they have already been defined in the abstract. Abbreviations such as IEEE, SI, ac, and dc do not have to be defined. Abbreviations that incorporate periods should not have spaces: write "C.N.R.S.," not "C. N. R. S." Do not use abbreviations in the title unless they are unavoidable (for example, "IEEE" in the title of this article).

[1]It is recommended that footnotes be avoided (except for the unnumbered footnote with the receipt date and authors' affiliations on the first page). Instead, try to integrate the footnote information into the text.

D. Equations

Number equations consecutively with equation numbers in parentheses flush with the right margin, as in (1). First use the equation editor to create the equation. Then select the "Equation" markup style. Press the tab key and write the equation number in parentheses. To make your equations more compact, you may use the solidus (/), the exp function, or appropriate exponents. Use parentheses to avoid ambiguities in denominators. Punctuate equations when they are part of a sentence, as in

$$\begin{aligned}\int_0^{r_2} F(r,\varphi)\, dr\, d\varphi &= [\sigma r_2 / (2\mu_0)] \\ &\quad \cdot \int_0^{\infty} \exp(-\lambda\, |z_j - z_i|)\, \lambda^{-1} J_1(\lambda r_2)\, J_0(\lambda r_i)\, d\lambda\,.\end{aligned} \tag{1}$$

Be sure that the symbols in your equation have been defined before the equation appears or immediately following. Italicize symbols (*T* might refer to temperature, but T is the unit tesla). Refer to "(1)," not "Eq. (1)" or "equation (1)," except at the beginning of a sentence: "Equation (1) is ... ."

E. Other Recommendations

Use one space after periods and colons. Hyphenate complex modifiers: "zero-field-cooled magnetization." Avoid dangling participles, such as, "Using (1), the potential was calculated." [It is not clear who or what used (1).] Write instead, "The potential was calculated by using (1)," or "Using (1), we calculated the potential."

Use a zero before decimal points: "0.25," not ".25." Use "cm^3," not "cc." Indicate sample dimensions as "0.1 cm × 0.2 cm," not "0.1 × 0.2 cm^2." The abbreviation for "seconds" is "s," not "sec." Do not mix complete spellings and abbreviations of units: use "Wb/m^2" or "webers per square meter," not "webers/m^2." When expressing a range of values, write "7 to 9" or "7-9," not "7~9."

A parenthetical statement at the end of a sentence is punctuated outside of the closing parenthesis (like this). (A parenthetical sentence is punctuated within the parentheses.) In American English, periods and commas are within quotation marks, like "this period." Other punctuation is "outside"! Avoid contractions; for example, write "do not" instead of "don't." The serial comma is preferred: "A, B, and C" instead of "A, B and C."

If you wish, you may write in the first person singular or plural and use the active voice ("I observed that ..." or "We observed that ..." instead of "It was observed that ..."). Remember to check spelling. If your native language is not English, please get a native English-speaking colleague to carefully proofread your paper.

VI. Some Common Mistakes

The word "data" is plural, not singular. The subscript for the permeability of vacuum μ_0 is zero, not a lowercase letter "o." The term for residual magnetization is "remanence"; the adjective is "remanent"; do not write "remnance" or "remnant." Use the word "micrometer" instead of "micron." A graph within a graph is an "inset," not an "insert." The word "alternatively" is preferred to the word "alternately" (unless you really mean something that alternates). Use the word "whereas" instead of "while" (unless you are referring to simultaneous events). Do not use the word "essentially" to mean "approximately" or "effectively." Do not use the word "issue" as a euphemism for "problem." When compositions are not specified, separate chemical symbols by en-dashes; for example, "NiMn" indicates the intermetallic compound $Ni_{0.5}Mn_{0.5}$ whereas "Ni–Mn" indicates an alloy of some composition Ni_xMn_{1-x}.

Be aware of the different meanings of the homophones "affect" (usually a verb) and "effect" (usually a noun), "complement" and "compliment," "discreet" and "discrete," "principal" (e.g., "principal investigator") and "principle" (e.g., "principle of measurement"). Do not confuse "imply" and "infer."

Prefixes such as "non," "sub," "micro," "multi," and "ultra" are not independent words; they should be joined to the words they modify, usually without a hyphen. There is no period after the "et" in the Latin abbreviation "*et al.*" (it is also italicized). The abbreviation "i.e.," means "that is," and the abbreviation "e.g.," means "for example" (these abbreviations are not italicized).

An excellent style manual and source of information for science writers is [9].

VII. Editorial Policy

Each manuscript submitted is subjected to the following review procedure:

- It is reviewed by the editor for general suitability for this publication
- If it is judged suitable, two reviewers are selected and a single-blinded review process takes place
- Based on the recommendations of the reviewers, the editor then decides whether the particular paper should be accepted as is, revised or rejected.

Do not submit a paper you have submitted or published elsewhere. Do not publish "preliminary" data or results. The submitting author is responsible for obtaining agreement of all coauthors and any consent required from sponsors before submitting a paper. It is the obligation of the authors to cite relevant prior work.

Every paper submitted to "Electronics" journal are single-blind reviewed. For conference-related papers, the decision to accept or reject a paper is made by the conference editors and publications committee; the recommendations of the referees are advisory only. Undecipherable English is a valid reason for rejection.

VIII. Publication Principles

The contents of "Electronics" are peer-reviewed and archival. The "Electronics" publishes scholarly articles of archival value as well as tutorial expositions and critical reviews of classical subjects and topics of current interest.

Authors should consider the following points:

1) Technical papers submitted for publication must advance the state of knowledge and must cite relevant prior work.
2) The length of a submitted paper should be commensurate with the importance, or appropriate to the complexity, of the work. For example, an obvious extension of previously published work might not be appropriate for publication or might be adequately treated in just a few pages.
3) Authors must convince both peer reviewers and the editors of the scientific and technical merit of a paper; the standards of proof are higher when extraordinary or unexpected results are reported.
4) Because replication is required for scientific progress, papers submitted for publication must provide sufficient information to allow readers to perform similar experiments or calculations and use the reported results. Although not everything need be disclosed, a paper must contain new, useable, and fully described information. For example, a specimen's chemical composition need not be reported if the main purpose of a paper is to introduce a new measurement technique. Authors should expect to be challenged by reviewers if the results are not supported by adequate data and critical details.
5) Papers that describe ongoing work or announce the latest technical achievement, which are suitable for presentation at a professional conference, may not be appropriate for publication in "Electronics".

IX. Conclusion

A conclusion section is not required. Although a conclusion may review the main points of the paper, do not replicate the abstract as the conclusion. A conclusion might elaborate on the importance of the work or suggest applications and extensions.

Appendix

Appendixes, if needed, appear before the acknowledgment.

Acknowledgment

The preferred spelling of the word "acknowledgment" in American English is without an "e" after the "g." Use the singular heading even if you have many acknowledgments. Avoid expressions such as "One of us (S.B.A.) would like to thank ... ." Instead, write "F. A. Author thanks ... ." **Sponsor and financial support acknowledgments are placed in the unnumbered footnote on the first page, not here.**

References

[1] G. O. Young, "Synthetic structure of industrial plastics (Book style with paper title and editor)," in *Plastics*, 2nd ed. vol. 3, J. Peters, Ed. New York: McGraw-Hill, 1964, pp. 15–64.

[2] W.-K. Chen, *Linear Networks and Systems* (Book style). Belmont, CA: Wadsworth, 1993, pp. 123–135.

[3] H. Poor, *An Introduction to Signal Detection and Estimation*. New York: Springer-Verlag, 1985, ch. 4.
[4] B. Smith, "An approach to graphs of linear forms (Unpublished work style)," unpublished.
[5] E. H. Miller, "A note on reflector arrays (Periodical style—Accepted for publication)," *IEEE Trans. Antennas Propagat.*, to be published.
[6] J. Wang, "Fundamentals of erbium-doped fiber amplifiers arrays (Periodical style—Submitted for publication)," *IEEE J. Quantum Electron.*, submitted for publication.
[7] C. J. Kaufman, Rocky Mountain Research Lab., Boulder, CO, private communication, May 1995.
[8] Y. Yorozu, M. Hirano, K. Oka, and Y. Tagawa, "Electron spectroscopy studies on magneto-optical media and plastic substrate interfaces (Translation Journals style)," *IEEE Transl. J. Magn.Jpn.*, vol. 2, Aug. 1987, pp. 740–741 [*Dig. 9th Annu. Conf. Magnetics* Japan, 1982, p. 301].
[9] M. Young, *The Techincal Writers Handbook.* Mill Valley, CA: University Science, 1989.
[10] J. U. Duncombe, "Infrared navigation—Part I: An assessment of feasibility (Periodical style)," *IEEE Trans. Electron Devices*, vol. ED-11, pp. 34–39, Jan. 1959.
[11] S. Chen, B. Mulgrew, and P. M. Grant, "A clustering technique for digital communications channel equalization using radial basis function networks," *IEEE Trans. Neural Networks*, vol. 4, pp. 570–578, Jul. 1993.
[12] R. W. Lucky, "Automatic equalization for digital communication," *Bell Syst. Tech. J.*, vol. 44, no. 4, pp. 547–588, Apr. 1965.
[13] S. P. Bingulac, "On the compatibility of adaptive controllers (Published Conference Proceedings style)," in *Proc. 4th Annu. Allerton Conf. Circuits and Systems Theory*, New York, 1994, pp. 8–16.
[14] G. R. Faulhaber, "Design of service systems with priority reservation," in *Conf. Rec. 1995 IEEE Int. Conf. Communications,* pp. 3–8.
[15] W. D. Doyle, "Magnetization reversal in films with biaxial anisotropy," in *1987 Proc. INTERMAG Conf.*, pp. 2.2-1–2.2-6.
[16] G. W. Juette and L. E. Zeffanella, "Radio noise currents n short sections on bundle conductors (Presented Conference Paper style)," presented at the IEEE Summer power Meeting, Dallas, TX, Jun. 22–27, 1990, Paper 90 SM 690-0 PWRS.
[17] J. G. Kreifeldt, "An analysis of surface-detected EMG as an amplitude-modulated noise," presented at the 1989 Int. Conf. Medicine and Biological Engineering, Chicago, IL.
[18] J. Williams, "Narrow-band analyzer (Thesis or Dissertation style)," Ph.D. dissertation, Dept. Elect. Eng., Harvard Univ., Cambridge, MA, 1993.
[19] N. Kawasaki, "Parametric study of thermal and chemical nonequilibrium nozzle flow," M.S. thesis, Dept. Electron. Eng., Osaka Univ., Osaka, Japan, 1993.
[20] J. P. Wilkinson, "Nonlinear resonant circuit devices (Patent style)," U.S. Patent 3 624 12, July 16, 1990.
[21] *IEEE Criteria for Class IE Electric Systems* (Standards style), IEEE Standard 308, 1969.
[22] *Letter Symbols for Quantities*, ANSI Standard Y10.5-1968.
[23] R. E. Haskell and C. T. Case, "Transient signal propagation in lossless isotropic plasmas (Report style)," USAF Cambridge Res. Lab., Cambridge, MA Rep. ARCRL-66-234 (II), 1994, vol. 2.
[24] E. E. Reber, R. L. Michell, and C. J. Carter, "Oxygen absorption in the Earth's atmosphere," Aerospace Corp., Los Angeles, CA, Tech. Rep. TR-0200 (420-46)-3, Nov. 1988.
[25] (Handbook style) *Transmission Systems for Communications,* 3rd ed., Western Electric Co., Winston-Salem, NC, 1985, pp. 44–60.
[26] *Motorola Semiconductor Data Manual,* Motorola Semiconductor Products Inc., Phoenix, AZ, 1989.
[27] (Basic Book/Monograph Online Sources) J. K. Author. (year, month, day). *Title* (edition) [Type of medium]. Volume (issue). Available: http://www.(URL)
[28] J. Jones. (1991, May 10). Networks (2nd ed.) [Online]. Available: http://www.atm.com
[29] (Journal Online Sources style) K. Author. (year, month). Title. *Journal* [Type of medium]. Volume(issue), paging if given. Available: http://www.(URL)
[30] R. J. Vidmar. (1992, August). On the use of atmospheric plasmas as electromagnetic reflectors. *IEEE Trans. Plasma Sci.* [Online]. *21(3).* pp. 876–880. Available: http://www.halcyon.com/pub/journals/21ps03-vidmar

Instruction for Authors

Editorial objectives

In the journal ”Electronics”, the scientific papers from different fields of electronics and electrical engineering in the broadest sense are published. Main topics are electronics, automatics, telecommunications, computer techniques, power engineering, nuclear and medical electronics, analysis and synthesis of electronic circuits and systems, new technologies and materials in electronics etc. The main emphasis of papers should be on methods and new techniques, or the application of existing techniques in a novel way.

The reviewing process

Each manuscript submitted is subjected to the following review procedures:

- It is reviewed by the editor for general suitability for this publication;
- If it is judged suitable, two reviewers are selected and a double-blind review process takes place;
- Based on the recommendations of the reviewers, the editor then decides whether the particular paper should be accepted as it is, revised or rejected.

Submissions Process

The manuscripts are to be delivered to the editor by e-mail: els-journal@etf.unibl.org.

Manuscripts have to be prepared in accordance with the instructions given in the template for paper preparation that can be found on the journal’s web page (www.electronics.etfbl.net).

Authors should note that proofs are not supplied prior to publication and ensure that the paper submitted is complete and in its final form.

Copyright

Articles submitted to the journal should be original contributions and should not be under consideration for any other publication at the same time. Authors submitting articles for publication warrant that the work is not an infringement of any existing copyright and will indemnify the publisher against any breach of such warranty. For ease of dissemination and to ensure proper policing of use, papers and contributions become the legal copyright of the publisher unless otherwise agreed.

ELECTRONICS, VOL. 21, NO. 2, DECEMBER 2017

PAPERS

PROFESSIONAL BIOGRAPHY VANČO B. LITOVSKI 51

MODULAR ENVIRONMENT FOR DEVELOPMENT AND CHARACTERIZATION OF TUNABLE ENERGY HARVESTING SYSTEMS.... 53
Casatorres-Agüero, Javier and Nieto-Taladriz, Octavio

HIGH EFFICIENCY PHOTOVOLTAIC SYSTEM WITH FUZZY LOGIC CONTROLLER 60
Branko Blanuša, Željko Ivanović and Branko Dokic

CHALLENGES AND OPPORTUNITIES IN APPLYING SEMANTICS TO IMPROVE ACCESS CONTROL IN THE FIELD OF INTERNET OF THINGS 66
Riste Stojanov, Vladimir Zdraveski and Dimitar Trajanov

BODE PLOTS REVISITED: A SOFTWARE SYSTEM FOR AUTOMATED GENERATION OF PIECEWISE LINEAR FREQUENCY RESPONSE PLOTS 76
Predrag Pejovic and Amela Zekovic

APPLICATIONS OF ARTIFICIAL NEURAL NETWORKS IN ELECTRONICS 87
Miona Andrejević Stošović and Vančo Litovski

SIMULATION OF A PICK-AND-PLACE CUBE ROBOT BY MEANS OF THE SIMULATION SOFTWARE KUKA SIM PRO 95
Duško Lukač, Miljana Milić

IMPLEMENTING MASTER PROGRAM ON DIGITAL BROADCASTING AND BROADBAND TECHNOLOGIES........ 100
Siniša Ilić, Mile Petrović, Branimir Jakšić, Slobodan Bojanić, Petar Spalević and Ranko Babić

ISSN 1450-5843
UDK 621.38